

LATTICE TRUSS STRUCTURAL RESPONSE USING  
ENERGY METHODS

by

Winfred Scottson Kenner  
B.S.M.E. May 1987, North Carolina A&T State University

A Thesis submitted to the Faculty of Old Dominion University in Partial  
Fulfillment of the Requirement for the Degree of

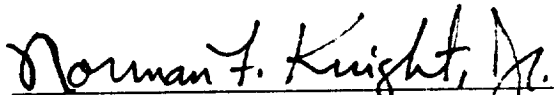
MASTER OF SCIENCE


MECHANICAL ENGINEERING

OLD DOMINION UNIVERSITY

August, 1996

Approved by:

  
Dr. Norman F. Knight, Jr. (Director)

  
Dr. Chuh Mei

  
Dr. Mark S. Lake

## **ABSTRACT**

### **LATTICE TRUSS STRUCTURAL RESPONSE USING ENERGY METHODS**

Winfred Scottson Kenner  
Old Dominion University, 1996  
Director: Dr. Norman F. Knight, Jr.

A deterministic methodology is presented for developing closed-form deflection equations for two-dimensional and three-dimensional lattice structures. Four types of lattice structures are studied: beams, plates, shells and soft lattices. Castigliano's second theorem, which entails the total strain energy of a structure, is utilized to generate highly accurate results. Derived deflection equations provide new insight into the bending and shear behavior of the four types of lattices, in contrast to classic solutions of similar structures. Lattice derivations utilizing kinetic energy are also presented, and used to examine the free vibration response of simple lattice structures. Derivations utilizing finite element theory for unique lattice behavior are also presented and validated using the finite element analysis code EAL.

## **ACKNOWLEDGEMENTS**

I would like to thank all the personnel of Langley Research Center and Old Dominion University who have assisted me and my research task. Specifically, I would like to thank Dr. Martin M. Mikulas, Jr., who inspired me to study lattice structures. Additionally, I would like to acknowledge Dr. Mark S. Lake, Dr. Charles M. Camarda, and my advisor Dr. Norman F. Knight Jr. for their support and encouragement. Finally I would like to thank my mother and father for their intangible gift of creativity.

# LATTICE STRUCTURAL RESPONSE USING ENERGY METHODS

## TABLE OF CONTENTS

	<b>Page</b>
LIST OF TABLES	vii
LIST OF FIGURES	viii
 <b>CHAPTER</b>	
I. INTRODUCTION.....	1
1.1 General.....	1
1.1.1 Historical Background.....	2
1.2 Foundation.....	3
1.3 Literature Review.....	4
1.3.1 Elementary Methods from Static.....	4
1.3.2 Elastic Stress-Strain Relations and Energy Methods..	5
1.3.3 Continuum Modeling.....	6
1.3.4 Finite Elements Analysis.....	7
1.4 Objectives and Scope.....	8
 II. LATTICE DESIGNS.....	 10
2.1 Overview.....	10
2.2 Lattice Geometries.....	11
2.2.1 Beam-like Lattices.....	12
2.2.2 Plate-like Lattices.....	12
2.2.3 Shell-like Lattices.....	13
2.2.4 Soft Plate-like Lattices.....	14
 III. LATTICE ANALYSIS PROCEDURES.....	 15
3.1 Overview.....	15
3.2 Static Determinacy.....	16
3.3 Static Indeterminacy.....	16

3.4	Castigliano's Second Theorem . . . . .	17
3.5	Exact Deflection Derivation . . . . .	18
3.6	Approximate Deflection Derivation for Static Indeterminacy ..	22
3.7	Finite Element Models. . . . .	24
3.8	Symmetry Exploitation for Static Indeterminacy Analysis . . . .	24
3.9	Comments on Analysis Considerations for Design. . . . .	25
<b>IV.</b>	<b>ANALYSIS RESULTS. . . . .</b>	<b>26</b>
4.1	Overview . . . . .	26
4.2	Linear Elastic Beam Overview . . . . .	26
4.2.1	Two-dimensional Lattices Overview. . . . .	27
4.2.1.1	Warren . . . . .	27
4.2.1.2	Quadrangular Warren. . . . .	29
4.2.1.3	Baltimore . . . . .	30
4.2.1.4	Baltimore with Fixed Supports. . . . .	30
4.2.1.5	Soft Warren and Baltimore. . . . .	30
4.2.2	Neutral Axis Deflection Principles. . . . .	31
4.2.3	Three-dimensional Lattice Beams . . . . .	32
4.2.3.1	Triangular Cross-section. . . . .	32
4.2.3.2	Warren. . . . .	33
4.2.3.3	Torsion. . . . .	34
4.2.3.4	Warren, Two-bays Wide. . . . .	35
4.2.4	Summary of Lattice Beams . . . . .	36
4.3	Linear Elastic and Lattice Plate Overview. . . . .	37
4.3.1	Three-dimensional Lattices with Square Geometries ..	39
4.3.1.1	Warren Membrane. . . . .	40
4.3.1.2	Warren Membrane, Orthotropic. . . . .	42
4.3.1.3	Warren Longerons. . . . .	43
4.3.1.4	Warren Membrane with Cutout. . . . .	44
4.3.1.5	Warren Longerons with Cutout. . . . .	45
4.3.2	Summary of Square Three-Dimensional Lattices . . . . .	45
4.3.3	Three-dimensional Infinitely Wide Planar Lattices . . . . .	46
4.3.3.1	Warren. . . . .	46
4.3.3.2	Tetrahedral. . . . .	49
4.3.4	Comments on Linear Elastic and Lattice Plate Theory .	50

4.4	Shell-like Overview .....	51
4.4.1	Two-dimensional Ring-like Lattices. ....	52
4.4.1.1	Triangular Bay. ....	53
4.4.1.2	Square Bay. ....	54
4.4.2	Curved Frame or Statically Determinate Circular Arch. ....	54
4.4.3	Spheres. ....	56
4.5	Soft Plate-like Lattices in Three-dimensions Overview. ....	57
4.5.1	Sixth Order with Surface Longerons. ....	57
4.5.2	Sixth Order Consisting of Diagonals. ....	58
4.5.3	Sixth Order Symmetric. ....	59
4.5.4	Sixth Order Symmetric Distributed Load ....	60
4.5.5	Eighth Order. ....	60
4.5.6	Eighth Order, Clamped On Two Sides. ....	61
4.5.7	Overview of Soft Lattices Displacement Fields. ....	62
4.5.8	Soft Lattice Mechanics. ....	62
4.5.9	Comments on Current and Theoretical Soft Lattices. . .	64
4.6	Vibration Overview .....	66
4.6.1	Rods. ....	66
4.6.2	Lattice Beams. ....	68
4.6.3	Lattice Ring. ....	68
V.	FINITE ELEMENT FORMULATION FOR SOFT LATTICES .....	70
5.1	Overview. ....	70
5.2	Exact Soft Finite Element Matrix Formulation. ....	71
5.3	Sixth Order Verification. ....	72
VI.	CONCLUSIONS AND RECOMMENDATIONS. ....	75
6.1	Overview. ....	75
6.2	Conclusions. ....	76
6.3	Recommendations. ....	76
VII.	REFERENCES. ....	78

## LIST OF TABLES

Table Number	Title	Page Number
4.1	Neutral axis deflection principles . . . . .	80
4.2	Elastic coefficients comparison for tetrahedral and Warren (hexahedral) plate-like lattices. . . . .	81
4.3	Summary and prediction of soft lattice performance in three-dimensions. . . . .	82
4.4	Outline of study derived equations. . . . .	83
5.1	Fifth-order finite element verification. . . . .	84

## LIST OF FIGURES

Figure Number	Title	Page Number
1.1	Assembly of panel structure on space station keel lattice structure. .	85
1.2	Candidate space lattice structures . . . . .	86
1.3	Foundation of lattice study. . . . .	87
2.1	Typical two-and three-dimensional lattice beams. . . . .	88
2.2	Typical planar Warren lattice geometry. . . . .	89
2.3	Typical planar Tetrahedral lattice geometry . . . . .	90
2.4	Typical shell-like lattice geometries . . . . .	91
2.5	Typical soft lattice geometries . . . . .	92
3.1	Displacement equation derivation for a cantilevered Pratt lattice beam . . . . .	93
3.2	Two displacement derivations of a statically indeterminate lattice. . .	94
4.1	Deflection equations of cantilevered Warren lattice beam. . . . .	95
4.2	Deflection equations of cantilevered quadrangular Warren lattice beam. . . . .	96
4.3	Deflection equations of cantilevered Baltimore lattice beam. . . . .	97
4.4	Deflection equations of Baltimore lattice beam with fixed supports. .	98
4.5	Deflection equations of cantilevered soft quadrangular Warren and Baltimore lattice beams in two-dimensions. . . . .	99
4.6	Deflection equation of cantilevered Warren lattice beam with triangular cross-section. . . . .	100
4.7	Deflection equations of cantilevered Warren lattice beam, three- dimensional. . . . .	101
4.8	Torsion equations of Warren beams with triangular and square cross-sections . . . . .	102
4.9	Deflection equations of cantilevered Warren lattice, two bay wide. . .	103



4.10	Warren planform lattice and component longeron and membrane lattices. . . . .	104
4.11	Deflection equations of Warren $\pm 45$ membrane lattice plate. . . . .	105
4.12	Deflection equation of Warren 0, $\pm 30, 90$ membrane lattice plate. . . .	106
4.13	Deflection equations of Warren 0, 90, longeron lattice plate. . . . .	107
4.14	Deflection equations of Warren membrane lattice plate with cutout..	108
4.15	Deflection equations of Warren longeron lattice plate with cutout. . .	109
4.16	Deflection equations and stiffness coefficient of Warren lattice plate	110
4.17	Deflection equations and stiffness coefficient of tetrahedral lattice plate. . . . .	111
4.18	Expansion equations of triangular bay lattice ring. . . . .	112
4.19	Expansion equations of square bay lattice ring. . . . .	113
4.20	Statically determinate symmetric circular arch lattice. . . . .	114
4.21	Spherical lattice member loads and displacements. . . . .	115
4.22	Deflection equations of a soft 6th-order Warren lattice with end load, two rows of longerons. . . . .	116
4.23	Deflection equations of a soft 6th-order Warren lattice with end load, longeronless. . . . .	117
4.24	Deflection equation of a symmetric soft sixth-order Warren lattice with end load . . . . .	118
4.25	Deflection equations of a symmetric soft sixth-order Warren lattice with distributed load. . . . .	119
4.26	Deflection equation of a soft eighth-order Warren lattice with end load. . . . .	120
4.27	Deflection equation of soft eighth-order Warren lattice with point load. . . . .	121
4.28	Overview of soft lattices induced loads and subsequent behavior. .	122
4.29	Axial eigenvalue relationship for two rod-like lattices. . . . .	123
4.30	Axial eigenvalue relationships for two beam-like lattices. . . . .	124
4.31	Fundamental eigenvalues for a lattice ring. . . . .	125
5.1	Finite Element stiffness matrices for elastic beam and frame elements. . . . .	126
5.2	Finite Element stiffness matrix derivation for soft sixth-order cantilevered lattice with end load . . . . .	127

5.3(a) Beam and frame stiffness matrix for cantilevered soft sixth-order lattice with end load .....	128
5.3(b) Beam and frame stiffness matrix for cantilevered soft sixth-order lattice with end load .....	129

# **CHAPTER I**

## **INTRODUCTION**

### **1.1 General**

Trusses are rigid skeletal frameworks utilized to provide support for structures or equipment. They are generally composed of long slender members. Typically these members are joined together with pin-connectors. Some attractive structural features of trusses are their low material to load carrying characteristics relative too solid beams, ease of construction, and predictable behavior while incurring load. Truss designers rely on geometry, redundancy and/or arch action to tailor and optimize trusses for various load applications. These and other design parameters play a crucial role in the performance of cranes, bridges, domes, and space-based structures. Examples of typical space-based trusses are presented in Figures 1.1 and 1.2. Various truss applications require designer evaluation of behavior for operational loading, vibrational excitations, or loads during truss construction. For preliminary analysis or conceptual studies, designers often study single- or double-layered planar lattice truss structures, which have regular and patterned geometries, to gain insight into their structural behavior. Lattice structures are attractive for stiffness and vibration analysis methods because their repetitive geometries are represented by mathematical models and numerical programs

in a more accurate manner than trusses with curvature or local variations. However, even the study of lattices encompasses a wide range of analysis techniques. Many reports and books have been published on lattice stiffness analysis, tailoring for load-transfer efficiency, and vibration response prediction (see [Ref. 1-7]). One of the most common types of analysis for lattice structures is the continuum approach in which a lattice's stiffness properties are represented by an equivalent continuum model. However, continuum analysis is most useful for large lattices with many repeating cells. In general transverse shear effects are not included in the analysis of lattices; however, shear effects can be included with additional mathematical terms. This and other lattice analysis drawbacks have prompted this study. In general, the overall objectives of the current work are to review current lattice analysis methods and to conduct a comprehensive study of lattices of varying geometry by accurately quantifying their static behavior. Resulting lattice expressions are compared to similar one-and two-dimensional linear elastic expressions in solid mechanics to provide new insight into structural behavior.

#### 1.1.1 Historical Background

Hellenistic builders invented the truss in the third century B. C. The theoretical basis for it may have been the finding of Greek geometers that the triangle is one type of rigid framework. Greek architects and engineers passed their knowledge of trusses to the Romans. Three of the better-known types of trusses - related to bridges are those of Howe, Pratt and Warren (see Ref. [8]).

## 1.2 Foundation

Basic similarities and differences between lattice analysis and linear elastic analyses for closed-form solutions in three-dimensions are depicted in Figure 1.3. The top left corner figure depicts a generic three-dimensional linear elastic material with load. The only means of analysis are the principle of virtual work and the principle of minimum total potential work. If no simplifying assumptions are made, closed-form solutions are virtually impossible to derive. To proceed further, the three-dimensional material field is usually simplified to a two-dimensional material field for a plane stress or a plate bending analysis, or a one-dimensional field for a beam analysis depending on the geometry. The upper right corner figure list some of the fundamental assumptions of one-and two-dimensional linear elastic materials which have closed form solutions. Additionally some assumptions not mentioned include: (1) uniform stress-strain fields; (2) neutral-axis is unstrained; (3) deflection is small compared to thickness; (4) structures designed to resist lateral loading are generally circular or rectangular in shape; and, (5) transverse shear behavior is seldom considered.

The analysis of a truss structure in three-dimensions differs from that of a linear elastic material in that trusses are deterministic structures. The lower left corner figure of Figure 1.3 represents a generic three-dimensional linear elastic truss, and listed below it are various analysis techniques common to lattices and three-dimensional linear elastic media. Although analysis of a random arrangement of truss members can theoretically be performed, it rarely

is because of mathematical complexities. The current study eliminates some of the analysis complexity by examining a subset of trusses, and lattices, which have repeating rectangular sections and tractable member loads. The study presents and examines lattices in one- and two-dimensions as in solid mechanics, and since all lattices are deterministic, lattices in three-dimensions are also presented and examined. The lower right corner figure of Figure 1.3 represents a typical one-, two- or three-dimensional lattice of this study. Some of the fundamental assumptions are listed below this figure. With these simplifying assumptions and analysis methods, an indirect means of multi-dimensional linear elastic structural analysis is presented.

### **1.3 Literature Review**

As mentioned previously, the analyses of lattice structures for civil application with various loading and boundary conditions for the acquisition of: 1.) member stress or strain values; 2.) nodal deflection; or, 3.) lattice stiffness parameters have been the focus of much research in the past. The leading lattice analysis methods are traditional methods from statics, energy methods, continuum modeling, and finite element analysis. A description of each type follows.

#### **1.3.1 Elementary Methods from Statics**

Historically, the field of statics has provided several adequate discrete nodal deflection and member load analysis techniques such as the methods of joints and of sections (e.g., [Ref. 9]). However, static techniques are time

consuming, tedious, produce very complicated solutions for redundant structures, and are inadequate for developing global lattice stiffness parameters. Global lattice stiffness parameters provide an overall indicator of truss static behavior.

### 1.3.2. Elastic Stress-Strain Relations and Energy Methods

As an alternative to static analysis, the analysis of trusses can be accomplished by determining the elastic stress-strain relationships of the material. Stress tensors,  $\tau_{ij}$ , arise from equilibrium considerations and strain tensors,  $\epsilon_{kl}$ , arise from kinematic considerations. These tensors are related by constitutive relationships. If the constitutive relationships relate stress and strain directly, uniquely, and linearly the material is referred to as linear elastic; the constitutive relationship becomes the generalized Hooke's law as given by

$$\tau_{ij} = C_{ijkl} \epsilon_{kl} \quad (1)$$

The definition of  $C_{ijkl}$  stiffness parameters distinguish isotropic, composite [10] and lattice-like materials. This technique is usually referred to as the Newtonian approach. Derivation of a stiffness parameter for a truss with this approach is very difficult because of the unknown stress-strain relationship. Simplifying assumptions lead to continuum analysis.

Elastic material analysis is also accomplished with energy methods or the Lagrangian approach. In the study of continuous media, variational methods based on energy principles provide additional analysis tools based on the underlying equations of equilibrium, assumed kinematics, and constitutive

relations [10]. These methods are commonly based on the principle of minimum total potential energy or the principle of virtual work. The strain energy of a elastic body is calculated from the constitutive relationships. For example, in a one-dimensional field, strain energy equals one half times stress times strain. Simplifying assumptions for isotropic materials also lead to commonly used stiffness parameters for rods and beams [11] such as

$$\frac{EA}{L} \quad (2)$$

$$\frac{EI}{L^3} \quad (3)$$

Once the strain energy expression is defined for the structure, Castigliano's theorems are frequently employed to determine deflections utilizing the unit load method. Therefore, discrete deflection values are commonly obtained through the use of Castigliano's theorems. However, Castigliano's theorem requires a lattice structure's total strain energy which involves significant computational effort to evaluate similar to the methods from statics.

### 1.3.3. Continuum Modeling

Continuum analysis is a closed-form solution technique used to derive lattice stiffness parameters that assumes the global elastic behavior of a lattice can be represented by an equivalent continuum. Several continuum analysis methods have been develop. Two such methods are the discrete field method [2-4] and Neyfeh's method [7]. Both methods are good for producing stiffness parameters for large lattice structures without transverse shear effects.



Discrete field methods assume various equivalences between the lattice and continuum at typical lattice nodes. These equivalences can involve equilibrium and compatibility equations, potential and kinetic energies, nodal deformations and rotations [3], and member forces and/or member strains [2]. The transition from lattice to continuum is performed by expanding one or more of the previously assumed fields in a Taylor series about the origin of the repeating element [4].

Neyfeh's continuum method [7] treats parallel lines of lattice members as single equivalent sheets of composite lamina. As in composite theory, a local stiffness matrix is derived for each lamina sheet, transformed to the primary axis, and the resulting matrices are summed to produce the global stiffness matrix of the lattice.

#### 1.3.4. Finite Element Analysis

During the past forty years, finite-element analysis methods have been developed. Very early formulations are related to the framework or lattice analogy for stress analysis. Finite element analyses produce very accurate discrete values, and it is applicable to a wide range of lattice structures [12-15]. However, it can be expensive in terms of personnel to develop and verify finite element models and their results, requires a high degree of computing efficiency, and is inadequate for developing global lattice stiffness parameters for use in design.

Using a finite element analysis system such as EAL [16], individual members are each represented as a spatial rod element with a corresponding Young's

modulus and cross-sectional area. Joint or node point locations are defined by global coordinates of the member end points. Assembly of the finite element model produces a global stiffness matrix that can be very large for large lattice structures. As the lattice design changes, modifications to the finite element model may be minor (i.e., selected changes in member cross-sectional areas) or more significant if the geometry is changed.

In summary, these methods vary from elementary methods of statics to complex methods involving equivalent continuum models to equivalent discrete models. These methods provide different levels of solution and perhaps are best used to verify the final design. However, as the lattice design evolves a more general method is needed.

#### **1.4 Objectives and Scope**

This paper provides a fundamental and integral approach to the study of lattices. First, lattice geometry, symmetry, topology, and design is examined. Next, lattice behavior or mechanics is examined, and a new methodology for the analysis of lattice structures is presented. The methodology provides insight into lattice design for strength or stiffness. Additionally, great emphasis is placed on exact solutions of various lattice parameters such as nodal displacements and member loads. This limits the scope of the study but allows for greater insight into the behavior of selected lattice geometries.

Specific objectives of this research are: 1.) To develop simple closed-form exact deflection and vibration equations using Castigliano's second

theorem over the nodal domain of uniform lattice structures; 2.) To develop expressions for highly redundant lattice structures by using compatibility requirements; 3.) To develop truss geometries which under uniform loading exhibit sixth- and eighth-order behavior for deflection; and, 4.) To develop associated finite element stiffness matrices and validation procedures.

Warren, tetrahedral and modified versions of the Warren lattice design are the primary configurations examined in this study due to the extensive amount of previous work on similar lattice geometries. Deflection equations are presented in mathematical form as functions of the number of bays or cells. All lattice members are assumed to have pinned nodal connections and to behave as linear elastic axial rods.

## **CHAPTER II**

### **LATTICE DESIGNS**

#### **2.1 Overview**

The structure of a solid material may vary from a crystalline-like material (e.g., metal, wood) to an amorphous material (e.g., glass). The fundamental characteristic of a crystalline material is periodicity of a unit atomic structure. There are only fourteen possible networks of lattice points for a unit structure and seven crystal systems [17]. Lattice structures have similar characteristics [5]. Lattice morphology or crystallography are common terms used to describe the science of certain repetitive structures. The basic relationship between geometry and behavior is studied to assist in the design of load efficient, reliable, and damage-tolerant lattice structures. However, most work in this area assumes that the basic unit lattice cell is infinitesimally small. In contrast, this study centers on the behavior of one cell, two cells, and progressively higher numbers of cells. By analyzing the basic cell to a higher degree, hopefully a better understanding of lattice behavior will be achieved.

Four groups of lattices with varying cell geometries are presented for analysis. Some lattices have traditional symmetric crystal-like cubic or tetrahedral cell geometries while others have asymmetric geometric cells. As will be illustrated, the lattice geometric domain is far larger (i.e., cross lacing,

asymmetric cells) than the seven crystalline geometric domain commonly studied. The lattices in each of the four groups are designed to capture this variation and hence, explore material behavior in structural mechanics which is undetermined.

## **2.2 Lattice Geometries**

The number of lattices studied are too numerous to describe individually, therefore a general definitions of the four major types of lattices is provided. The various geometries are aligned to an axis, and represent lattices of finite length of n-bays or n-cells. Lattice depth is held constant along the length. Bays are the repetitive lattice unit in two-dimensions, and cells are the repetitive lattice unit in three-dimensions. Lattice bays and cells consist of three types of members: longerons, diagonals, and battens. Longerons usually lie parallel to the horizontal axes or plane. Battens usually lie parallel to the vertical axis, and diagonal members usually bisect the rectangle formed by the longeron and batten members. Each member is defined by its geometric location in the lattice. Surface members lie on the parallel upper and lower expanding horizontal planes of a lattice, and core members lie in between the two parallel surfaces. The four types of lattice structures considered include: 1.) beam-like lattices in both two-and three-dimensions; 2.) plate-like lattices in two- and three-dimensions; 3.) shell-like lattices in two-and three-dimensions; and, 4.) soft plate-like lattices in three-dimensions.

### 2.2.1 Beam-like Lattices

Several two-and three-dimensional Warren-type lattices representative of classic beam-type lattice structures are presented in Figure 2.1. Beam-type lattices consist of linearly replicated bays in two-dimensions and cells in three-dimensions. The repeating elements of the Pratt lattice in two-dimensions and of the Warren lattice in three-dimensions are highlighted in gray. Various lattice members are also identified.

The two-dimensional top lattice is commonly called a Pratt lattice wherein the diagonal members are oriented in the same manner connecting two longerons. Warren lattices have alternating diagonal members, and quadrangular Warren lattices have crossing diagonal members. Alternative forms, such as the Baltimore design often involve additional longerons, diagonals, or batten members per bay as illustrated in Figure 2.1(a).

Three-dimensional beam-like lattice structures have rectangular and triangular cross-sections as illustrated in Figure 2.1(b). The three-dimensional Warren beams consist of two two-dimensional Warren beams connected by out of plane diagonal and batten members. Beam-like lattices are studied for a wide range of applications.

### 2.2.2 Plate-like Lattices

Various views of Warren and tetrahedral plate-like lattice geometries are presented in Figures 2.2 and 2.3. Plate-like lattices consist of cells which are bilinearly replicated. Warren plate-like lattices have a rectangular volumetric design, with one diagonal per cubic face. Tetrahedral plate-like lattices consist

of tetrahedral and octahedral cells. All of the members in a regular tetrahedral lattice have the same length. A tetrahedral lattice is derived from a Warren lattice by rearranging the diagonal members and displacing alternating rows of nodes by one. Therefore, the total number of members in equal bay configurations of both lattices are the same. Warren and tetrahedral lattice geometries are attractive for analysis because they can be tailored to have pseudo-isotropic (i.e., analogous to a laminated composite plate with a stacking sequence of  $0/\pm 45/90$ , or  $\pm 60/0$ ) face-sheet arrangements of members for the top and bottom surfaces, and they are highly redundant (e.g., Ref. 5). The repeating cells of each lattice are highlighted in gray, and various groups of members (i.e., surface, core) are identified.

### 2.2.3 Shell-like Lattices

Ring, cylindrical, and spherical geometries are presented in Figure 2.4 as representative of shell-like lattice structures. The ring cylindrical lattices have bays which are axially symmetrically replicated, and the spherical lattices have cells which are spherically symmetrically replicated. The two-dimensional ring lattices have the same bay geometry as the two-dimensional Warren lattices; however, the inner surface members are shorter than the outer surface members. The spherical geometry is representative of a polyhedral sphere comprised of  $n$ -equilateral triangles. Few lattice stiffness papers [1-7] have been written on shell geometries, because stiffness values can be obtained from analogous plate analysis. However, there is a stiffness difference do to

unequal inner and outer member lengths especially for geometries with few bays.

#### 2.2.4. Soft Plate-like Lattices

Two types of hybrid Warren plate-like lattices or soft lattices are presented in Figure 2.5. Soft plate-like lattices consist of cells which are linearly replicated. The geometries are derived from the basic Warren lattice geometry presented in Figure 2.2 by the removal of surface longerons and/or diagonals. These members are selected for removal because they seem critical to the bending stiffness of Warren lattices in two-and three dimensions. These lattices are designed to be inherently weak in bending, and to serve indirectly as test cases to assess the accuracy of the analysis method qualitatively.



## **CHAPTER III**

### **LATTICE ANALYSIS PROCEDURE**

#### **3.1 Overview**

To understand lattice behavior, various lattice components and analysis techniques are defined. Lattice structures consist of two main components: 1.) members which are only capable of transmitting compression and tension reactions; and, 2.) pinned nodes which are the frictionless connection points of the lattice members. The arrangement of members will depend on the structural function to be desired. Constraints serve to prevent lattice structures from translation or rotation due to loading. In two-dimensions, constrained lattice structures by definition adhere to a minimum member  $m$  to node  $n$  relationship. This relationship for a two-dimensional lattice is

$$m = 2n \quad (4)$$

and for a three-dimensional lattice the relationship is

$$m = 3n \quad (5)$$

Equations (4) and (5) are referred to as Maxwell's equations for structural stability or kinematic stability. Lattices which have more than the required number of members have redundant members. Lattices which have more than the required number of constraints to prevent translation or rotation have redundant constraints.

### **3.2 Static Determinacy**

A statically determinate lattice structure exposed to external forces is defined as an internal system of pinned members and constraint arrangement from which internal forces and displacements can be determined exactly by the equations of statics (i.e., using the method of joints, or method of sections) [8]. A vast majority of statically determinate lattices, adhere to Maxwell's equations. However, if the number of members in a lattice is less than  $2n$  or  $3n$  then a mechanism results. All of the lattices in groups one and four defined in Section 2.2 are statically determinate.

### **3.3 Static Indeterminacy**

A lattice structure is considered statically indeterminate if member loads can not be determined through static analysis. Statically indeterminate analysis considers member elasticity and the equations of equilibrium. A lattice structure is defined as kinematically stable if it is statically determinate or statically indeterminate.

There are several procedures for solving statically indeterminate lattice problems exactly. The Maxwell-Mohr method and the Castigliano method [17] are two such methods. Both methods start with the removal of all redundant members from a lattice structure. Each member is replaced by equal and opposite reactive forces at the associated nodes. The lattice is now statically determinate and can be analyzed. The magnitude of the unknown reactive loads are found from the requirement that initial lattice nodal deflections must

vanish with the application of the original load and the member replacement loads. These techniques become very complicated for highly redundant lattices and therefore are rarely utilized. All of the lattices in group's two and three are statically indeterminate.

### 3.4 Castigliano's Second Theorem

To acquire statically determinate and statically indeterminate lattice behavior, a highly rigorous analysis method is desired. Knowing that the application of Castigliano's second theorem derived from a total complementary energy functional captures all of a material's displacement behavior due to point forces prompted its use. The generalized Castigliano's second theorem is presented mathematically as,

$$\delta_i = \frac{\partial U'}{\partial P_i} \quad (6)$$

where  $U'$  is complementary strain energy,  $P_i$  is a generalized force, and  $\delta_i$  is the generalized displacement in the direction of  $P_i$ . In words, Castigliano's second theorem states that the partial derivative of the complementary strain energy with respect to any independent generalized force  $P_i$  is equal to the generalized displacement  $\delta_i$  located at the force  $P_i$  and in the direction of  $P_i$ . Equation (6) is simplified for this study due to the analysis of linearly elastic members at constant temperature. Hence, the complementary strain energy is equal to strain energy,  $U = U'$ , and equation (6) reduces to

$$\delta_i = \frac{\partial U}{\partial P_i} \quad (7)$$

This form of Castigliano's second theorem, utilized for this study, states that for a linear elastic system at constant temperature, the partial derivative of the strain energy with respect to any independent generalized force  $P_i$  is equal to the generalized displacement  $\delta_i$  located at the force  $P_i$  and in the direction of  $P_i$ .

### 3.5 Exact Deflection Derivation

To analyze statically determinate lattice groups one (beams) and four (soft, plate-like), a simple exact static analysis procedure is used consisting of Castigliano's second theorem, and extrapolation functions. The analysis procedure consist of four main steps: 1.) generating a lattice model with defined repeating bays or cells, boundary conditions, and specified loads; 2.) calculating lattice member loads per bay or cell; 3.) deriving nodal displacements per bay or cell using Castigliano's second theorem; and, 4.) deriving a displacement function using an extrapolation function for an exact fit.

To provide an understanding of the procedure, an example is presented. Figure 3.1 contains a cantilevered Pratt design lattice beam with an end load , $P$ , and associated internal member loads. A Pratt lattice has two rows of longerons, vertical battens and intermediate diagonal members. Member load results are obtained through any type of static analysis (i.e., the method of joints). Analysis of the first four bays is illustrated on the Figure 3.1. Analysis of the first bay is presented in the upper left corner. A deflection value ( $\delta$ ) is obtained by summing up the strain energy of the five members. This step is

given by

$$\delta = \sum_{i=1} \frac{F_i(\delta F_i)L_i}{E_i A_i} \quad (8)$$

where  $F_i$  is the member load due to actual forces,  $\delta F_i$  is the member load due to a unit virtual load, applied at the desired point of displacement, and  $L_i$  are the member lengths. This is an application of Castigliano's second theorem. Analysis of a two-bay configuration is presented in the upper right corner. Again a deflection value is generated. Deflection values are generated through member load analysis of lattice beams with successively higher number of bays as indicated. Generated deflection values for one, two and three bays are presented in the table form in Figure 3.1. As additional bays are analyzed, their contribution to the tip deflection is zero for more than four bays. Hence, the tip deflections for these four bays allow a fit to a cubic function in terms of the number of bays  $n$ . The derived exact deflection values presented in the table are then fit to a third-order polynomial function. Note, member load and deflection values are rational expressions due to geometry, boundary conditions, and the applied load. These are critical design and analysis criteria, because the derivation of rational coefficients for the third-order extrapolation polynomial is only possible with rational displacement values. The resulting third-order deflection function is given by

$$y(n) = \frac{Pl}{AE} \left[ \frac{2}{3}n^3 + \frac{4n}{3} + 2\sqrt{2}n \right] \quad (9)$$

bending	shear
term	terms

which represents the exact vertical deflection equation of the node where the point load is applied for a finite number (n) of bays, and can be verified through analytical methods or finite element programs (EAL, NASTRAN). Note the bending term results from surface longeron members, and the shear terms result from core members. A third-order polynomial function is chosen as an extrapolation function because of the analogous solid mechanic solution for end deflection of a cantilevered beam of length L given by

$$y = \frac{PL^3}{3EI} \quad (10)$$

and because surface member loads of the four-bay configuration increase from the applied load in a linear fashion. In general, the type of extrapolation or interpolation function is dependent on the change in member load from cell to cell. Since rational values can be fit to any type of mathematical function (i.e., nth-order polynomial function, or trigonometric function), this analysis has wide appeal for linear and nonlinear elastic material problems.

A comparison of the Pratt derived displacement equation using strain energy and a solid mechanic beam displacement equation is presented to highlight the difference. The moment of inertia, I, in equation (10) is calculated using the parallel axis theorem

$$I = 2Ad^2 = \frac{1}{2}A\ell^2 \quad (11)$$

where d is  $\ell$  times one half. Equation (11) substituted into equation (10) generates

$$y = \frac{2P\ell}{3AE} \quad (12)$$

Therefore the classic beam derivation, equation (12), is the first term of lattice equation (9) with  $n$  equal to one. An even more rigorous solution with shear terms can be produced using Timoshenko beam theory or a plane stress analysis with an Airy stress function [9]. However, in general, plane elasticity analysis is limited relative to strain energy analysis for lattice structures. The versatility of the presented energy method for other lattice structures will be illustrate with additional example problems in subsequent sections. As a result of this analysis method, derived solutions are referred to as exact.

It is interesting to note that the expression derived for the end deflection on an  $n$ -bay truss given by equation (12) may be generated to obtain the end deflection for the  $m$ -th bay of an  $n$ -bay truss by successive application of Castigliano's second theorem. Such an expression will be analogous to the deflection equation of a cantilevered beam where the distance measure along the truss axis is  $m$  instead of  $x$ . In the case of classical beam theory, repeated differentiation of the beam deflection equation until a constant right-hand-side term appears results in the governing differential equation of the beam. Repeated integration of this single differential equation and application of boundary conditions will again give the deflection equation. It is believed that similiar steps may be performed using these exact deflection expressions for various lattices where the independent variable is  $m$  instead of  $x$  for the beam. Close examination of the resulting differential-like expressions may provide insight for further extensions to buckling and vibration problems.

### **3.6 Approximate Deflection Derivation for Static Indeterminacy**

Statically indeterminate lattice analysis is an approximate method which views parallel rows of surface members as representative layers of composite lamina. This method is not exact; however, it provides highly accurate solutions, shear terms and is applicable to a wide range of highly redundant lattices. The surfaces of an infinitely wide planar lattice (e.g., Figures 2.2 and 2.3) consist of parallel rows and columns of members oriented at different angles. For example, the Warren planar lattice has parallel members oriented at  $0$ ,  $\pm 45$ , and  $90$  degrees, and the tetrahedral planar lattice has parallel members oriented at  $0$  and  $\pm 60$  degrees. The presented analysis procedure assumes that a redundant planar lattice can be decomposed or simplified and represented by several statically determinate lattices with one row or two symmetric rows of parallel surface members. For example, a statically indeterminate  $0$ ,  $\pm 60$ -degree lattice is represented by a statically determinate  $0$ -degree lattice and a statically determinate  $\pm 60$ -degree lattice. The core member arrangement remains the same since core members only contribute to lower order shear terms. After the deflection equations are derived for each lattice, a compatibility requirement is applied to sum the reciprocal of the respective deflection equations and derive the statically indeterminate deflection equation. The accuracy of the equation is verified through analytical methods. Stiffness parameters, (e.g.,  $EI$  or  $D$ ), are obtained through comparison to classic solid mechanics deflection equations. This procedure applied to redundant lattice plates and beams is illustrated in Chapter 4.



The previously discussed procedure is utilized to analyze a redundant lattice structure and to derive extension equations. Two parent statically indeterminate lattices are presented at the bottom left and right of Figure 3.2 with axial loads. Associated nodal extensional derivations are presented above each figure. The lattice in Figure 3.2 (a) is oriented along the x-axis in a one-dimensional displacement field, and the lattice in Figure 3.2 (b) is in the x-y plane two-dimensional displacement field. In Figure 3.2 (a) the parent lattice is decomposed into a rod-like 0-degree longeron lattice and a diagonal  $\pm 45$  degree type lattice. The strain energy and displacement principles illustrated in Figure 3.1 are applied, and a displacement equation is derived and presented below each statically determinate lattice. With a compatibility requirement, the reciprocal of both displacement equations are summed, and the final displacement equation for the statically indeterminate lattice is presented below the parent lattice in Figure 3.2 (a). This equation is exact because both statically determinate displacement equations are derived in the same x-axis displacement field. Each displacement equation represents the average displacement of the three nodes where point loads are applied.

The lattice in Figure 3.2 (b) is decomposed into a rod-like 0-degree longeron lattice and a  $\pm 45, 90$ -degree lattice due to the inclusion of the y-dimension. Both displacement equations are derived and presented in Figure 3.2 (b) below each lattice. Again, with a compatibility requirement, both equations are summed, and the resulting equations is presented below the redundant parent lattice. This equation is not exact because the two statically determinate lattices

have different displacement fields. However, nodal displacement results are highly accurate and can be verified through finite element analyses.

### **3.7 Finite Element Models**

The following study is conducted with a finite element analysis program called Engineering Analysis Language (EAL) [15]. Each lattice is modeled and analyzed within EAL. Each member is represented by a rod tension and compression element with pinned ends. All loads are applied directly to the nodes, and material and section properties have arbitrary unit values of one. The use of a computer facilitates the derivation of member loads and validates derived equation results. Computer use is critical since hand calculations of some lattice problems is a daunting task.

### **3.8 Symmetry Exploitation for Statically Indeterminate Analysis**

The previous definition for statically indeterminacy is generally accepted; however, symmetry is often utilized to simplify analysis of statically indeterminate structures in solid mechanics. For example, a beam with two fixed ends has one redundant constraint, and a hollow sphere with a uniform pressure load is structurally redundant. However, through the use of symmetry assumptions both statically indeterminate structures are analyzed as determinate structures using only the equations of equilibrium.

In a similar way, symmetric designs and loads are utilized to help analyze statically indeterminate lattices. This is facilitated in lattice designs through: (1) neutral load planes; (2) symmetric shapes; (3) symmetric loading; and, (4)

symmetric boundary conditions. These characteristics do not guarantee statically determinate behavior of a statically indeterminate lattice, but in general, they represent basic requirements.

### **3.9 Comments on Analysis Considerations for Design**

In designing the lattices of the upcoming four lattice groups, all of the previous definitions are incorporated. Statically determinate and symmetric indeterminate beam-like lattices of group one are very common, and since they can be solved exactly with the equilibrium equations, they provide a good validation of the new analysis procedure presented herein. Plate-like lattices are inherently indeterminate (several researchers have attempted to discover statically determinate plate-like lattices and still none have been found) and therefore don't lend themselves to exact analysis. The lattices of the third group have nonlinear geometries in addition to being statically indeterminate, and therefore present additional complexity over the linear lattices of the first two groups. Last, soft plate-like lattice designs inherently exhibit higher-order displacement fields than those considered in typical continuum analysis. The present techniques are uniquely capable of capturing these complex response characteristics. All of the previously mentioned lattice characteristics (e.g., static indeterminacy, symmetry, and circular geometry) are inherent in the four groups of lattice geometries, and their effects on lattice behavior are communicated through upcoming analysis equations presented in Chapter 4.

## **CHAPTER IV**

### **ANALYSIS RESULTS**

#### **4.1 Overview**

Deflection equations are presented for four lattice geometries to illustrate the analysis procedure and to provide insight into one-, two-, and three-dimensional statically determinate and indeterminate lattice behavior. Lattice geometries and derived deflection equations are discussed through references to linear elastic solid mechanic structures (e.g., rods, beams, plates). As previously mentioned, all lattices are modeled, analyzed, and validated with EAL.

#### **4.2 Linear Elastic Beam Overview**

Beams are often statically determinate structures designed to carry loads along one major axis (e.g., length). They are usually designed with a minimal length to width and depth ratio of ten to one. Euler investigated and derived the primary bending behavior of beams while Timoshenko expanded beam theory with shear terms [10]. However, shear terms are usually not calculate during elementary beam derivations. The stiffness parameter of a beam is  $EI$ , which is the product of Young's modulus and the moment of inertia.

#### 4.2.1 Two-dimensional Lattices Overview

The following five lattice beams are statically determinate with uniform loading. Vertical point loads are applied evenly to upper and lower surface nodes. The five lattice geometries all possess rectangular bays like the Pratt lattice geometry presented earlier. In contrast to an elastic beam, lattice beam transverse shear is explicitly represented in a truss, and lattice beam width theoretically does not exist. Lattice nodal deflection equations are simple to derive, as illustrated in Section 3.5, and bending and shear terms are easily associated with surface or core members. All values of  $n$  give exact solutions. Members are assumed not to buckle or deform in a nonlinear fashion due to loadings. Equivalent beam stiffness parameters such as  $EI$  are derived for the lattice beams as illustrated earlier. The cross sectional area of a member is  $A$ ,  $E$  represents Young's modulus of the member material,  $P$  represents an applied point load, and  $P'$  represents an applied distributed load. The unit length  $\ell$ , and  $n$ , number of bays or cells, are defined relative to each lattice group.

##### 4.2.1.1 Warren

The geometry and deflection equations for a cantilevered Warren lattice beam with an end load and a distributed load are shown in Figure 4.1. A Warren lattice has parallel upper and lower surface longeron members with vertical batten members and connecting diagonal members. One bay is highlighted in gray on the lattice where  $H$  represents the beam's height,  $\ell$  represents the length of a longeron member and one bay of the lattice,  $n$

represents the number of bays in a particular lattice design,  $n$  times  $\ell$  equals the length of the lattice.

Deflection equations are also presented on Figure 4.1 for rectangular and square bay lattice configurations with point and distributed loads. Note that in these equations  $n$  squared is excluded. This means that moments generated as a result of the loadings do not include a component which is constant along the beam length. The derived lattice deflection equations are analogous to classic linear elastic beam deflection equations. Since point loads are equally divided among upper and lower nodes, the deflection equation generates values on the horizontal neutral axis between the surface nodes. As previously noted, the third- and fourth-order terms of the deflection equations represent bending while the lower order terms represent shear. Third- and fourth-order bending terms are generated from surface members while lower order terms are generated by core batten, and diagonal members. Note, for the square bay case with an end load, the bending term is the same as the bending term of the Pratt lattice due to equivalent beam depth (see Figure 3.1). The diagonal member lacing pattern of the Warren lattice allows a more efficient load transfer than Pratt lacing, hence Warren shear terms are smaller. Constant terms represent deformation within the end bay of the truss, equivalent to St. Venant effect in continuum. Since this lattice design is statically determinate, loads applied to any node result in relative deflection equations. A member count equation as a function of the number of bays is also presented.

#### 4.2.1.2 Quadrangular Warren

A quadrangular Warren lattice beam is presented in Figure 4.2. It is derived from the Warren lattice by adding an additional diagonal member per bay. Again, general deflection equations are presented for end and distributed loadings, and deflection equations are presented for a square bay configuration. The derived lattice deflection equations are analogous to elastic beam deflection equations. One bay is highlighted in gray. Surface longeron members generate third- and fourth-order bending terms, while core members generate lower order terms. All quadrangular Warren third- and fourth-order bending terms equal Warren bending terms for equivalent depths. Quadrangular Warren diagonal members allow a more efficient load transfer than Warren or Pratt geometries.

Inherent geometric characteristics significantly distinguish this lattice design from previous lattice beam designs. Uniquely, batten members are not strained while the beam is loaded, and constant terms are not generated in the deflection equation derivations. Additionally, this lattice has one redundant member per bay, and lattice behavior is statically determinate only with the application of two equivalent point loads on vertically aligned nodes. Hence, the determination of a deflection equation for this geometry is one example of symmetric statically determinate analysis of a statically indeterminate lattice design. Note the symmetric nature of the lattice geometry, loading conditions and boundary conditions. For previous statically determinate lattice beams, deflection equations can be explicitly derived for all load conditions; however,

this and future redundant lattice deflection equations are only derivable for symmetric lattice designs, loading and boundary conditions. Redundant lattice analysis is desirable in cases of member failure due to buckling or other types of mechanical failures.

#### 4.2.1.3 Baltimore

A redundant cantilevered Baltimore lattice with an end load and respective deflection equations is illustrated in Figure 4.3. The gray highlighted area represents one bay. Again bending and shear terms are generated by surface longeron members and shear terms are generated by core members. The added feature of redundancy and the design of two layers offers an advantage of limited lattice performance in case of member failure. Note the middle row of horizontal members lie on a neutral axis and therefore carry no load.

#### 4.2.1.4 Baltimore with Fixed Supports

A redundant Baltimore lattice with fixed supports and a mid-span point load is illustrated in Figure 4.4. This lattice has redundant members and a redundant support. Mid-span deflections are presented below the geometry. Bending and shear terms both differ from previous lattice values. This example illustrates how bay definition and boundary conditions affect deflection equation coefficients. One bay is defined by the two gray highlighted areas. This lattice is also designed with a neutral middle row of horizontal members.

#### 4.2.1.5 Soft Warren and Baltimore

A cantilevered soft quadrangular Warren lattice, where the bottom row of longerons have been removed, is presented in Figure 4.5 (a), and a soft



Baltimore lattice, where all surface members have been removed is presented in Figure 4.5 (b). These examples are presented to illustrate the flexibility of lattice design and the capability of the analysis method for nontraditional lattice geometries. The highlighted gray areas represent typical repeating bays. Deflection equations for an end are presented below each lattice geometry. Note, longeron and batten core members both contribute third-order terms, and that the third-order coefficient for both square bay configuration is no longer two thirds. Hence, the moment of inertia,  $I$ , of both lattices has changed. With these lattice geometries, the calculation of moment of inertia terms and subsequent Bernoulli-Euler beam deflection equations seem difficult. However, deflection equations are quite easily derived using strain energy methods.

#### 4.2.2 Neutral-Axis Deflection Principles

Lattice beam deflections are calculated for the neutral axis to emulate linear elastic beam behavior. The energy principles behind these lattice beam deflection assumptions and future deflection assumptions are presented on Table 4.1. Statically determinate lattices are represented on the left side of Table 4.1 by three Warren lattice beams. The sum of the deflections of the two lower Warren lattices equals the deflection of the top Warren lattice with two point loads. Hence, neutral axis deflection assumptions are based on the method of superposition for statically determinate lattices. The center lattice represents all statically indeterminate lattices with a point load on a desired point of deflection coinciding with the neutral axis. This is the basic definition of Castigliano's second theorem. The fact that this lattice can be solve as a

statically determinate lattice is ignored. The Warren lattice presented on the right side of Table 4.1 represents statically indeterminate lattices with point loads offset from the desired point of deflection. This behavior is not within the domain of Castigliano's second theorem or the method of superposition, because the summed lower two lattice deflections due to individual point loads do not equate to the deflection of an individual lattice with equivalent point loads. To justify neutral-axis deflection behavior, the principle of complementary energy is utilized.

#### 4.2.3 Three-dimensional Lattice Beams

Three-dimensional lattice beams are examined as a natural progression from two-dimensional beams. With the added dimension, beam width is a consideration. Previous analysis procedures apply, and deflection equations are presented in the same format.

##### 4.2.3.1 Triangular Cross-section

A Warren lattice beam with a triangular cross-section with an end load is presented in Figure 4.6. This geometry is generated by assembling three two-dimensional Warren lattice beams with square bays in the form of a structure with a triangular cross-section. A deflection equation is presented for the averaged nodal displacement at the end of the beam. The design has equal length longeron and batten members and equal length diagonal members. One cell is highlighted in gray. The diagonal members have a Warren lattice design, and either six or four members connect to a node. Load is equally

applied to the nodes at the free end of the beam parallel to a selected flat lattice side. The lattice deflection equation is similar to the deflection equation of the analogous two-dimensional Warren lattice beam presented in Figure 4.1. This is because, due to geometry, off-plane members of the beam are not loaded. Therefore the deflection equation is independent of beam width. A member count equation is also presented on Figure 4.6. It is a function of the number of cells in a particular lattice design. Note that it is equivalent to Maxwell's equations presented in Chapter 3 since each additional lattice cell adds three nodes.

#### 4.2.3.2 Warren

Deflection equations and the geometry of a three-dimensional Warren lattice beam with an end load are present in Figure 4.7. One cell is highlighted in gray. The basic geometry of this lattice is derived by combining four two-dimensional Warren lattice beams with an interior diagonal member to form a rectangular cross-section. The deflection equation is one half of a two-dimensional Warren lattice beam deflection equation for comparable configurations due to loading conditions. This and the previous three-dimensional beam deflection equation are independent of beam width. Although the three-dimensional Warren lattice beam has one redundant member per bay, it behaves as two uncoupled two-dimensional Warren lattice beams due to the geometry and interaction of diagonal members. Note, that redundant lattices require Warren diagonal member geometries and uniform loads for analysis. A redundant Pratt diagonal member geometry and off-center

loads complicates three-dimensional deflection equation derivations because torsion and bending stiffnesses become coupled. Additionally, a member count equation is also presented.

#### 4.2.3.3 Torsion

Torsional rotation equations are presented in Figure 4.8. They are developed for two versions of the triangular cross-sectional and square cross-sectional Warren-type beams to determine diagonal member arrangement effects on torsional stiffness. Both versions have the same number of members, just different diagonal member arrangements. The orthogonal tetrahedral or OTT-type and Warren-type geometry is presented above each lattice. A torque, consisting of four point loads applied at 90-degree angles for the square cross-section and three point loads applied at 120 degrees for the triangular cross-section, is applied to the free end of each beam and corresponding member loads are used to derive torsional or rotational displacement equations. The Warren-type triangular cross-section lattice stiffness coefficient is 52.7 % larger than the OTT-type stiffness coefficient. The Warren-type square cross-section lattice stiffness coefficient is 70.7 % larger than the OTT-type lattice coefficient. The Warren-type lattice designs are stiffer because loads bypass batten members and remain primarily in diagonal members. Additional information on the torsional stiffness and vibration behavior of lattice beams can be found in Reference 19.

#### 4.2.3.4 Warren, Two-bay Wide

As previously mentioned, the next logical step in lattice analysis drives us to wider lattices. Currently the analysis of two-dimensional and three-dimensional beams is very similar, except for the ability to investigate torsional stiffnesses. However, lattices two bays wide are of interest because interior surface nodes are present, and with interior nodes potentially a third dimension is added to a lattice's deformation behavior. Therefore, the previously defined three-dimensional Warren lattice is designed two bays wide and with the removal of selected redundant members analyzed as a statically determinate beam with an end load. The standard repeating cell, now changes into a repeating cell with interior nodes. For convenience, all of the lattices presented hereafter have repeating cells with square surface geometries with symmetric nodal arrangements; therefore a cell is now defined by the number of component cubic cells or in terms of length (e.g., two bays wide). Length is therefore chosen, specifically the number of bays widthwise along an edge of a cell. This will hopefully simplify the description of various lattice geometries. Cells are far more versatile than bays for representing and capturing three-dimensional lattice behavior as will be illustrated in the following lattice examples.

One version of a cantilevered two-bay-wide lattice beam with three rows of longeron surface members is illustrated in Figure 4.9. This geometry is created by combining two three-dimensional Warren lattice beams. By removing the upper two edge rows of longeron members, the lower surfaces center row of

longerons members and selected batten members the lattice geometry is achieved. A deflection equation for the lattice with an end load is presented on Figure 4.9. The repeating cell is highlighted in gray. Note that  $n$  now represents the gray rectangular cell, not one cubic cell, and therefore this equation is only exact for even  $2\ell$  values. This design is weaker than the three-dimensional Warren lattice beam but stiffer than the two-dimensional version. A part count equation is also present for this lattice geometry on Figure 4.9. As can be shown it equals Maxwell's equation. Additionally a maximum member load value equation is presented to illustrate another type of exact lattice derivation. Note this is a linear equation for an end loaded beam.

#### 4.2.4 Summary of Lattice Beams

In conclusion, deflection equations for statically determinate lattice beams have been derived through a fairly simple procedure based on Castigliano's second theorem. Having member loads, the stresses are readily obtained. Due to the simplicity of the deflection derivation, the fundamental question of why this derivation has eluded engineers for so many years comes to mind. One explanation is that this derivation has been presented and somehow over time has been omitted from the general literature. Another explanation is that with an emphasis on closed-form solutions and numerical analyses, these particular derivations are not sought. In either case, the derivations provide a simple highly accurate measure of lattice deflection behavior and is an excellent educational tool for young engineers.

### **4.3 Linear Elastic and Lattice Plate Overview**

Flat linear elastic plates are structures designed to carry load over an area. They are usually designed with two expanding major dimensions, length, and width and one minor constant dimension, depth with a ratio of twenty to one or larger. They are inherently statically indeterminate and their behavior is usually represented mathematically with partial differential equations. Solutions usually involve Fourier series, and Navier [18] conducted initial work and early derivations in 1820.

Flat lattice plates have some of the same characteristics as elastic plates. They are inherently statically indeterminate, and they are designed to expand along two axes. However as with lattice beams, the present theory is not restricted to large length-to-depth ratios because shear terms are explicitly obtained for any value of lattice plate depth. To address the issue of statically indeterminacy, lattice plates are designed with unique geometries. Thereafter, lattice nodal deflection equations are simple to derive and bending and shear terms are easily associated with surface or core members. Lattice deflection equations are obtained by utilization of the statically indeterminate analysis procedures listed in Section 3.6. Hence, some of the following equations are exact and some are approximate. Equivalent linear elastic plate parameters, such as  $D$ , are derived for lattice plates by comparisons to classic linear elastic, closed-form plate deflection equations.

As mentioned, flat lattice plates with uniform geometry are statically indeterminate structures. This is in contrast to lattice beams which can be

designed as statically determinate or statically indeterminate structures. Anderson and Nimmo [20] proposed a method for generating free-free nonuniform lattices derived from a parent Warren lattice geometry. These nonuniform planar lattice designs are built upon statically determinate lattice beams. Collins and Lalvani [21] investigated free-free uniform lattices derived from a parent tetrahedral lattice geometry. They uniformly removed members from the lattice using a trial-and-error process. However, they were unable to isolate a statically determinate geometry for analysis. Lake [5] also investigated this issue and was able to mathematically prove that statically determinate uniform lattices in two dimensions can not be designed. Hence, it has come to be accepted that the design of statically determinate lattice structures in three dimensions is also impossible. Therefore, the design of a statically indeterminate uniformly expanding planar lattice which can be analyzed is a required task.

The Warren and tetrahedral lattice designs presented in Figures 2.2 and 2.3 are two commonly studied highly redundant lattice structures; therefore, they are analyzed herein. Two types of plate studies are conducted on the lattices.

The first study examines plate-like Warren lattices with square geometries. The primary objectives are to obtain analyzable lattice geometries consisting of parallel  $\pm 45$ -degree members and 0,90-degree members, and to generate corresponding deflection equations for both. The second study examines infinitely wide plate-like Warren and tetrahedral lattices. The primary objectives are to generate analyzable rectangular lattice geometries, and to obtain



deflection equations and stiffness parameters. Inherently, all planar lattices are statically indeterminate therefore even component lattices are redundant.

#### 4.3.1 Three-dimensional Warren Lattices with Square Geometries

This study examines plate-like Warren lattices with square planform geometries. A Warren lattice has parallel 0,  $\pm 45^\circ$  and 90-degree members. To study the highly redundant Warren lattice structure required some simplification. Hence, it is assumed that the parent Warren lattice can be treated as a composite laminate consisting of component laminae represented by the parallel surface members of the lattice. With this initial assumption, the Warren lattice is divided into two component lattices: membrane and longeron. The parent Warren planform, membrane and longeron lattices are presented on Figures 4.10. Both planar lattice configurations are similar to the beam configuration presented in Figure 4.5 (a). All sides of both lattices are clamped. A member count equation for the parent lattice is provided below Figure 4.10 (a).

A membrane lattice with parallel lines of  $\pm 45^\circ$ -degree oriented members is shown in Figure 4.10 (c). The membrane lattice is designed by the removal of all upper surface longerons, core battens and the entire lower surface. This geometry is serendipitously derived with the examination of planar Warren lattice permutations where various groups of members are removed. The configuration meets structural criteria, since it has redundant members and a uniform configuration, and analysis criteria, since rational member values can be obtained through analysis.

A longeron lattice with parallel lines of 0,90-degree oriented members is shown in Figure 4.10 (b). The longeron lattice has the same design as the membrane lattice except upper surface diagonal members are removed and all longeron members are retained. Core batten members are also retained. This longeron lattice geometry is also serendipitously derived. The longeron lattice configuration has more redundant members than the membrane lattice, and the configuration also meets structural criteria and analysis criteria.

#### 4.3.1.1 Warren Membrane

Various views of the membrane lattice are shown in Figure 4.11 including center deflection equations for a center applied point load and planar distributed load. The upper surface consisting of parallel rows of  $\pm 45$ -degree members is highlighted on the perspective view. A top view of the lattice showing surface and core members and the four clamped boundary conditions are presented along with a side view. The side view also illustrates the two loading conditions. The lower surface of core members, not shown, has a crimped design since the lower surface has been removed. As mentioned, Figure 4.5 (a) illustrates a two-dimensional version of the three-dimensional geometry shown in Figure 4.11. A typical lattice ring is highlighted in gray,  $n$  represents the number of rings in a lattice design,  $\ell$  represents unit length,  $P$  represents a point load, and  $P'$  represents a distributed load. For example, the lattice shown in Figure 4.11 has three rings and therefore  $n$  equals three. The unit length is usually set at one. A standard unit batten, diagonal or longeron member length helps simplify analyses.

The point-load deflection equation given on Figure 4.11 is of the third order in terms of the number of repeating rings  $n$ . Closed-form solutions for square elastic plates with point loads are hard to generate due to high stress concentrations. However, deflection equations for circular plates with center applied point loads are second order. Therefore, the planar lattice with a point load does not have a comparable linear elastic structure with a closed-form deflection solution. Therefore, plate behavior is investigated by examining load distribution among surface members. After a member-load analysis, it becomes apparent that point loads do not disperse to surrounding diagonal members. Loads stay localized and are transmitted along four straight lines of members to corresponding corners, just as in the two-dimensional beam cases with point loads. This illustrates the lattice's geometric inability to disseminate point loads, and hence the reason for the lattice's third-order beam-like behavior. However, the point load is disseminated among core members and a second-order equation results.

The distributed load deflection equation given on Figure 4.11 is a fourth-order equation in terms of the number of repeating rings  $n$ . Surface load dissemination is inherent due to the distributed load field. The equation corresponds analogously to thin square plate deflection equations. Note, core members also contribute a fourth-order equation similar to the core members of the end loaded beams in Figure 4.5 which contribute a third-order equation.

#### 4.3.1.2 Warren Membrane, Orthotropic

To illustrate the capability and limitations of this procedure for plate-like lattices; a modified Warren or orthotropic lattice with surface members oriented at  $0, \pm 30, 90$  degrees is examined. A  $0, \pm 30, 90$  Warren membrane lattice is illustrated in Figure 4.12. This geometry is a modified version of the previous planar lattice. A typical ring is highlighted in gray. A point load is applied to the center node, and the four lattice edges are clamped. Through analysis, only selected surface member loads can be determined in rational form. However, these are the same members which produced the third-order term for the  $\pm 45$ -degree membrane lattice. The presented third-order equation in Figure 4.12 is generated from these members. As the number of lattice rings increases, the accuracy of the present solution improves. However, even for a ten-bay truss the present solution has significant error. This trend is observed in the finite element results comparison table shown on Figure 4.12.

By comparison, there is an 84-percent difference between the third-order deflection coefficient term of the  $0, \pm 30, 90$  lattice shown in Figure 4.12 and the same term of the  $0, \pm 45, 90$  lattice shown in Figure 4.11. This is due to the different parallel member orientations of the two lattices, and the square geometry of the  $0, \pm 45, 90$  lattice is the square root of two times larger than the rectangular geometry for the  $0, \pm 30, 90$  lattice. Since all of the member loads of the  $0, \pm 30, 90$  geometry are not determined, the lattice may be identified as a limiting geometry. The study of alternative parallel member cases is useful in planar lattice design for strength or stiffness requirements.

#### 4.3.1.3 Warren Longerons

Warren longeron lattice geometry is presented in Figure 4.13. Ring and load definitions previously defined for the membrane lattice are applicable to the longeron lattice. Note, the desired parallel members 0- and 90-degree orientations presented in the top view. Center deflection equations for point and distributed loading are presented in Figure 4.13 below the lattice geometry. A typical lattice ring is highlighted in gray. The point-load deflection equation is a second-order equation in terms of the number of repeating rings  $n$ . This is comparable to a circular plate deflection equation with a point load. Loads are distributed throughout the surface of the lattice due to a point load in contrast to a membrane lattice. Core members also contribute a second-order deflection equation. Thus, the longeron lattice with a point load is stiffer by a polynomial order than the membrane lattice.

The center deflection of the longeron lattice with a distributed load is a fourth-order equation which correlates with the membrane lattice and elastic plate theory. Note the coefficient of the longeron deflection equation with a distributed load is larger than the coefficient of the membrane deflection equation. Longerons weakness is due to core member arrangements. This is determined by examining the core member deflection equations of both lattices. This difference illustrates an inefficient load path through core members due to geometry.

#### 4.3.1.4 Warren Membrane with Cutout

A planar Warren membrane lattice with a centrally located square hole or cutout is presented in Figure 4.14. This example represents some type of lattice damage or cutout for a generic package. If the cutout is not present, as in the previous lattices, stress distributes uniformly through members over the surface. With the cutout present, stress reaches a high value around the cutout or is concentrated. This example highlights the capability of the present analysis procedure over continuum analysis methods in which a continuous surface is required. The cutout is equivalent to one ring of the lattice where  $n$  still represents the actual number of rings in a lattice. For example, the lattice presented in Figure 4.14 has two rings, and therefore  $n$  equals two. Calculated deflection values for point as well as distributed loading represent the nodal displacement under the four arrows shown in the perspective view. The side and perspective views illustrate the four point loads. The order of the deflection equations given in Figure 4.14 are analogous to equations given in Figure 4.11. There is an increase in the third-order coefficient for a point load which is to be expected because of the cutout's weakening effect on lattice stiffness. A similar comparison is made between core members. Increases in member load value around the cutout are not detrimental. The deflection equation for the distributed load case shown in Figure 4.14 is a fourth-order equation, and it is comparable to the analogous equation in Figure 4.10 and the result from elastic plate theory.

#### 4.3.1.5 Warren Longerons with Cutout

A longeron lattice with a centrally located square hole or cutout is presented in Figure 4.15. Again, this example can represent some type of lattice damage or cutout for a generic package. The order of the deflection equations is analogous to equations given in Figure 4.13. There is an increase in the bending third-order coefficient for a point load which is to be expected because of the cutout's detrimental effect on lattice stiffness. A similar comparison can be made between core members. The deflection equation for the distributed load case given in Figure 4.15 is a fourth-order equation, and it is comparable to analogous equation in Figure 4.12.

#### 4.3.2 Summary of Square Three-Dimensional Lattices

The previous examples illustrate a simple way of generating a highly redundant plate-like Warren lattice with a square geometry. The previous examples also illustrate several statically indeterminate lattices which through symmetric loading, geometry and boundary conditions have tractable member loads. This is unique in that previous reports have cast doubt on the probability of obtaining a uniform lattice which can be analyzed using statics. Therefore, the logic hereafter is that closed-form analysis of such uniformly expanding lattices is possible.

Additionally, the previous examples illustrate a simple way of determining and examining the bending stiffness parameters of a highly redundant square lattice plate. The parameters are representative of linear elastic plate stiffnesses. From the examples, the longeron lattice primarily provides elastic

uniform surface plate stiffness for point loads as well as distributed loads. In contrast, the membrane lattice contributes a limited amount of surface radial stiffness for a point load and traditional plate stiffness for a uniform load. Core member stiffness parameters for both component lattices are consistent with classic plate theory. However, for global behavior relative to the parent lattice, they only contribute to shear stiffness, a first-order term.

#### 4.3.3 Three-dimensional Infinitely Wide Planar Lattices

A second study is conducted on the redundant Warren and tetrahedral plate lattices to obtain plate deflection equations and stiffness parameters. To simplify plate analysis, the lattices are idealized and designed as infinitely wide lattice plates experiencing cylindrical bending while subjected to an end load. To acquire cylindrical bending, lattice boundaries consist of one free side, one clamped side and two guided sides. Members on the two guided edges have half of the area of interior members and half the applied load. The lattice, as in the previous study, is divided into two lattices. However, upper and lower surfaces are retained since global bending behavior is being investigated. This is in contrast to the previous square planar lattice study.

##### 4.3.3.1 Warren

A rectangular version of a planar Warren lattice is illustrated in Figure 4.16 which has been modeled as a very long and narrow plate or an infinitely wide plate. Boundary conditions consist of one clamped side, a free opposite side, and two sides with rollers. With a distributed end load applied to the free



edge, the lattice theoretically deforms as a cylindrical surface. These assumptions for design, in effect, eliminate two terms from the governing partial differential equation and yield a beam-like ordinary differential equation. With this equation, a D term or equivalent plate stiffness for a lattice is derived. Two component lattices, a primary Warren longeron lattice and a membrane octahedral lattice, derived from the parent lattice are presented to the right of the parent Warren lattice.

The primary 0,90 longeron lattice is an expanded version of the three-dimensional Warren beam presented in Figure 4.7. Note that both upper and lower surfaces have been retained. Its load transfer behavior is unique in that member loads per row of longeron are uncoupled. Therefore, the lattice uniquely behaves as if its Poisson's ratio equaled zero. The lattice deflection equation due to a uniform end load given in Figure 4.16 is represented by a third-order equation in terms of the number of bays  $n$ . The bending term is identical to the two-dimensional Warren lattice deflection equation. However, shear terms differ due to varying diagonal member arrangements.

The membrane octahedral lattice is located below the longeron lattice on the right of Figure 4.16. It represents the arrangement of parallel  $\pm 45$ -degree diagonal members. Again, note that both the upper and lower surfaces have been retained. This geometry is achieved by removing all longeron and batten members from the parent Warren lattice. The lattice bending loads are coupled and, hence for analysis and rational member loads, square cell geometries have to be generated with increasing lattice width. The resulting

deflection equation is shown below the membrane octahedral lattice. The deflection equation is of the third-order and independent of the lattice width. By inspection, the coefficients of the third-order deflection term equations of the membrane lattice are larger than those of the longeron lattice therefore the membrane lattice is weaker than the longeron lattice due to the arrangements of surface members.

In contrast to the lattices presented in Figures 4.11 and 4.13, both of these lattice deflection equations are of the same order, and both lattices have respective upper and lower surfaces. To derive the redundant lattice deflection equation, these deflection equations are inverted and summed. A simpler example is illustrated in Section 3.6. The resulting redundant planar deflection equation is presented on Figure 4.16 above the parent lattice. With equation (3), a stiffness term  $D$  is generated from the deflection equation terms highlighted in gray. To verify the presented  $D$  value, it is compared to  $D$  terms from earlier lattice reports; and the comparison is presented in a later section of the present paper. The additional terms in the deflection equation are shear terms.

Deflection results generated by the closed-form deflection equation are compared to results generated in EAL for validation of the analysis procedure and generated deflection values. Differences between the present approach and the finite element results occur due to the assumption that the Warren lattice can be decomposed into a Warren longeron lattice and an octahedral lattice with no interaction. Results are presented in the table on Figure 4.16

below the parent lattice. The percent error between the two values is also presented as the number of bays increases from two to 20. The percent error decreases as the number of bays increases; therefore, the procedure and resulting values are validated.

#### 4.3.3.2 Tetrahedral

Tetrahedral lattices are designed in planar rectangular or circular form. Circular hexagonal shapes are desirable as support structures for land or space-based reflectors. Another unique feature is the ability to construct the lattice with equal length members. This geometry is obtained at a planar lattice height of square root of two thirds. The tetrahedral lattice presented in Figure 4.17 is designed with equal length members and a rectangular geometry. The  $0, \pm 60$ -degree tetrahedral lattice is divided into two statically determinate lattices as shown on the right side of Figure 4.17. The primary longeron lattice represents the  $0$ -degree angled members, and the isolated diagonal members represent the  $\pm 60$ -degree membrane lattice.

The tetrahedral longeron lattice is analogous to the Warren longeron lattice. Note, selected surface diagonal members are removed to prevent redundancy. The longeron lattice generates a third-order deflection equation shown on Figure 4.17 similar to the deflection equation obtained for Warren lattices  $0, 90$ -angle lattice. However, the longeron tetrahedral lattice deflection equation also generates a second order moment term, which makes the deflection equation dependent on width on the number of bays in the width direction of  $m$ . This is due to coupling between torsion and bending stiffnesses of this lattice design.

The second  $\pm 60$ -degree membrane lattice also generates a third-order deflection equation. Its deflection equation is independent of plate width. To derive the redundant lattice deflection equation, these deflection equations are inverted and summed with a compatibility requirement. The final deflection equation is presented in Figure 4.17 above the redundant lattice geometry. The width term of the longeron lattice is included in the plate deflection calculation. A bending stiffness term,  $D$  is generated from the terms highlighted in gray and is presented below the deflection equation on Figure 4.17.

#### 4.3.4 Comments on Linear Elastic Plate and Lattice Plate Theory

Both Warren and tetrahedral plate-like lattices are analogous to classic elastic plates. Therefore, both Warren and tetrahedral redundant deflection equations are analogous to classic plate deflection equations. The governing partial differential equation of an elastic isotropic uniform plate with a uniform load is:

$$\frac{\partial^4 w}{\partial x^4} + 2 \frac{\partial^4 w}{\partial x^2 \partial y^2} + \frac{\partial^4 w}{\partial y^4} = \frac{p}{D} \quad (13)$$

Assuming cylindrical bending equation (13) reduces to

$$\frac{\partial^4 w}{\partial y^4} = \frac{p}{D} \quad (14)$$

The solution of equation (14) with an end load is fairly well known and is represented by:

$$w(L) = \frac{pL^3}{3D} \quad (15)$$

By comparing equation (15) to the Warren and tetrahedral deflection equations a  $D$  stiffness value is obtained. Table 4.2 contains a general comparison of the

stiffness terms derived in this study and previously derived stiffness terms. The deflection equations of the parent Warren lattice and the tetrahedral lattice are presented in the top box along with the general stiffness coefficient equations of the Noor, Anderson, and Greene [2], the study of Warren or Hexagonal lattices, and the study by Mikulas, Bush, and Card [1] of tetrahedral lattices. Stiffness parameters for lattices with specified heights are presented in the center box. Since the Warren lattice cell geometry of this study corresponds to the cell geometry of the Noor, Anderson, and Greene study [2], stiffness terms match exactly. The tetrahedral cell geometry between this study, the Noor, Anderson and Greene [2] and Mikulas, Bush and Card [1] do not match. Therefore a length modification is required, subsequent stiffness values match exactly. This validates the present analysis procedure for obtaining stiffness values for planar lattice structures. Additionally, the planar deflection equations have shear stiffness terms which the other studies ignored. Hence, these analysis procedure provides highly accurate measure of static lattice behavior. A general view of each type of lattice cell is presented on Figures 4.16 and 4.17 and at the bottom of Table 4.2.

#### **4.4 Shell-like Overview**

Flat lattice beams and plates have been the focus of this study so far. Now the analysis is extended to curved surface lattices or shell-like lattices. Examples of shells include pressure vessels, airplane wings, pipes, domes and fuel tanks for rockets. Governing partial differential equations for shells usually

have trigonometric solutions, and Kirchhoff and Love derived the relevant equations.

Rings are statically indeterminate beams and therefore are analyzed with energy theorems. The governing differential equation for radial expansion of a thick ring with an internal pressure [22] is presented by

$$\frac{d^2u}{dr^2} + \frac{1}{r} \frac{du}{dr} - \frac{u}{r^2} = 0 \quad (16)$$

The solution of equation (16) where the constants  $A_1$  and  $A_2$  are determined by boundary conditions is given by

$$u = A_1 r + A_2 / r \quad (17)$$

$$A_1 = \frac{(1 + \nu)(1 - 2\nu)}{E} \frac{p_i r_i^2}{r_o^2 - r_i^2}$$

$$A_2 = \frac{(1 + \nu)}{E} \frac{p_i r_i^2 r_o^2}{r_o^2 - r_i^2}$$

In solid mechanics, rings under pressure loads expand due to axial tension and transverse shear stresses.

#### 4.4.1 Two-dimensional Ring-like Lattices

Lattice rings are two-dimensional statically indeterminate structures, and for this study, Castigliano's second theorem is used in conjunction with simple mathematical techniques to determine radial ring expansion equations. Rings are studied because of their simple nonlinear axially symmetric geometries. Lattice ring geometry is simplified by modeling inner and core members with a unit length,  $\ell$ . Outer perimeter member length is a variable (decreases as bay

number increases). Two parent lattice geometries, with square and triangular bays, are studied in cylindrical coordinates  $(r, \theta)$  with uniform pressure loads. Each parent ring is divided into less redundant structures and constrained for radial expansion. With these assumptions, nodal expansion equations are derived.

#### 4.4.1.1 Triangular Bay

The parent triangular bay ring geometry is presented on the top left side of Figure 4.18. It consists of a series of inverted and standard isosceles triangles. The lattice ring is divided into two component lattices with two different loading conditions. A typical repeating bay of a component lattice is highlighted in gray in Figure 4.18 (a). A uniform load applied at the nodes is also presented. The rings in Figures 4.18 (a) and 4.18 (b) are representative of classic thin-walled rings since loads only reside in respective outer and inner surface members. These member loads produce a one over sine squared expansion equation for the radial expansion of a lattice ring with  $n$  bays multiplied by member length as indicated in Figure 4.18. This equation is derived by inspection through simple geometric relationships. Trigonometric functions in contrast to polynomials are generated due to the lattice cylindrical geometry. The exact expansion equation for each lattice is presented adjacent to the respective geometry on Figure 4.18. The ring in Figure 4.18 (c) is representative of a thick ring with transverse shear effects. Its expansion equation is solved using the following steps: (1) isolating a bay; (2) generating a representative stiffness matrix in cylindrical coordinates; (3) applying symmetric

loading conditions; (4) matrix inversion; and, (5) nodal displacement acquisition. The cosine term represents the transverse shear effect in the core members, and the cosine times sine term is associated with axial tension.

#### 4.4.1.2 Square Bay

The square bay lattice ring is presented in Figure 4.19. This lattice is divided into a core member lattice shown in Figure 4.19 (a) and a Vierendeel lattice shown in Figure 4.19 (b). The Vierendeel member loads are calculated by solving three simultaneous equations, while the double-laced lattice member loads are calculated by solving two simultaneous equations as presented on Figure 4.19. Again trigonometric expansion equations result. Note that as bay number approaches infinity, surface and core member loads of the lattice in Figure 4.19 (a) approach infinity, this is representative of a thin-walled ring. In contrast, surface member load values in the Vierendeel lattice shown in Figure 4.19 (b) approach infinity while core member loads approach a constant value. This is representative of a thick ring with transverse shear effects included.

#### 4.4.2 Curved Frame or Statically Determinate Circular Arch

A curved frame is typically a structure which spans an area and acts in bending as a beam with additional force components of transverse shear and axial tension or compression. A circular symmetric curved frame (arch-like) lattice is presented in Figure 4.20. The lattice is pinned on the right end and simply supported on the left end. This lattice is statically determinate. A typical repeating bay, represented by the outer perimeter members, has a unit length of  $l$ . The length of the inner members varies for different  $n$  values. The



curved frame presented on Figure 4.20 has a  $n$  value of 12. A point load is applied to the crown of lattice.

As a result of loading, the lattice incurs compressive loads in outer surface members and tension loads in inner surface members. As with linear beams and plates shear and axial terms are determined explicitly. Since the lattice is statically determinate, exact trigonometric equations for member loads (m.l.) are tractable. Load equations for the lower two outer surface members are presented on Figure 4.20. Exact member load equations become very complex as the number of bays increases. Therefore to acquire a global curved lattice deflection equation due to a point load an approximation equation is derived instead of an exact equation. The derivation of the deflection equation assumes a lattice of many bays. With this assumption cosine terms reduce to rational numbers and sine terms approach zero. A table consisting of outer surface member loads as  $n$  approaches a large value is presented on Figure 4.20. With member loads represented by rational numbers, the deflection derivation procedure of Section 3.5 is utilized to generate a deflection equation. The deflection equation of the curved lattice is presented at the bottom of the figure. Note, that the deflection equation is of the fifth order, and that the traditional solid mechanic curved frame deflection equation is of the third order. The increase of the order of the deflection equation is due to the geometry of the lattice. Note, the single layer of perimeter nodes which is unique in lattice design. The geometric effect is illustrated with an isolated repeating structural unit on the figure where the primary load is uniquely enhanced with the

secondary load condition. Hence, the curved lattice is weaker than the traditional fourth-order frame.

The unique behavior of the curved frame lattice represents a new class of structures referred to as soft lattices. More information on soft lattices with exact solutions will be presented in Section 4.5.

#### 4.4.3 Spheres

Lattice spheres have another type of curved surface, which is of interest for lattice analysis. By definition, a sphere is a three-dimensional surface for which all points of which are equidistant from the center. This definition complicates lattice sphere analysis because only three polyhedron geometries with equal member length exist.

The three polyhedron geometries are presented in Figure 4.21 along with a generic  $n$ -sided lattice where  $n$  is very large. Uniform internal point loads are applied to lattice nodes of the three polyhedron, and EAL results and geometric values are presented in the table on Figure 4.21. The first column lists the number of sides associated with each lattice. The second column lists the member load associated with each lattice, note all member loads are identical. To calculate theoretical member loads of lattices with larger bay numbers, the member load equation, presented on Figure 4.21 is postulated. It is generated by relating the three member loads of the presented polyhedron and the radii, presented in column four of the table. Column five lists the number of members in each lattice and column six lists the number of vertices. Both are used along

with the member load to derive a spherical expansion displacement equation. The resulting equation is highlighted in gray. To validate the expansion equation, a comparison is made between an infinite  $n$ -sided lattice and a linear elastic sphere with an internal pressure load. Poisson's ratio is assumed to be one third [1]. Resulting lattice and solid mechanic terms are comparable and provide some insight into the behavior of a spherical lattice with uniform internal point loads.

#### **4.5 Soft Plate-like Lattices in Three-dimensions Overview**

The fourth group consist of uniquely designed cantilevered planar lattices in three dimensions. Lattice behavior so far has been analogous to traditional elastic structures such as beams and plates. Even shell-like lattices have analogous structures in solid mechanics and predictable linear elastic expansion behavior. If Figure 4.9 is revisited, and the removal of more members is initiated, behavior unique to pinned soft lattice structures occurs.

##### **4.5.1 Sixth-Order with Surface Longerons**

A cantilevered modified two-bay wide lattice with a top surface of two rows of longerons and battens is shown in Figure 4.22. The lower surface consist of a  $\pm 45$ -degree arrangement of diagonal members; diagonal core members separate the two surfaces. The repeating cell has been isolated for observation, and another one is highlighted in gray. This lattice has an end load applied to the five exterior nodes. After analysis, a fifth-order term arises in the deflection equation as given in Figure 4.22 due to the diagonal members.

This is unique in that traditional end loaded cantilevered beam deflection equations are of the third order. However, examination of the lattice cross section, in contrast to the Warren beam presented in Figure 4.7, illustrates a very weak geometry for load transfer in bending. In general, a cantilevered elastic beam deflects downward while widthwise cross-sections remain plane and rotate. To contrast, a cantilevered soft sixth-order lattice geometry induces artificial side moments along the lengthwise edges which inwardly warp the lattice and create an exaggerated Poisson's ratio effect. Hence, nodes deflect downward, widthwise cross sections remain plane and rotate, and lengthwise edge nodes rotate inward. This additional rotation leads to the addition of a fifth-order deflection term. To parallel fourth-order beam theory in solid mechanics, lattices with fifth-order deflection equations due to an end load are referred to as soft sixth-order lattices. An equation for the number of members is also presented in Figure 4.20. Note, Maxwell's equations are satisfied.

#### 4.5.2 Sixth-Order Consisting of Diagonals

The removal of the two remaining rows of longeron members and batten members and associated nodes, gives a lattice of the configuration in Figure 4.23. This lattice consist solely of diagonal members. A repeating cell is isolated for observation and is highlighted in gray on the top view shown in Figure 4.23. It also has a fifth-order bending term in the deflection equation due to the geometry of upper and lower diagonal surface members. Again, the fifth-order deflection equation is generated due to induced side moments which in turn produce an exaggerated Poisson's ratio effect. A deflection equation for

loading in the x-y plane is also presented in Figure 4.23. Note that this lattice deflection equation is of the third order. Therefore, soft lattices presented herein have a weak axis and a traditional beam-like stiff axis.

Work on additional designs of soft lattices is presented next to illustrate the capability of the strain energy analysis and to better understand soft lattice mechanics. Note that cross sections of the soft lattices remain plane during loading and that if the sides of the lattices are simply supported a third-order deflection equation results.

#### 4.5.3 Sixth-Order Symmetric

The next soft lattice is designed with a symmetric geometry and a neutral load plane. The lattice and associated deflection equation for an end loaded lattice is presented in Figure 4.24. The lattice geometry is four bays wide and two bays deep. Note, the core member geometry has changed to consist of perimeter diagonal members. One cell is isolated and selected parts are shown. Another cell is highlighted in gray on the top view. The repeating cell consist of four cubes of diagonal surface members with a midplane of longeron members. During loading midplane longeron, member loads are eliminated as anticipated and an exaggerated Poisson's ratio effect occurs as in the previous examples. Top surface member loads and bottom surface loads are identical. With the determination of the neutral load plane and a symmetric geometry, loads can be applied uniformly and behavior is quantified in a truer sense, in contrast to the asymmetric soft lattices shown in Figures 4.22 and 4.23.

#### 4.5.4 Sixth-Order Symmetric Soft Lattices With Distributed Load

Next, the soft symmetric lattice is examined with a distributed load. The deflection equation for nodal deflection along the length of the lattice is presented in Figure 4.25. The deflection equation is of the sixth order due to the same factors of previous lattices. One way of investigating the associated governing differential equation of the lattice is by differentiating the displacement equation six times. Differential equations are of interest for lattice buckling or vibration behavior.

#### 4.5.5 Eighth-Order

Another asymmetric soft lattice is derived by removing the bottom half of the symmetric soft lattice and expanding by two bays. This lattice is six bays wide and one bay high. The repeating cell of this lattice and associated deflection equation for an end load are presented in Figure 4.26. With a uniformly distributed end load, this lattice exhibits seventh-order deflection behavior due to the geometry of the top surface diagonal members. This behavior is a result of the top  $\pm 45$ -degree and bottom  $0, 90$ -degree member orientations which induce side moments and widthwise axial compression. Therefore, a seventh-order deflection equation results. An eighth-order equation is presumed to occur for a distributed loading case. Again, to parallel fourth-order beam theory in solid mechanics, lattices with seventh-order deflection equations due to an end load are referred to as eight-order lattices.

#### 4.5.6 Eighth-Order, Clamped On Two Sides

The last soft lattice is designed to illustrate softness along the width of a lattice in contrast to the length. The lattice geometry and repeating cell are shown in Figure 4.27. It is derived from the previous lattice by removing batten members from the lower surface and expanding by two bays. The core member geometry is also changed back to the corrugated style of the planar Warren lattice. Therefore, the lattice is eight bays wide, one bay deep, and has the traditional corrugated core member arrangement as shown in Figure 4.23. The lattice has a  $\pm 45$ -degree top surface and single rows of longeron members on the bottom surface. Hence, the bottom surface is the weakest component of the lattice. Member load values are not deterministic with the application of a distributed end load. However with the application of two opposing point loads as illustrated or by constraining the neutral vertical nodes of the x-z plane, member load values are obtainable. The resulting seventh-order deflection equation is presented in Figure 4.27. To appreciate the softness of this lattice note that classic beams, and the previous fifth- and seventh-order lattices have first-order torsional equations. Note, with the removal of batten members from the lower surface lattice loads have to travel the length of the lattice in contrast to traveling to the closer constrained side. With a seventh-order deflection equation for a point loaded lattice with two constrained sides, a cantilevered version potentially requires a very high-order polynomial equation to capture bending behavior.

#### 4.5.7 Overview of Soft Lattice Displacement Fields

The derived soft lattice behaviors are compared and summarized on Figure 4.28. Classic two-dimensional beam theory dictates that beams deflect and rotate due to vertical loading. This is illustrated in Figure 4.28 (a). The lattice geometries presented in Figures 4.22 through 4.25 experience an additional inward rotational degree of freedom due to loading. This behavior is illustrated in Figure 4.28 (b). This effect occurs in the x-z longitudinal, lengthwise plane of symmetric or asymmetric lattices. Stiffness remains of the third order on the opposite axis and of the first order during axial loading. With a modification to the lattice presented in Figure 4.25, the lattice presented in Figure 4.26 is achieved. This lattice is unique in that it has a seventh-order bending term due to an addition of z-axis compression as a result of load. Deflection, rotation, and inward rotation behavior are still present as in the previous lattices. All nodal behaviors are presented for this lattice in Figure 4.28 (c). The seventh-order bending lattice is the last lattice where a bending equation is derived. To further illustrate lattice softness design a lattice is examined in torsion. Seventh-order equations result, in contrast to first-order equations for previous designs. This illustrates a severe weakness in torsion and presumably also in bending. The two constrained sides and lattice behavior are presented in Figure 4.28 (d).

#### 4.5.8 Soft Lattice Mechanics

In order to gain more insight into soft lattice mechanics, related geometric deformation relations are discussed. Strain energy expressions are utilized to



derive deflection equation throughout this paper. Three-dimensional strain-displacement relations reduce to the following set of two-dimensional relations for planar material

$$\epsilon_x = \frac{\partial u}{\partial x} \quad (18a)$$

$$\epsilon_y = \frac{\partial v}{\partial y} \quad (18b)$$

$$\epsilon_z = \frac{\partial w}{\partial z} = 0 \quad (18c)$$

$$\gamma_{xy} = \frac{\partial u}{\partial y} + \frac{\partial v}{\partial x} \quad (18d)$$

$$\gamma_{xz} = \frac{\partial w}{\partial x} + \frac{\partial u}{\partial z} = 0 \quad (18e)$$

$$\gamma_{yz} = \frac{\partial w}{\partial y} + \frac{\partial v}{\partial z} = 0 \quad (18f)$$

Note these expressions are also referred to as the kinematic relations [12].

These expressions are valid for soft lattice structures. To gain insight into bending behavior Equations (18e) and (18f) are integrated giving

$$u = -z \frac{\partial w}{\partial x} \quad (19 a-b)$$

$$v = -z \frac{\partial w}{\partial y}$$

These strain displacement equations are invalid for soft lattice structures.

Hence, the difference between elastic materials and soft lattices is identified.

This leads one to postulate that soft lattices uniquely represent the material zone between membranes which have in-plane stiffness and no out-of-plane stiffness and plates which have in-plane stiffness and out-of-plane fourth-order bending stiffness.

#### 4.5.9 Comments on Current and Theoretical Soft Lattices

Table 4.3 lists some key features and future work associated with soft lattices relative to composite theory. Composite theory is one of many ways of describing the surface member orientation of soft lattice cells. Note lattice behavior is not being compared to composite behavior; however, some type of relationship is desired between member orientation and higher-order deflection equations.

A traditional lattice with parallel members oriented at  $0, \pm 45, 90$  degrees is presented in row one of Table 4.3. A fourth-order deflection equation results with distributed load. In composite theory, such lamina ply arrangements form an antisymmetric angle-ply laminate. By definition, an antisymmetric angle-ply laminate has laminae oriented at  $+\alpha$  degrees to the laminate coordinate axes on one side of the middle surface and corresponding equal thickness laminae oriented at  $-\alpha$  degrees on the other side.

A soft lattice with  $\pm 45$ -degree surface member angles is presented in row two, where a sixth-order deflection equation results with distributed load. Such lamina ply arrangements are also create an antisymmetric angle-ply laminate.

Additionally in the third row, a soft lattice with  $\pm 45$ -degree upper and 0,90-degree lower member angles is presented. This geometry is quasi-isotropic (with member areas properly balanced as in Ref. [5]) and defined as antisymmetric angle-ply laminate. The term quasi-isotropic is used to describe laminates that have essentially isotropic extensional stiffnesses, all in the same directions. The next lattice geometry has  $\pm 45$ , 90-degree member arrangements. This type of composite laminate is described as a symmetric angle-ply laminate. A symmetric angle-ply laminate exhibits no coupling between bending and extension therefore  $B_{ij}$  terms equal zero. A deflection equation for bending load is not presented for this lattice due to difficulty in generating rational member loads. Whether this is due to the symmetric geometry, in contrast to the antisymmetric geometry of previous lattice geometries, is unknown. The  $\pm 45$ , 90-degree lattice geometry is derived by rotating the previous lattice by 90 degrees and adding sufficient bays. A zero angle lattice and a 0, 90-degree lattice are theoretically created by modifying the  $\pm 45$ , 0 and  $\pm 45$ , 90-degree lattices. The acquisition of rational member loads is an uncertainty. However, these are the limiting cases for lattices since single-layer lattices are not kinematically stable. To conclude, Table 4.4 is presented as a guide of the present study and for future work on soft lattices. Just as in two-dimensions, a fourth-order deflection equation for uniform loading is the limiting case; and a similar limiting case should exist for three-dimensional lattice structures. The derivation of this limiting case is of great interest for the study of lattices and three-dimensional linear elastic materials.

Symmetric laminates are desirable for several reasons. First,  $B_{ij}$  terms equal zero eliminating coupling between bending and extension. Second, symmetric laminates do not have a tendency to twist from thermally induced contractions that occur during cooling following the curing process.

In contrast, many physical applications of laminated composites require nonsymmetric laminates to achieve design requirements. For example, coupling is necessary to manufacture jet turbine fan blades with pretwist, and coupling is desired for heat shields which are heated on only one side to prevent warping [11].

#### **4.6 Vibration Overview**

The natural free vibration behavior of some lattice structures (e.g., antennas, solar arrays) is of great interest because these systems are designed to be lightweight and to incur low or minimal loads. The following vibration examples are simple but provide insight into lattice axial and ring vibrational behavior. Additionally, the domain of the analysis is extended from exact strain energy analysis to exact kinetic energy analysis.

##### **4.6.1 Rods**

Exact eigenvalues are obtained for fixed-end, rod-like lattices and presented on Figure 4.29. The lattices are analyzed as discrete systems with an axial degrees of freedom and point masses at the nodes. For this free harmonic vibrational study, one lattice member is represented by a two by two stiffness matrix and a two by two lumped mass matrix. The analyses consist of

generating a global stiffness and mass matrix, characteristic equation, and the associated eigenvalues. A series of exact eigenvalues are calculated this way for lattices with two, three and more members. Eigenvalues are presented for lattices with two, four, and eight members on Figure 4.29. Through observation a recurrence relationship for these eigenvalues and higher multiples of two is presented. Likewise, a similar relationship exist for lattices with three, nine, 27, and higher multiples of three members. The recurrence relationship enables the prediction of higher eigenvalues without solving higher  $n$ -th-order characteristic equations, and they provide some insight into the vibrational behavior of lattices. The Young's modulus multiplied by area and divided by length ratio, represented by  $\mathbf{a}$  on Figure 4.29 is a variable, for simplicity mass is a constant.

A rod-like lattice with two fixed ends is also examined and presented on Figure 4.29. Eigenvalues are presented for lattices with four, and eight members. The eigenvalues of the four member lattice equal the eigenvalues of a lattice with two members and one fixed end. The third eigenvalue is  $\mathbf{a}$ , the material and geometry parameter. The eigenvalues of the eight member lattice equal the eigenvalues of the two and four member lattices and  $\mathbf{a}$ . Therefore a rod lattice with two fixed ends and  $n$  members generates all previous eigenvalues of lattices with one fixed end. With this observation, a recursion relationship is presented for eigenvalues as a function of two times the number of members plus one on Figure 4.29.

#### 4.6.2 Lattice Beams

The lattice vibration study is continued by investigating the axial vibration of the quadrangular and Warren lattice beams with one side fixed. Batten members are removed from both lattices. Both lattices are presented in Figures 4.30 (a), and (b). Eigenvalues and the recursion relationship generated by the quadrangular lattice beam are identical to the rod-like lattice when the number of bays equals the number of members. Repeating eigenvalues consisting of the material and geometry parameter are also generated; they are a result of the diagonal members. Eigenvalues for four, eight and 16 bay configurations are presented along with the recursion relationship on Figure 4.30.

The Warren lattice also generates eigenvalues and a recursion relationship identical to the rod-like lattice. However, diagonal members generate an additional series of rod-like values, where the material and geometry coefficient is divided by two. Note, lattice behavior is derived with specific material and geometric properties, listed at the bottom of Figure 4.30.

#### 4.6.3 Lattice Ring

The natural extensional vibration of a ring is another simple one dimensional problem encounter in the study of material behavior. The studied lattice ring is presented in Figure 4.31. Ring boundary conditions, and member length assumptions remain the same. The first mode of vibration for a lattice ring is uniform expansion or contraction. Since a ring consists of repeating bays each bay's nodal radial displacement is identical. Therefore, the analysis of one bay for extensional vibration represents the analysis of the lattice ring. A selected

bay highlighted in gray consisting of three members is presented in Figure 4.31. To analyze the lattice bay, outer member lengths are represented by trigonometric functions. Core members have an assumed length of one unit. A three by three stiffness matrix is derived for the three members in cylindrical coordinates, and a lumped mass matrix is also formulated. A characteristic equation is calculated from the stiffness and mass matrix. The lowest solution of the characteristic equation represents the first eigenvalue of the lattice ring for n-bays. This eigenvalue equation is presented in Figure 4.31. Associated parameters are also defined. The equation is analogous to a classic ring vibration equation, in contrast to the lattice rod recursion relationships. A table of lattice ring parameters and results are presented due to the complexity of the eigenvalue equation. A similar equation can be derived for a circular lattice with square bays. Note, that a lattice of six bays has a higher frequency than one of four bays due to geometry.

## **CHAPTER V**

### **FINITE ELEMENT FORMULATIONS FOR SOFT LATTICES**

#### **5.1 Overview**

The finite element method is a common and computationally useful numerical method for solutions of complex structural problems. The method simplifies structures which may include beams, plates and/or shells into discretized elements and represents them mathematically by matrices. Beam and frame elements are presented in Figure 5.1 above their respective finite element matrix representations.

Elastic and lattice beams have previously been defined. In the method of finite elements a beam is represented by a horizontal element with two nodes. Each node has two degrees of freedom, displacement and rotation. Hence, the finite element matrix representation is a four by four matrix. Since one beam element only has two nodes, several beam elements are utilized to represent true structural behavior under distributed or combined loadings. Shear terms are usually not included in the basic matrix derivation.

Frame elements are similar to beam elements in that they have two nodes which deflect and rotate. Additionally frames have axial deformation and varied rotational orientations. This angle is represented by  $\alpha$  on the figure. Hence, the finite element matrix representation is a six by six matrix. Again



since one frame element only has two nodes, several frames are utilized to represent true structural behavior.

The displacement finite element formulation of a linear elastic beam or frame consist of four basic steps: 1.) discretization of the structural domain; 2.) derivation of variational formulation from governing differential equations; 3.) derivation of shape or interpolation functions between element nodes; and, 4.) generation of stiffness and force matrices. To initiate Step 2, a selected lattice displacement equation has to be differentiated to generate a governing differential equation. However, this step eliminates lower order terms and the  $n$  variable. To retain these terms and maintain the studies emphasis on exactness, another finite element formulation is utilized.

## **5.2 Exact Soft Finite Element Matrix Formulation**

The following three steps outline an exact lattice finite element matrix formulation. First, a lattice displacement equation is derived for every degree of freedom, boundary condition and load condition desired. These equations are grouped to form a vector. Second, a vector consisting of the three applied loads is factored from the displacement equations. Third, a stiffness matrix is generated by inverting the lattice equation matrix. These three steps are utilized in deriving a representative stiffness matrix for a fifth-order cantilevered lattice beam with an end load. The previously mentioned three steps relative to the beam are presented in Figure 5.2. The exact displacement matrix for vertical displacement, widthwise rotation, and lengthwise rotation is presented at the top of the figure. The center matrix contains a truncated displacement

matrix where lower order terms are not used for brevity. Next, a load vector is factored off of the displacement equations. The displacement matrix is inverted and presented in Figure 5.2 (c) as the K-stiffness matrix of a soft cantilevered beam. The formulation presented in Figure 5.2 (c) is analogous to the gray highlighted lower right hand quadrant of the global beam element stiffness matrix presented in Figure 5.1.

The lattice beam stiffness matrix presented in Figure 5.2 (c) is transformed into a local frame matrix with the addition of an axial stiffness value and presented as matrix  $k'$  at the top of Figure 5.3. The local frame matrix is transformed into a global frame matrix through the use of a transformation matrix,  $L$ . This step is illustrated in the middle of Figure 5.3. The resulting global lattice frame matrix is presented at the bottom of Figure 5.3. This matrix formulation is analogous to the gray highlighted lower right hand quadratic of the frame element presented in Figure 5.1. Notice that  $n$  values have been retained and that through this formulation as many displacement terms are retained in the original displacement matrix as desired for accuracy. This element derivation validates the present formulation assumptions and provides new insight into lattice behavior under combined loading.

### **5.3 Sixth-order Verification**

The soft lattice beam-like and frame-like finite element matrixes presented in Figure 5.3 are verified by comparison to exact results generated by EAL as given in Table 5.1. Three test cases are presented for  $n$  values of two, five, and

ten. An  $n$  value of two verifies shear behavior while an  $n$  value of ten verifies bending behavior. The four variables of interest are vertical deflection along the  $z$ -axis, traditional rotation in the  $x$ - $z$  plane, inward rotation in the  $y$ - $z$  plane, and axial displacement along the  $x$ -axis.

The first test case is representative of a cantilevered soft beam with a vertically applied end load. The end load has a magnitude of one unit. Matrix generated deflection,  $x$ - $z$  rotation and  $y$ - $z$ -rotation values are presented in the top table of Table 5.1. In addition, values generated by EAL are also presented. The percent error between values represents the error in the matrix coefficients. In bending, percent errors range from three point six percent for two bays to zero for ten bays. Therefore, matrix solutions for bending due to an end load are validated. For rotation in the  $x$ - $z$  plane, errors range from one point one to zero. Hence, matrix solutions are validated, and similar results occur for rotation in the  $y$ - $z$  plane.

The second case represents a cantilevered beam with combined loads in the three degrees of freedom. The combined loads consist of a ten unit vertical load, a ten unit rotational torque and a ten unit widthwise torque. Similar to the end loaded lattice, the percent errors between matrix and EAL generated values for combined loads are acceptable for bending, and both rotations as given in Table 5.1. However, the percent error between axial extension values slightly increases as the number of bays increases. This is due to an inexact calculation for axial displacement. Horizontal, longeron members are stressed during axial loading; in contrast, during bending and rotation they lie on a

neutral plane. To lessen the error a displacement analysis similar to the axial displacement problem presented in Section 3.6 would have to be conducted.

The last case represents a frame-like soft lattice oriented at forty-five degrees with an end load. The end load is applied in the vertical direction and has a magnitude of ten units. Again generated percent errors between results obtained using the present matrix formulation and results obtained using EAL decrease as the number of bays increases (see Table 5.1). Initial error values are largely due to an increase in shear loads due to the forty-five degree angle.

## **CHAPTER VI**

### **CONCLUSIONS AND RECOMMENDATIONS**

#### **6.1 Overview**

Structural evaluation of lattices, Warren and tetrahedral, using energy methods is a comprehensive study of the behavior of four groups of lattices with pin-connectors. Finite elements are used to generate the lattice models. Lattice geometric parameters include cell geometry, symmetry, topology, and redundancy. Energy methods, Castigliano's theorems, are used to generate exact member loads and nodal displacement values which greatly enhance the study and quantification of lattice structural behavior. With exact displacement values and extrapolation functions, exact lattice governing displacement equations are obtained as functions of the repeating cell number. Deflection equation coefficients for bending are used as lattice stiffness or strength parameters.

To reiterate, the specific objectives of this research are: 1.) to develop simple closed-form exact deflection and vibration equations using Castigliano's second theorem over the nodal domain of uniform lattice structures; 2.) to develop expressions for highly redundant lattice structures by using compatibility requirements; 3.) to develop truss geometries which under uniform loading exhibit sixth-and eighth-order behavior for deflection; and, 4.)

to develop associated finite element stiffness matrices and validation procedures.

## **6.2 Conclusions**

The use of strain and kinetic energies to achieve the four objectives have been demonstrated by numerous examples. On the foundation of those examples the following conclusions are drawn. First, closed-form deflection and eigenvalue equations for statically determinate lattice beams consist of exact third-and fourth-order polynomial functions in bending and lower order polynomial terms in shear for static analysis and exact recurrence relations for free vibrational analysis for  $n$  lattice bays. Second, after generating a uniform redundant lattice geometry, lattice deflection equations and stiffness values are consistent with linear elastic plate theory. Third, lattice geometries which exhibit sixth, eighth, and higher order deflection equations are generated by expanding the width of a lattice beam and removing redundant members. Deflection equations are derived by increasing the order of the polynomial interpolation function. Finally beam- and frame-like matrix derivations for a fifth-order soft lattice maintaining  $n$ -bay and shear terms are validated through comparison to EAL finite element results.

## **6.3 Recommendations**

Future work on lattice structures parallel material and solid mechanics work. Work on lattice vibration analysis could be expanded to include buckling analysis. Work could continue on the effects of cutouts on lattice stiffness.

Thermal effects on lattices are also of interest. All of the previous concerns could be applied to the study of soft lattices. Hence, there potentially exist a wide and broad spectrum of work to be done on lattice structures.

## **REFERENCES**

1. Mikulas, Martin M., Jr.; Bush, Harold G.; and Card, Michael F.: Structural Stiffness, Strength and Dynamic Characteristics of Large Tetrahedral Space Truss Structures. NASA TM X-74001, 1977.
2. Noor, Ahmed K.; Anderson, Melvin S.; Greene, William H.: Continuum Models for Beam- and Plate-like Lattice Structures. AIAA/ASME 19th Structures, Structural Dynamics and Material Conference, Bethesda, Md., April 3-5, 1978.
3. Nemeth, Michael P.: Continuum Models for Repetitive Lattice Structures with Rigid Joints, Master's Thesis, George Washington University, 1979.
4. Noor, Ahmed K.; and Mikulas, Martin, Jr.: Continuum Modeling of Large Lattice Structures - Status and Projections. NASA TP 2767, February, 1988.
5. Lake, Mark S.: On the Analysis and Design of Uniform Truss Structures, Doctoral Dissertation, North Carolina State University, 1992.
6. Collins, Timothy J.; Fichter, W. B.; Adams, R. R.; and Javeed, M.: Structural Analysis and Testing of an Erectable Truss for Precision Segmented Reflector Application. NASA TP 3518, July, 1995.
7. Neyfeh, Adnan H.; and Hefzy, Mohamed Samir: Continuum Modeling of Three-Dimensional Truss-Like Space Structures, AIAA Journal, Vol. 16, No. 8, August, 1978, pp. 779-787.
8. The Encyclopedia America-International edition, Grolier Incorporated, 1991, p.180.
9. Timoshenko, Stephen P.; and Young, D. H.: Theory of Structures. McGraw-Hill Book Co., 1965.
10. Shames, Irving H.; and Dym, Clive L.: Energy and Finite Element Methods in Structural Mechanics. Hemisphere Publishing Corporation, 1985.



11. Jones, Robert M.: **Mechanics of Composite Materials**. McGraw-Hill Book Co., 1984.
12. Ugural, A. C.: **Stresses in Plates and Shells**, McGraw-Hill Book Co., 1981.
13. Chandrupatla, Tirupathi R.; and Belegundu, Ashok D.: **Introduction to Finite Elements in Engineering**, Prentice-Hall, Inc., 1991.
14. Reddy, J. N.: **An Introduction to the Finite Element Method**. Second Edition, McGraw-Hill, Inc., 1993.
15. Cook, Robert D.; Malkus, David S.; and Plesha, Michael E.: **Concepts and Application of Finite Element Analysis**. Third Edition, John Wiley & Sons, Inc. 1989.
16. Whetstone, W. D.: **EISI-EAL Engineering Analysis Language Reference Manual-EISI-EAL System Level 2091**. Volume 2: Structural Analysis-Primary Processors. Engineering Information Systems, Inc., July, 1983.
17. Jastrzebski, Zbigniew D.: **The Nature and Properties of Engineering Materials**. John Wiley & Sons, Inc., 1976.
18. Timoshenko, Stephen P.: **History of Strength of Materials**. Dover Publications, Inc., 1983.
19. Sutter, Thomas R.; and Bush, Harold G.: **A Comparison of Two Trusses for the Space Station Structure**. NASA TM 4093, March, 1989.
20. Anderson, M. S.; and Nimmo, N. A.: **Dynamic Characteristics of Statically Determinate Space-Truss Platforms**. AIAA Journal of Spacecraft and Rockets, Vol. 23, No. 3, May-June, 1986, pp. 303-307.
21. Collins, Timothy J.; and Lalvani, Haresh: **Generation and Analysis of Reduced-Part-Count Truss Structures for Spaced-Based Applications**. AIAA Paper No. 91-1193, Presented at the AIAA/ASME/ASCE/AHS/ASC 32nd Structures, Structural Dynamics and Materials conference, Baltimore, Maryland, April 8-10, 1991.
22. Popov, Egor P.: **Engineering Mechanics of Solids**. Prentice-Hall, Inc., 1990.
23. Wolfram, Stephen: **Mathematica - A System For Doing Mathematics by Computer**. Addison-Welsey Publishing Company, Inc., 1988.

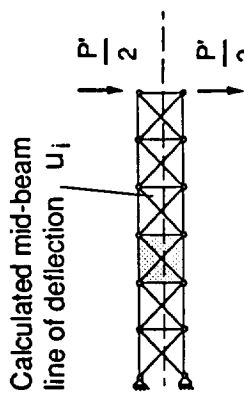
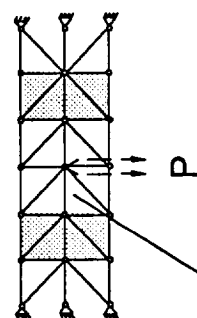
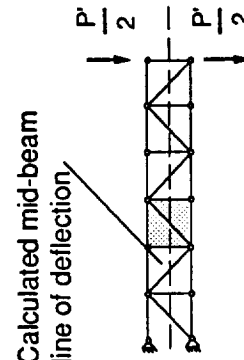
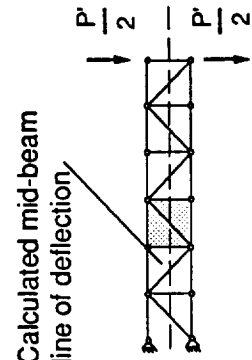
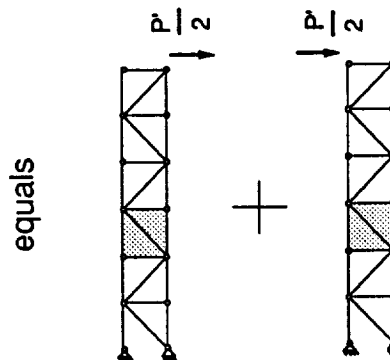
 <p>Calculated mid-beam line of deflection <math>U_i</math></p> <p>does not equal</p> 	 <p>Calculated mid-beam line of deflection <math>\delta_i</math></p>	 <p>Calculated mid-beam line of deflection <math>U_i</math></p> <p>equals</p> 
Statically determinate	Statically Indeterminate	Statically Indeterminate
Deflection principle - method of superposition	Deflection principle - Castiglione's second theorem	Deflection principle - Principle of complementary energy
The method of superposition states that the deflection at any point in a beam is equal to the sum of deflections caused by each load separately.	$\delta_i = \frac{\partial U}{\partial P_i}$	$U_1 = \int \int_V \epsilon_{ij} \delta \tau_{ij} dv$

Table 4.1. Neutral axis deflection principles.

	Derived equation and coefficients	
	Hexagonal	Tetrahedral
Mikulas, Bush, Card	n.a.	$\frac{\sqrt{3}}{4} EA$
Noor, Anderson, Greene	$3 \frac{\sqrt{3}}{16} \frac{h^2}{L} (E_1 A_1 + E_2 A_2)$	$\frac{h^2}{4L} \left(1 + \frac{1}{2\sqrt{2}}\right) (E_1 A_1 + E_2 A_2)$
Present study	$y(n) = \frac{P\ell}{EA} \left[ \frac{8\sqrt{2}n^5 + 96n^3 + 26\sqrt{2}n^3 + 264n + 11\sqrt{2}n}{6n^2 + 12\sqrt{2}n^2 + 3 + 69\sqrt{2}} \right]$	$y(m,n) = \frac{P\ell}{EA} \left[ \frac{3456n^5 + 11208n^3 + 24m^2n^3 + 8m^2n^2 + 3352n}{3888n^2 + 3m^2 + 2409} \right]$

Stiffness value D	Hexagonal $L=1; H=1$	Tetrahedral $L=1; H=.8165$	Tetrahedral $L=1.155; H=.8165$
Mikulas, Bush, Card	n.a.	$\frac{\sqrt{3}}{4} EA$	n.a.
Noor, Anderson, Greene	$\left( \frac{4 + \sqrt{2}}{8} \right) EA$	$\frac{\sqrt{3}}{4} EA$	$\left( \frac{3}{8} \right) EA \quad L=1.155$
Present study	$\left( \frac{4 + \sqrt{2}}{8} \right) EA$	n.a.	$\left( \frac{3}{8} \right) EA \quad L=1$

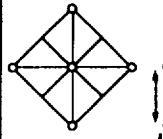
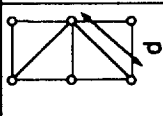
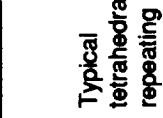
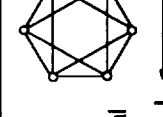
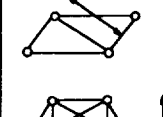
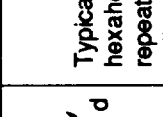
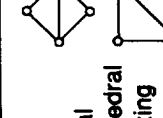
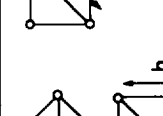
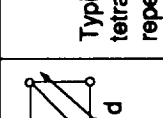
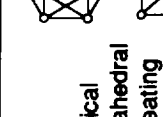
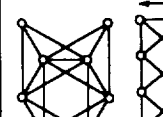

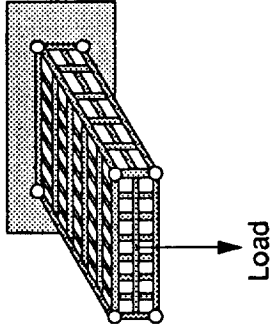
 Typical hexahedral repeating cell	 Typical tetrahedral repeating cell	 Typical hexahedral repeating cell	 Typical tetrahedral repeating cell	 Typical hexahedral repeating cell	 Typical tetrahedral repeating cell	 Typical hexahedral repeating cell	 Typical tetrahedral repeating cell	 Typical hexahedral repeating cell	 Typical tetrahedral repeating cell	 Typical hexahedral repeating cell	 Typical tetrahedral repeating cell
Mikulas, Bush, Card and Noor, Anderson, Greene Studies											
Present study											

Table 4.2. Elastic coefficients for tetrahedral and Warren (hexahedral) plate-like lattices.

Cell member orientation		Order of deflection equation (distributed load)	Presented lattices and comments on other designs	Relative to composite theory
Surfaces				
Upper	Lower			
0/±45/90	0/±45/90			
±45	±45	fourth	Geometry (quasi-isotropic) and equation	Antisymmetric angle-ply lattices
		sixth	Geometry and equation	Antisymmetric angle-ply lattices
±45	0/90	eighth	Geometry (quasi-isotropic) and equation	Antisymmetric angle-ply lattices
±45	0	unknown	Geometry and related equation	Symmetric angle-ply lattices
±45	90	unknown	Geometry derivable, ±45/0	Bij = 0
0	0	unknown	Theoretical geometry	Single orthotropic layer
0	90	unknown	Theoretical geometry	Antisymmetric cross-ply lattices

Table 4.3. Summary and prediction of soft lattice performance in three-dimensions.



Polynomial order of derived equation									
		2-Dimensional Elasticity			3-Dimensional Elasticity				
Load		bending			bending			torsion	
		point	distributed		point	distributed		point	
Group 1	Beams	3rd	4th		3rd	4th		1st	
	Plates			n.a.	2nd, 3rd	4th		n.a.	
Group 2	Highly redundant lattice plates			n.a.			3rd		n.a.
Group 3	Rings (expansion)	Trigonometric functions			n.a.			n.a.	
Group 4	Soft	n.a.			5th, 6th and 7th			n.a.	7th

Type of vibration equation	
Free vibration	2-Dimensional Elasticity
rods	recursion relationship
rings	classic square root of stiffness over mass

Table 4.4. Outline of study derived equations.

Case 1 (beam-like lattice, end load)									
n bays	Bending			Rotation-y			Rotation-x		
	EAL	matrix deriv.	% Err.	EAL	matrix deriv.	% Err.	EAL	matrix deriv.	% Err.
2	.524 -4	.505 -4	3.6	.145 -4	.147 -4	1.1	.208 -5	.189 -5	9.4
5	.38 -2	.376 -2	1.1	.463 -3	.463 -3	.03	.299 -4	.294 -4	1.5
10	.115	.115	.0	.715 -2	.715 -2	.0	.237 -3	.236 -4	.7

Case 2 (beam-like lattice, combined loading)									
n bays	Bending			Rotation-y			Rotation-x		
	EAL	matrix deriv.	% Err.	EAL	matrix deriv.	% Err.	EAL	matrix deriv.	% Err.
2	.644 -3	.671 -3	4.	.191 -3	.18 -3	6.	.261 -4	.277 -4	6
5	.422 -1	.425 -2	.7	.519 -2	.526 -2	1.2	.339 -3	.343 -3	1.4
10	1.22	1.22	0.	.761 -1	.764 -1	.4	.253 -2	.254 -2	.4
							Axial-Extension		
							EAL	matrix deriv.	% Err.
2							.224 -5	.22 -5	1.8
5							.564 -5	.55 -5	2.5
10							.113 -4	.11 -4	2.7

Case 3 (frame-like lattice, end load)									
n bays	Bending			Rotation-y			Rotation-x		
	EAL	matrix deriv.	% Err.	EAL	matrix deriv.	% Err.	EAL	matrix deriv.	% Err.
2	.144 -2	.123 -2	14.6	.41 -3	.376 -3	14.6	.422 -4	.377 -4	10.7
5	.108	.103	4.6	.141 -1	.128 -1	9.2	.607 -3	.589 -3	3.
10	3.3	3.26	1.2	.198	.201	2.	.48 -2	.47 -2	1.5
							Axial-Extension		
							EAL	matrix deriv.	% Err.
2							.144 -2	.123 -2	14.6
5							.108	.103	4.6
10							3.3	3.26	1.2

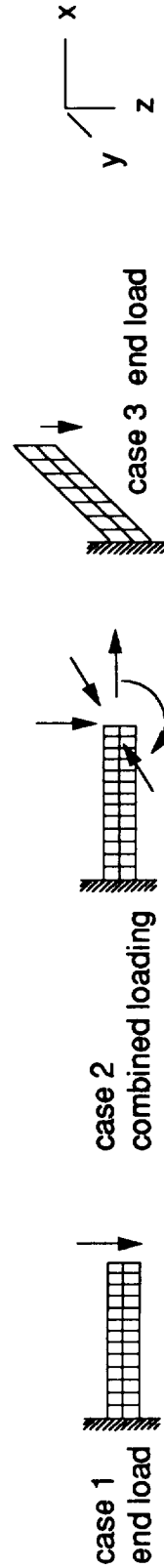
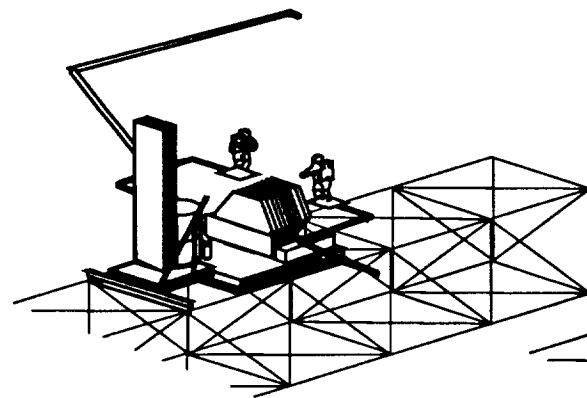
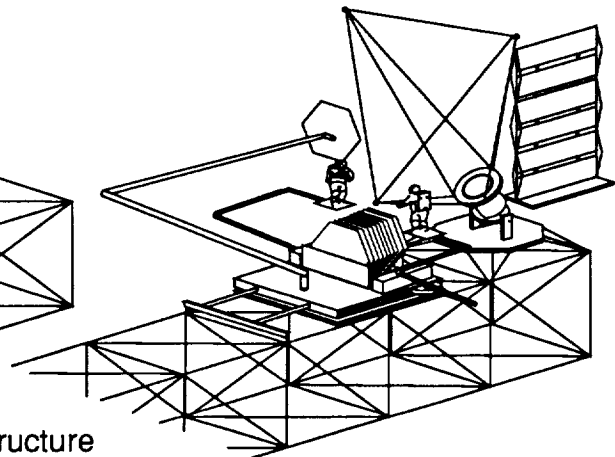


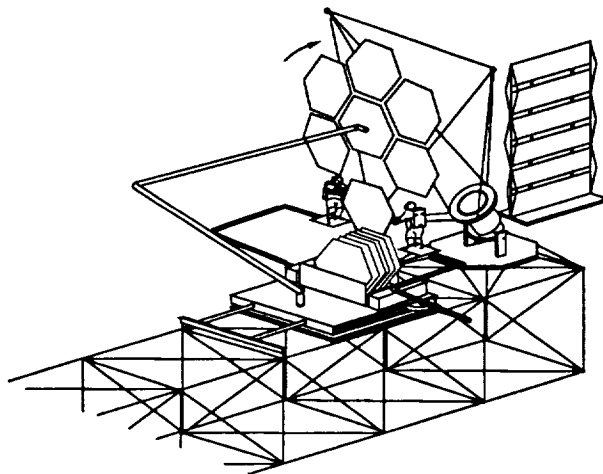
Table 5.1. Sixth-order finite element verification.



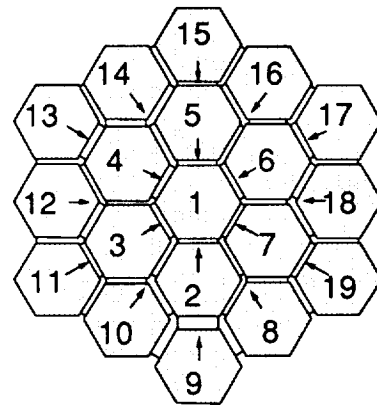
(a) Space Station keel and stored structure



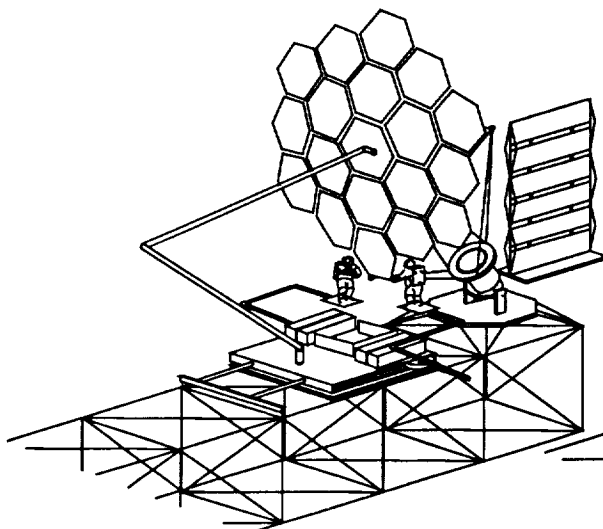
(b) Support truss assembly



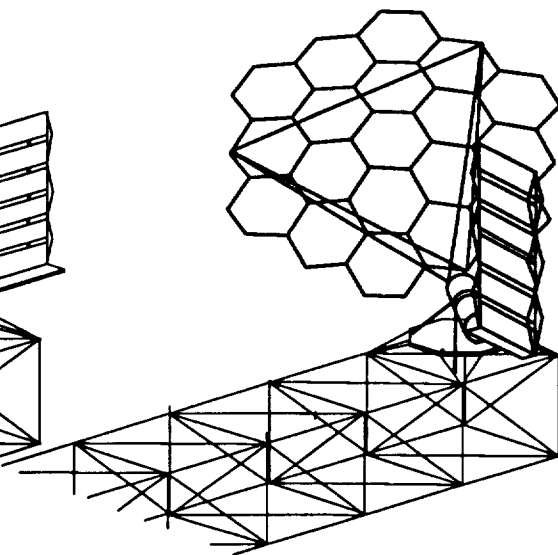
(c) Structure assembly



(d) Generic circular panel assembly



(e) Attachment of panel assembly to support truss



(f) Assembled structure

Figure 1.1. Assembly of panel structure on space station keel lattice structure.

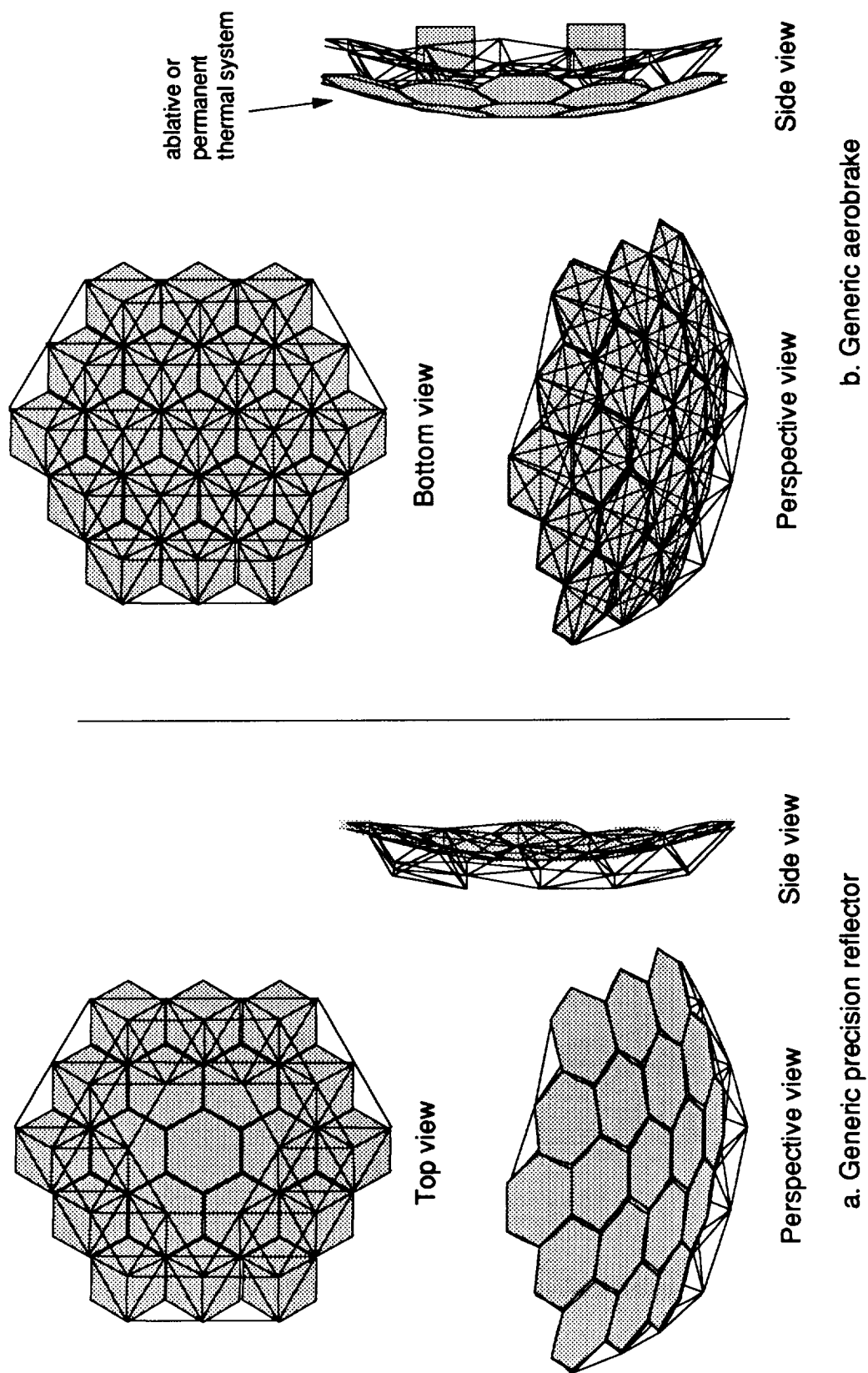
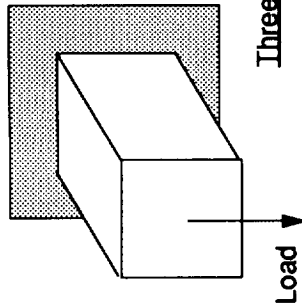


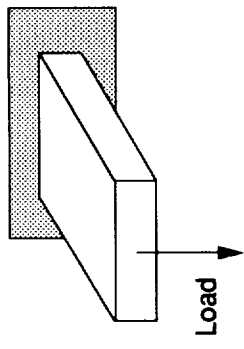
Figure 1.2. Candidate space lattice structures.





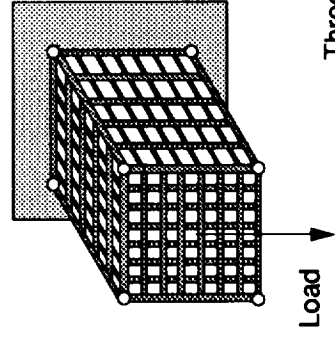
Three-dimensional elasticity

Analysis (energy methods, Principle of total complementary energy)  
 Material (linear elastic)  
 Geometry (unbounded), Loading (unbounded)



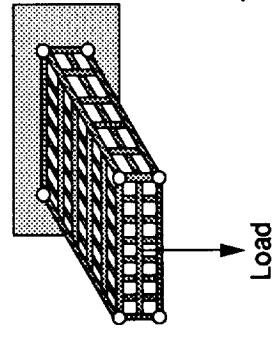
One-dimensional and two-dimensional elasticity

Analysis (energy methods, plate theory)  
 Material (linear elastic)  
 Geometry (uniform rectangular), Loading (uniform, point)  
 Classic solutions (plates, beams)  
 Based on the geometry of deformation



Three-dimensional elasticity

Analysis (energy methods, Principle of total complementary energy)  
 Material (linear elastic)  
 Geometry (unbounded), Loading (point)

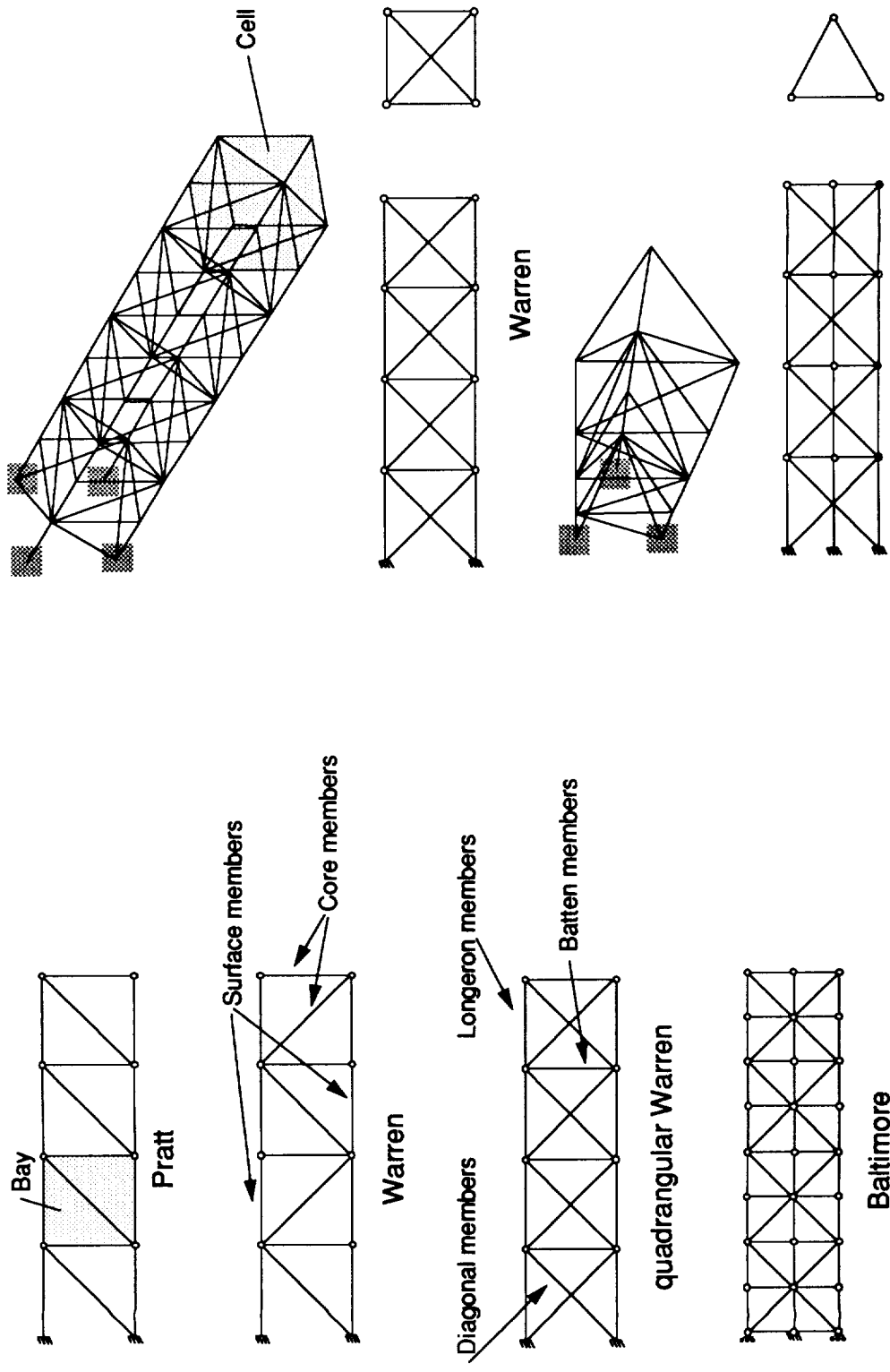


Current study

Two-dimensional and three-dimensional elasticity

Analysis (energy methods, Castigliano's 2nd theorem)  
 Material (linear elastic, tension compression rods)  
 Geometry (repeating unit square cell), Loading (point)  
 Classic solutions (beam-like, plate-like lattices)  
 Based on total strain energy

Figure 1.3. Foundation of lattice study.



a.) two-dimensional

b.) three-dimensional

Figure 2.1. Typical two-dimensional and three-dimensional lattice beams.

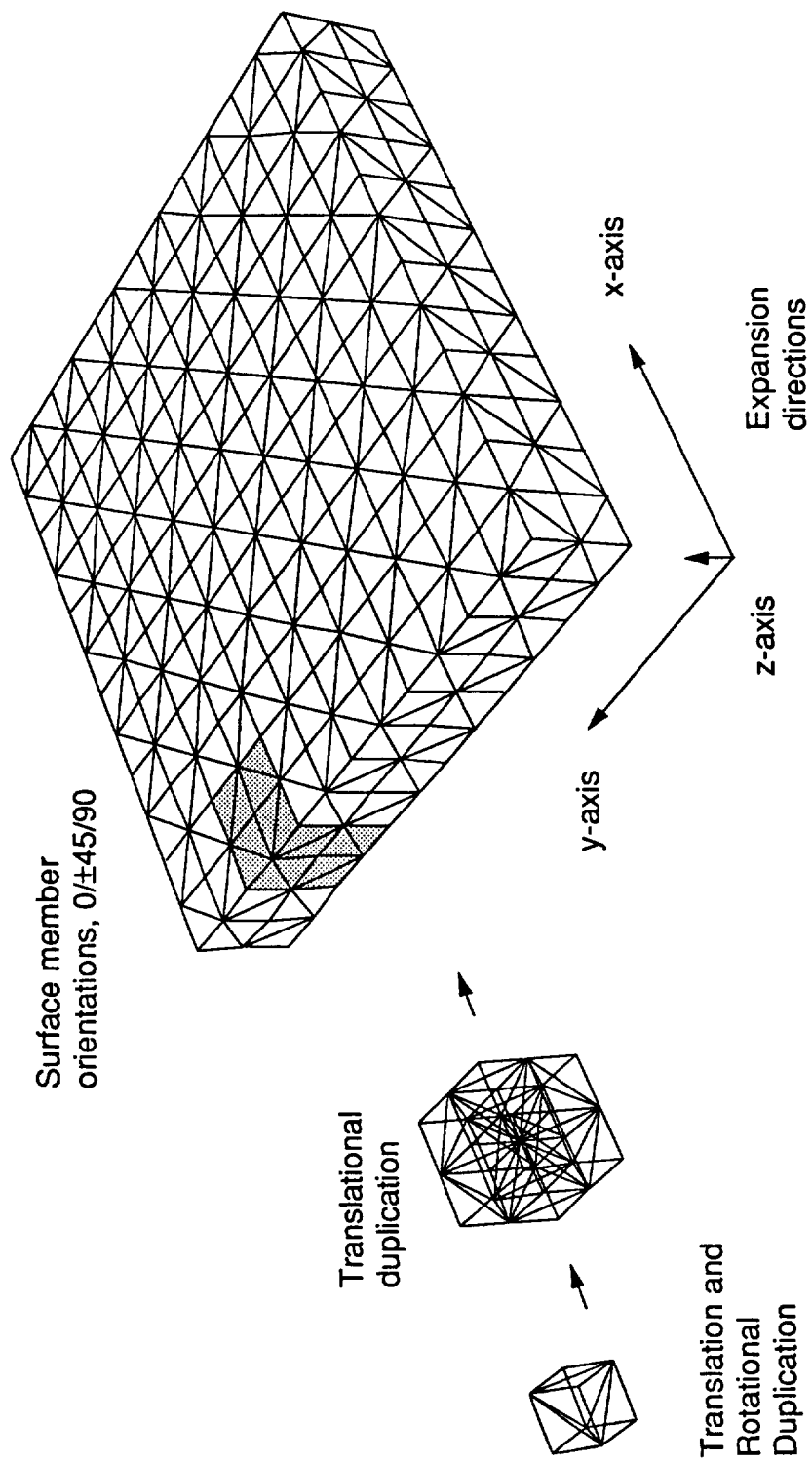


Figure 2.2. Typical planar Warren lattice geometry.

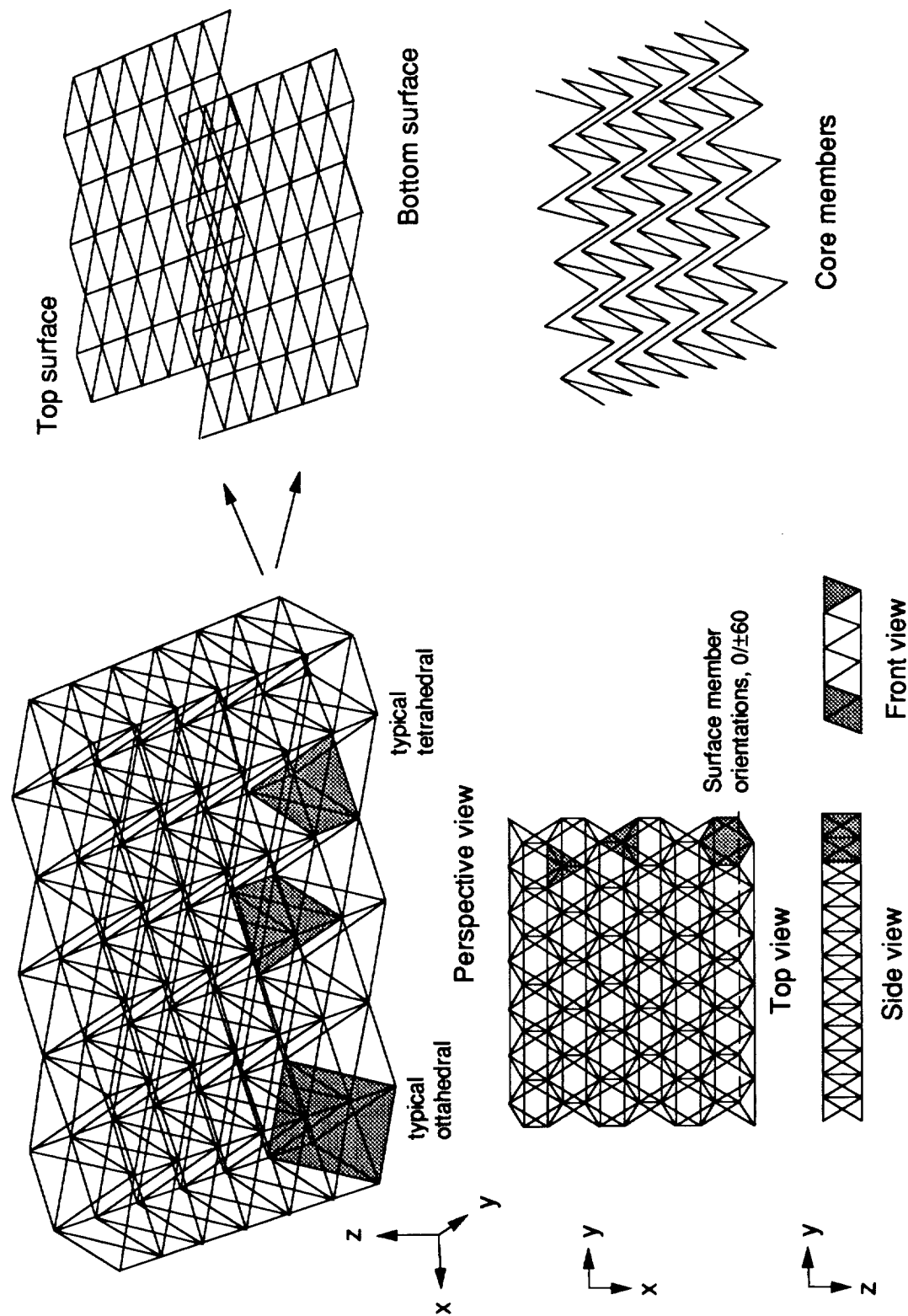


Figure 2.3. Typical planar tetrahedral lattice geometry.

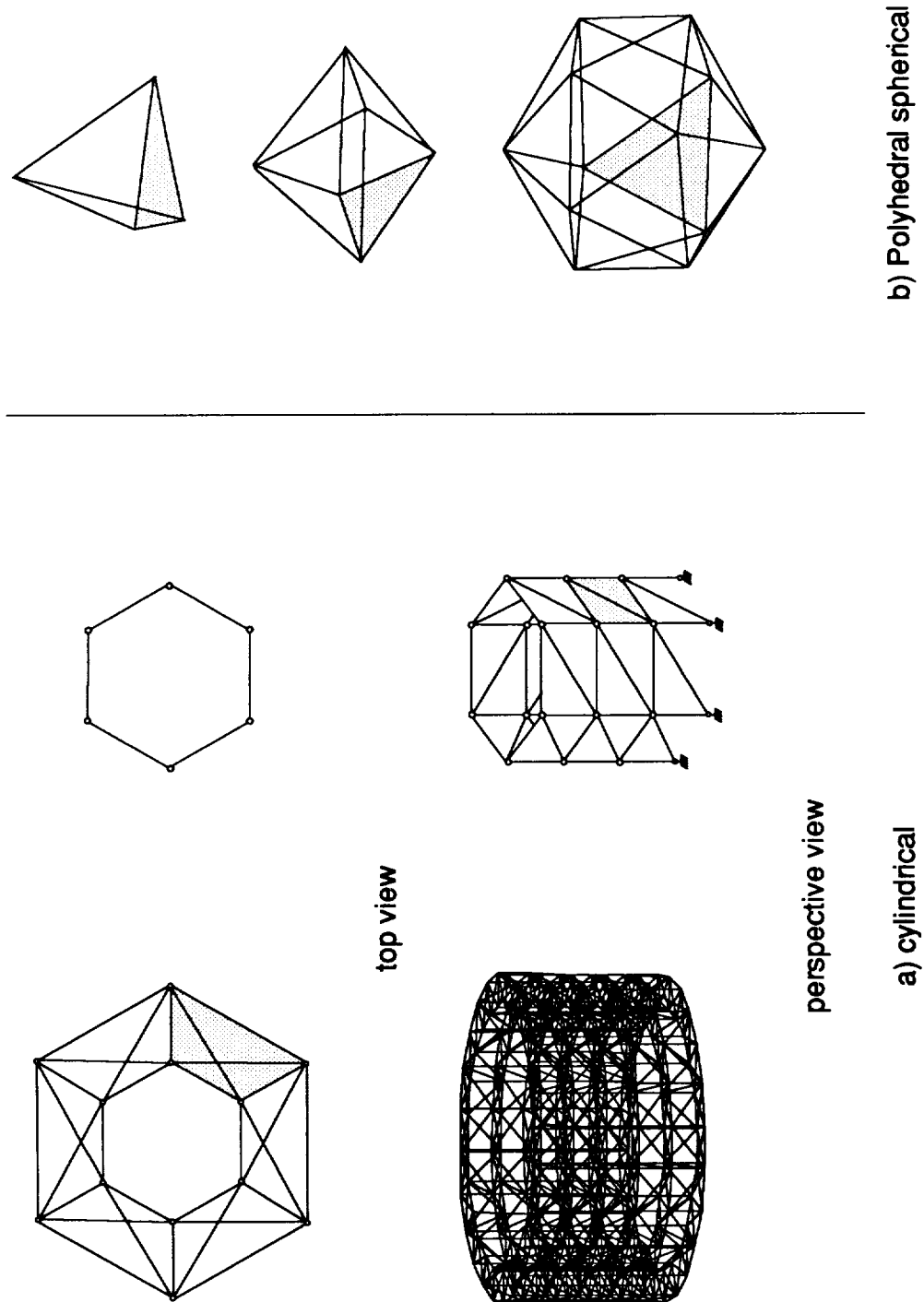


Figure 2.4. Typical shell-like lattice geometries.

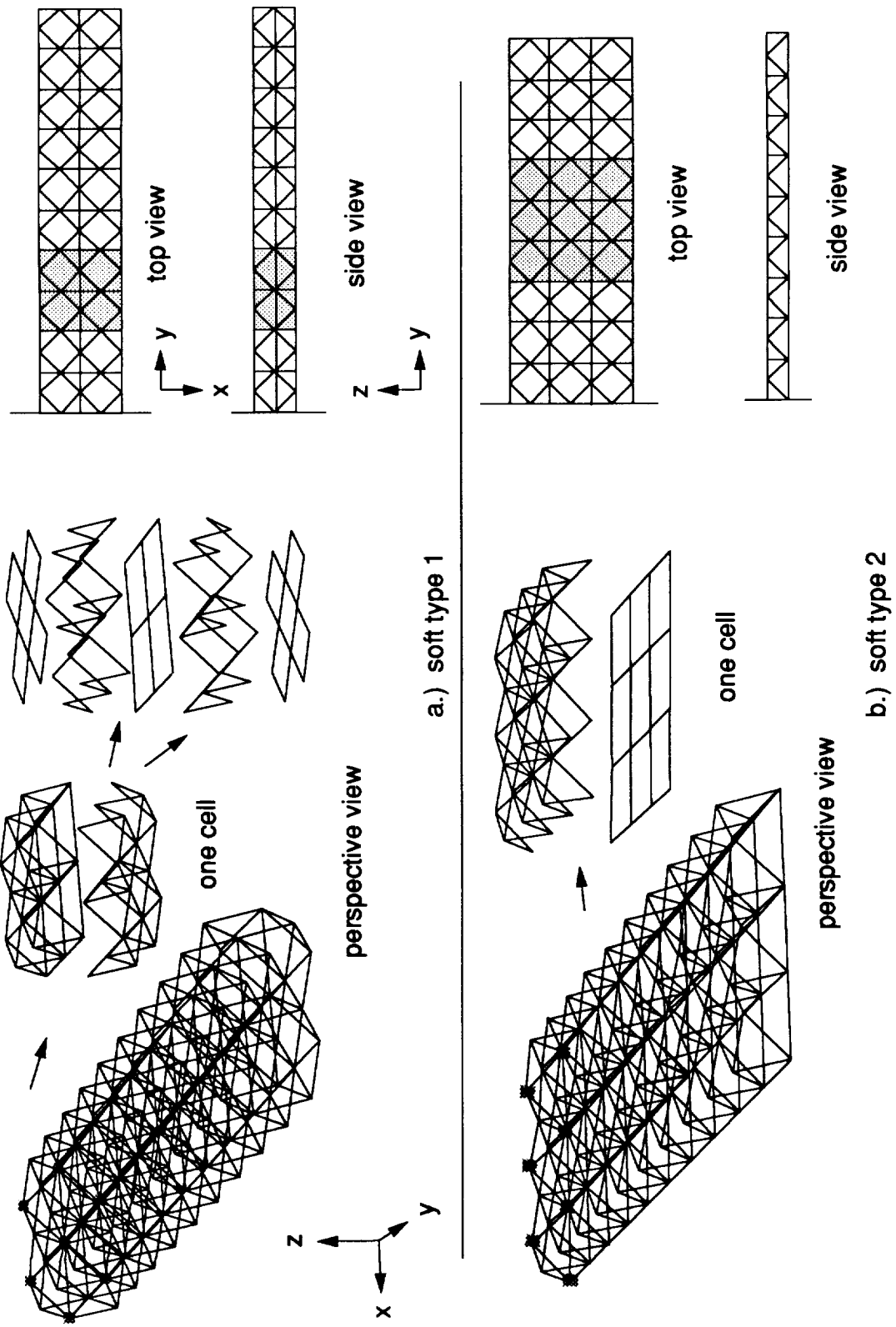


Figure 2.5. Typical soft lattice geometries.

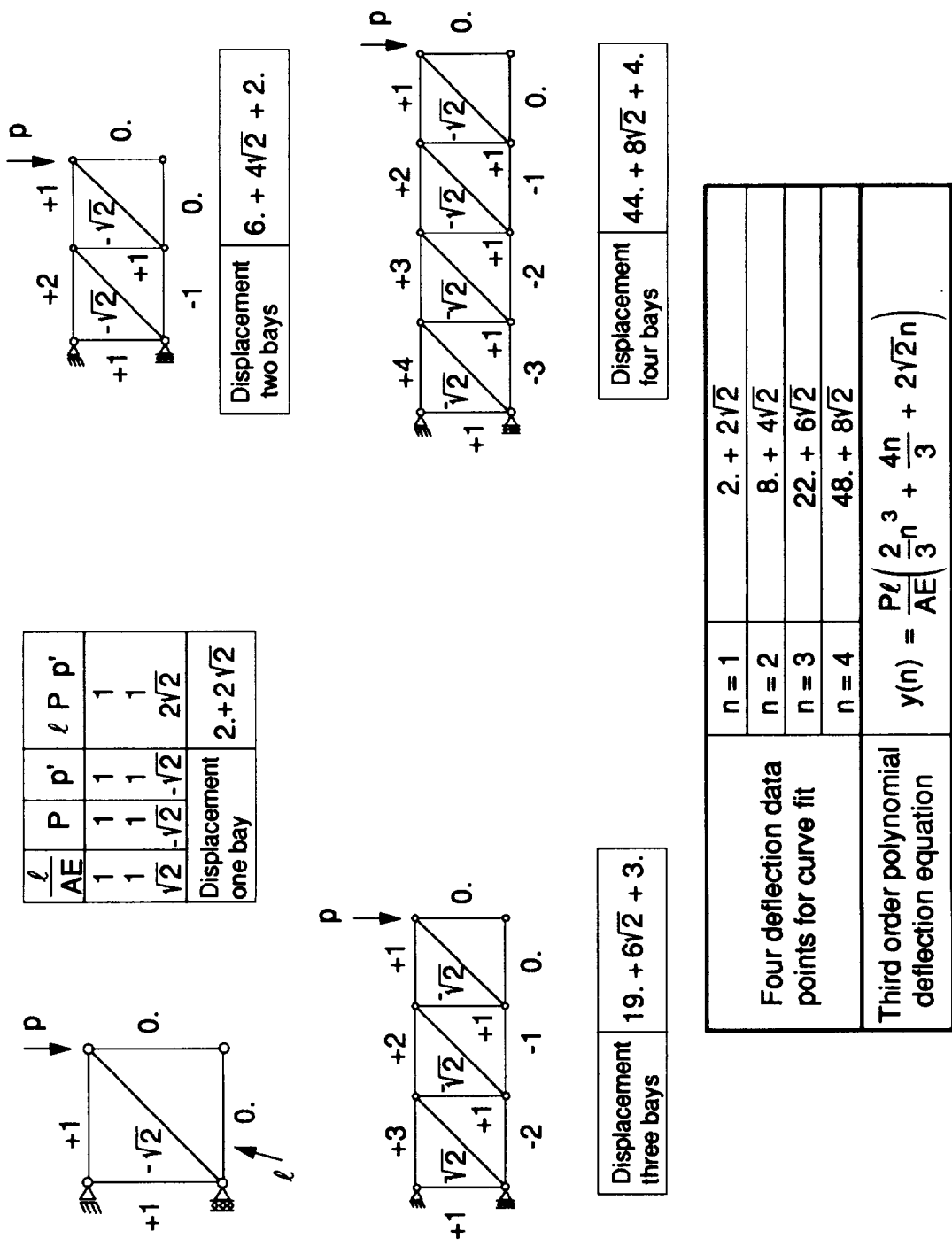


Figure 3.1. Displacement equation derivation for a cantilevered Pratt lattice beam.

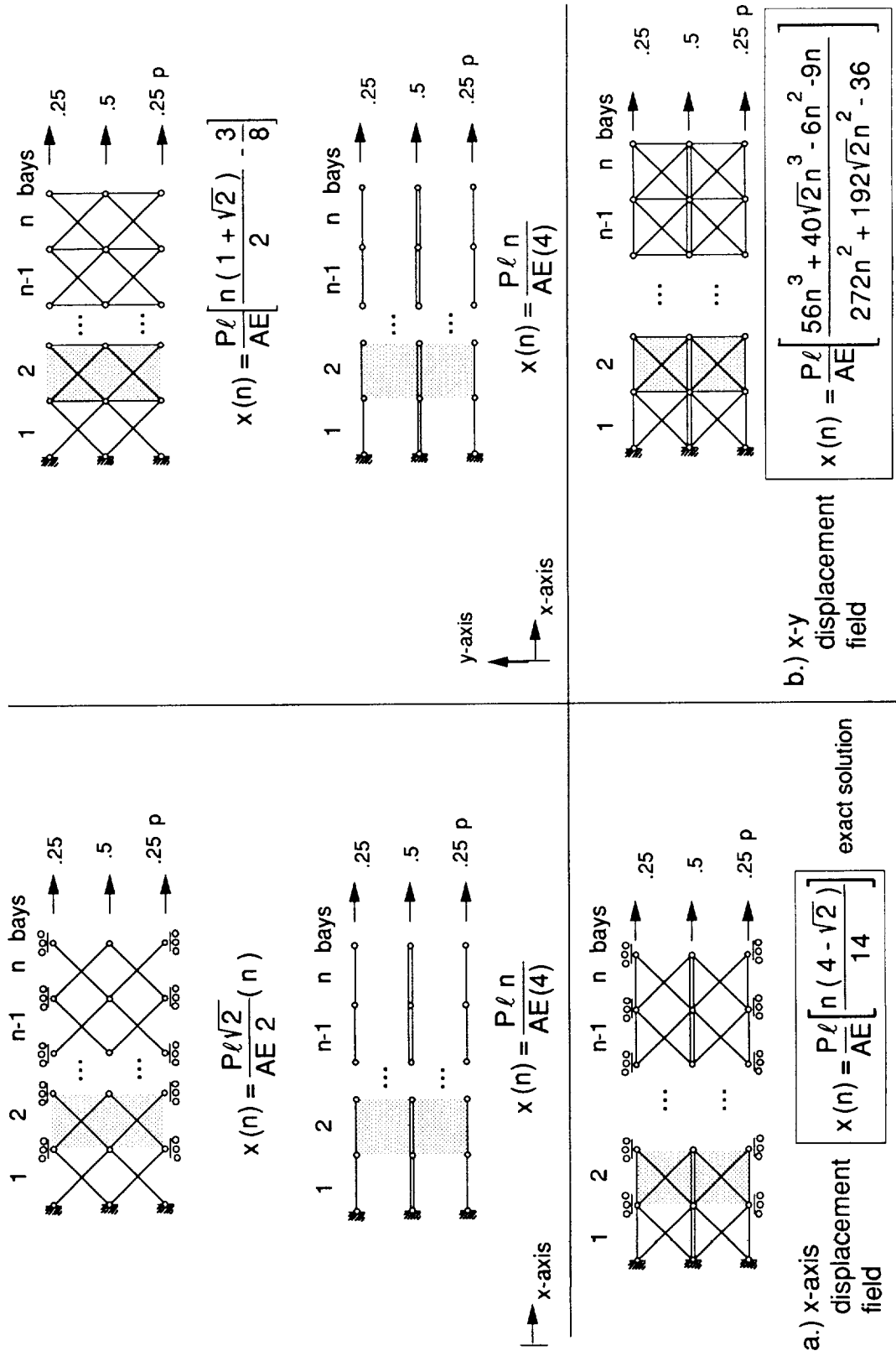
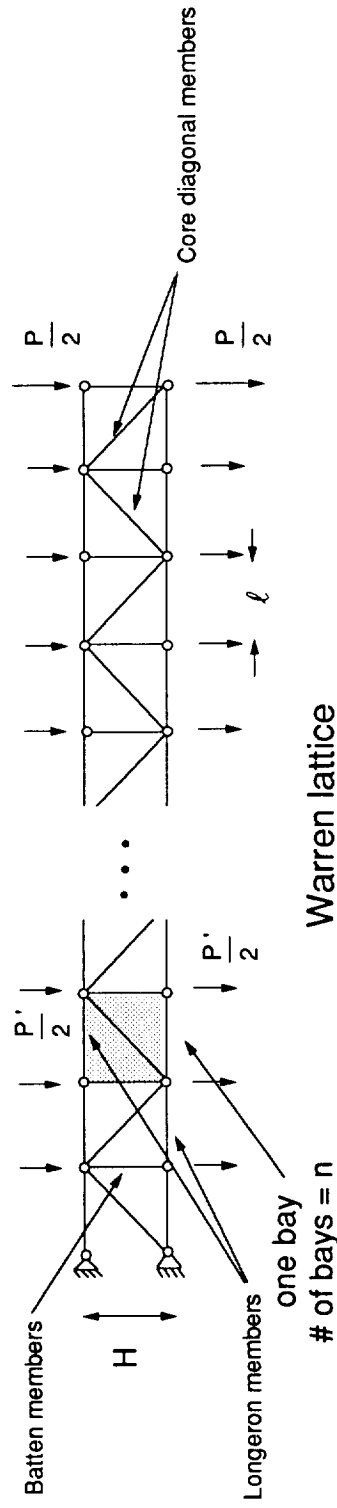


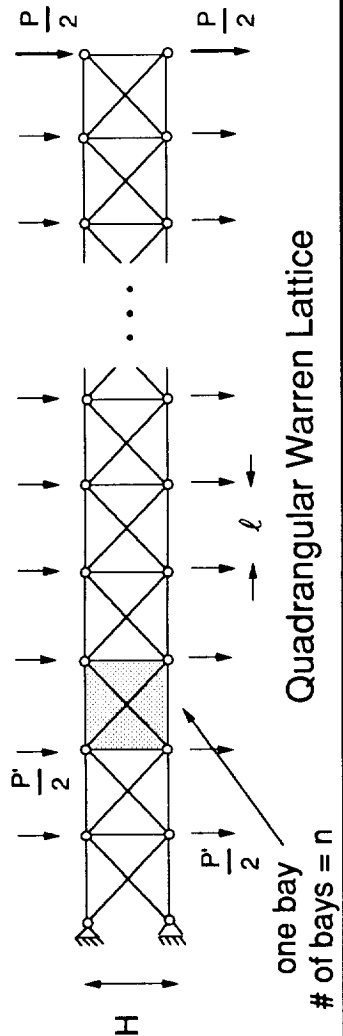
Figure 3.2. Two displacement derivations of a statically indeterminate lattice.





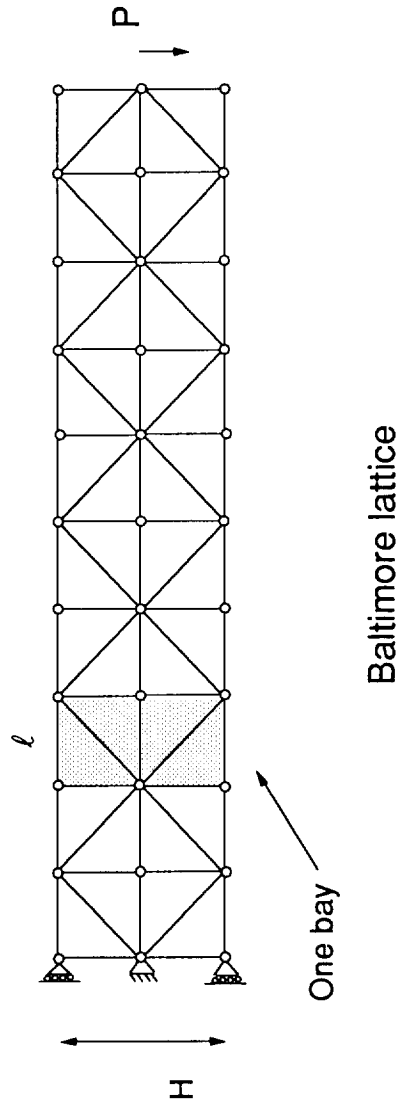
Deflection equation (end load)	$y(n) = \frac{P\ell}{AE} \left[ \left( \frac{2}{3}n^3 + \frac{n}{3} \right) \frac{\ell^2}{H^2} + \frac{(\ell^2 + H^2)^{3/2}}{H^2\ell} n + \frac{H}{\ell^4} \right]$
Deflection equation, square bay (end load)	$y(n) = \frac{P\ell}{AE} \left[ \frac{2}{3}n^3 + \frac{n}{3} + 2\sqrt{2}n + \frac{1}{4} \right]$
Deflection equation (distributed load)	$y(n) = \frac{P'\ell}{AE} \left[ \left( \frac{n^4}{4} + \frac{n^3}{3} + \frac{n}{6} \right) \frac{\ell^2}{H^2} + \frac{H}{4\ell} + \left( \frac{n^2}{2} + \frac{n}{2} \right) \frac{(\ell^2 + H^2)^{3/2}}{H^2\ell} \right]$
Deflection equation, square bay (distributed load)	$y(n) = \frac{P'\ell}{AE} \left[ \frac{n^4}{4} + \frac{n^3}{3} + \frac{n}{6} + \frac{1}{4} + \left( \frac{n^2}{2} + \frac{n}{2} \right) 2\sqrt{2} \right]$
Member count	$m(n) = 4n$

Figure 4.1. Deflection equations of cantilevered Warren lattice beam.



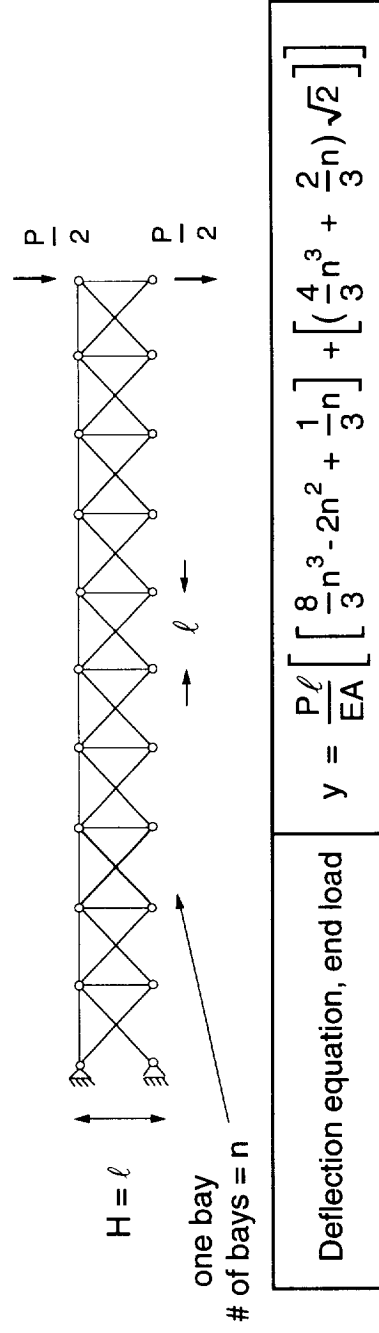
Deflection equation (end load)	$y(n) = \frac{P\ell}{AE} \left[ \left( \frac{2}{3}n^3 - \frac{n}{6} \right) \frac{\ell^2}{H^2} + \frac{(\ell^2 + H^2)^{3/2}}{2H^2\ell} n \right]$
Deflection equation, square bay (end load)	$y(n) = \frac{P\ell}{AE} \left[ \frac{2}{3}n^3 - \frac{n}{6} + \sqrt{2}n \right]$
Deflection equation (distributed load)	$y(n) = \frac{P'\ell}{AE} \left[ \left( \frac{n^4}{4} + \frac{n^3}{3} - \frac{n}{12} \right) \frac{\ell^2}{H^2} + \left( \frac{n^2}{4} + \frac{n}{4} \right) \frac{(\ell^2 + H^2)^{3/2}}{H^2\ell} \right]$
Deflection equation, square bay (distributed load)	$y(n) = \frac{P'\ell}{AE} \left[ \frac{n^4}{4} + \frac{n^3}{3} - \frac{n}{12} + \left( \frac{n^2}{2} + \frac{n}{2} \right) \sqrt{2} \right]$
Member count	$m(n) = 4n$

Figure 4.2. Deflection equations of cantilevered quadrangular Warren lattice beam.

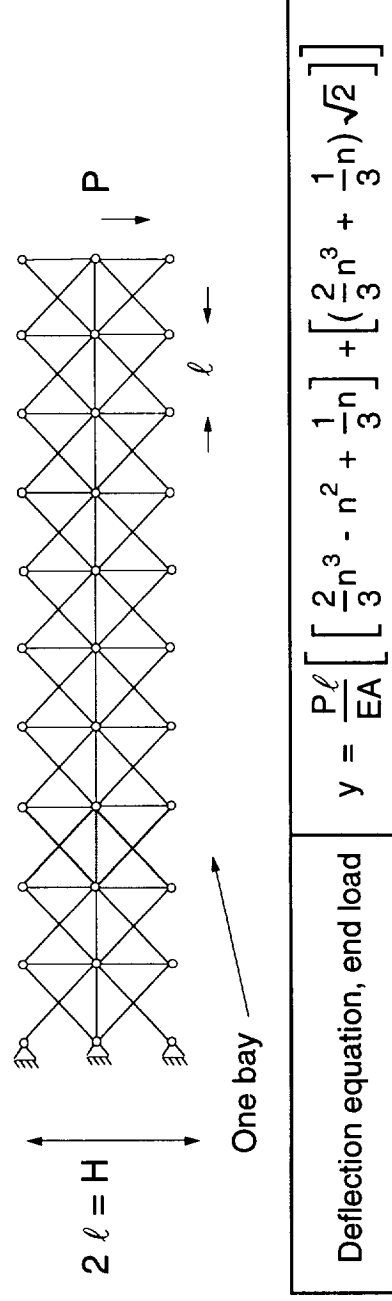


Deflection equation (end load)	$y(n) = \frac{P\ell}{AE} \left[ \frac{2}{3} \left( n^3 - n \right) \frac{\ell^2}{H^2} + \frac{H}{2\ell} + 2n \frac{(\ell^2 + H^2)^{3/2}}{H^2 \ell} \right]$
Deflection equation, square bay (end load)	$y(n) = \frac{P\ell}{AE} \left[ \frac{2n^3}{3} + \frac{2n}{3} + \frac{1}{2} + \frac{5\sqrt{5}n}{4} \right]$
Member count	$m(n) = 7n + 2$

Figure 4.3. Deflection equation of cantilevered Baltimore lattice beam.

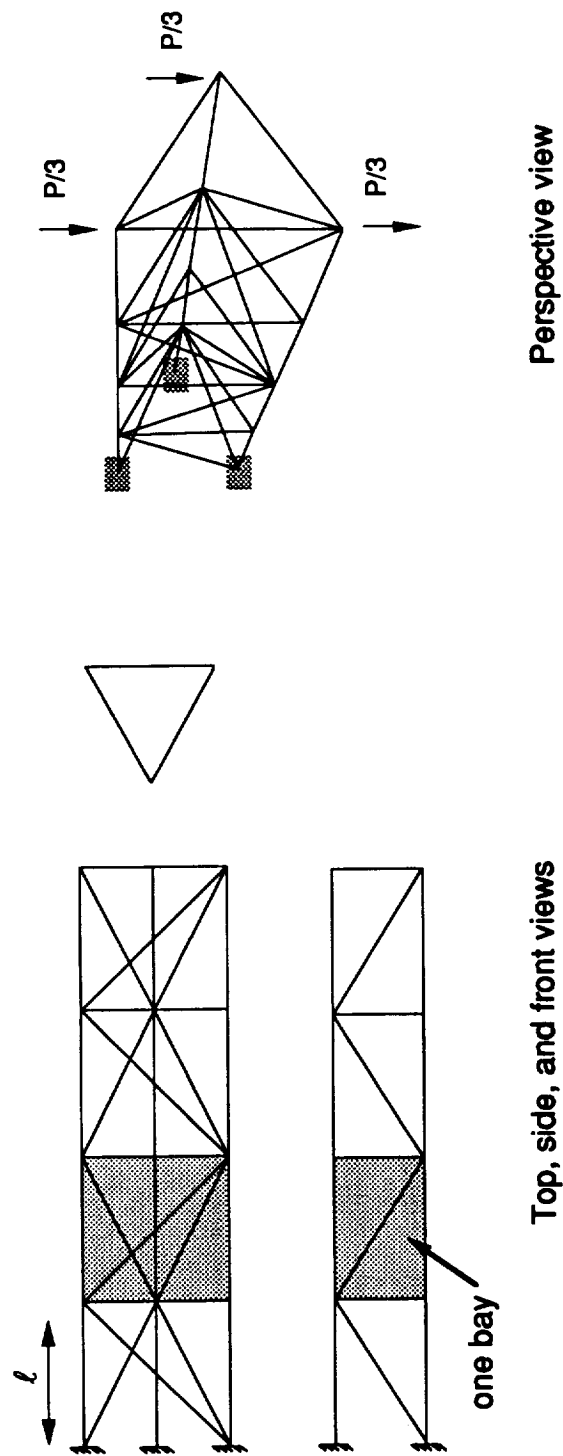


(a.) Soft quadrangular Warren lattice.



(b.) Soft Baltimore Warren lattice.

Figure 4.5. Deflection equations of cantilevered soft quadrangular Warren and Baltimore lattice beams in two-dimensions.



Warren lattice beam, triangular cross-section

Deflection equation (End load)	$y(n) = \frac{Pl}{AE} \left( \frac{2}{3}n^3 - \frac{2}{9}n + \frac{4\sqrt{2}}{3}n + \frac{1}{3} \right)$
Member count	$m(n) = 9n$

Figure 4.6. Deflection equation of cantilevered Warren lattice beam with triangular cross-section.

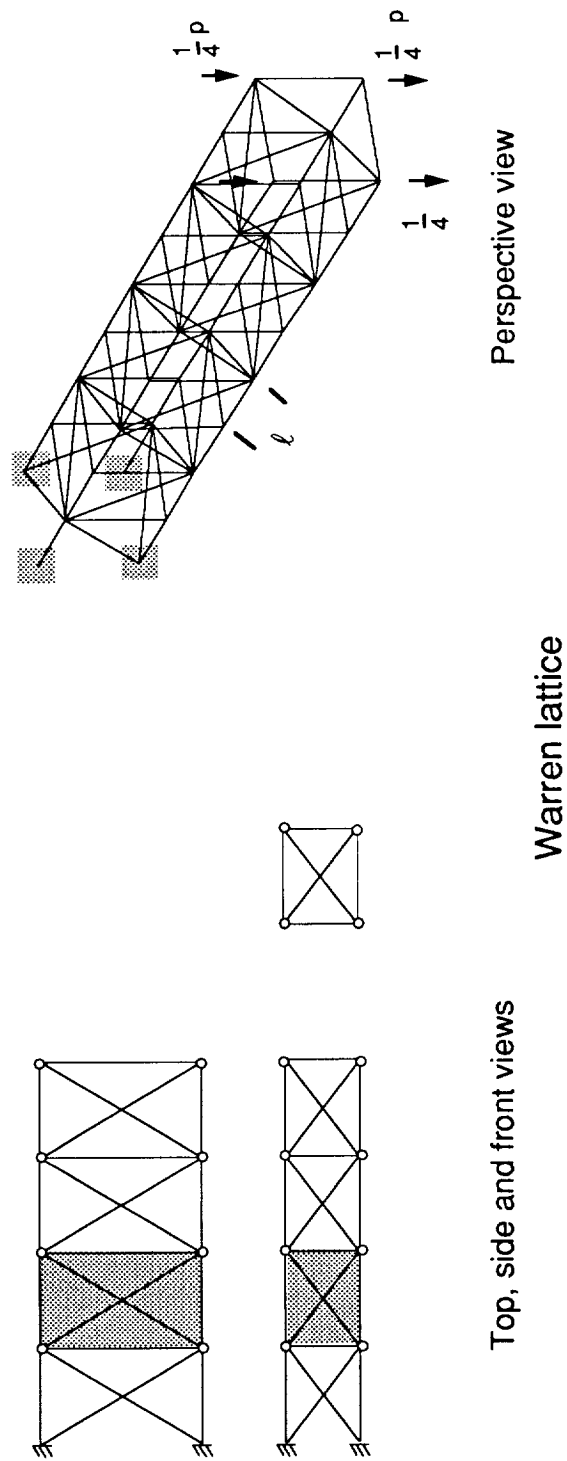
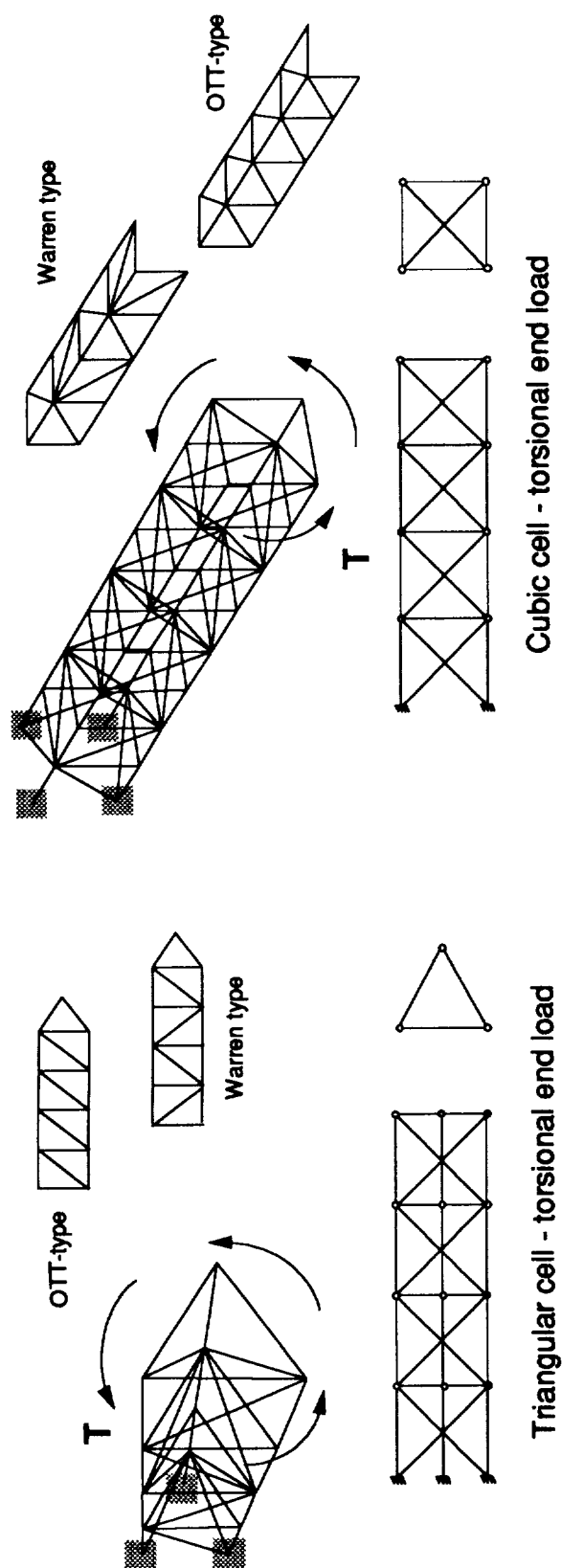


Figure 4.7. Deflection equations of a cantilevered Warren lattice beam, three-dimensional.



Warren-type triangular cells	$\theta_{\text{warren}} = \frac{T}{\ell_{\text{bay}} AE} \left( \frac{180}{\pi} \left[ \frac{n4\sqrt{3}(1 + 6\sqrt{2}) + 3\sqrt{3}}{27} \right] \right)$
OTT-type triangular cells	$\theta_{\text{OTT}} = \frac{T}{\ell_{\text{bay}} AE} \left( \frac{180}{\pi} \left[ \frac{n8\sqrt{3}(1 + \sqrt{2}) - 3\sqrt{3}}{9} \right] \right)$
Warren-type cubic cells	$\theta_{\text{warren}} = \frac{T}{\ell_{\text{bay}} AE} \left( \frac{180}{\pi} \left[ n + \frac{\sqrt{2}}{16} \right] \right)$
OTT-type cubic cells	$\theta_{\text{OTT}} = \frac{T}{\ell_{\text{bay}} AE} \left( \frac{180}{\pi} \left[ \frac{n(2 + \sqrt{2})}{2} - \frac{3\sqrt{2}}{16} \right] \right)$

Figure 4.8. Torsion equations of Warren beams with triangular and square cross-sections.

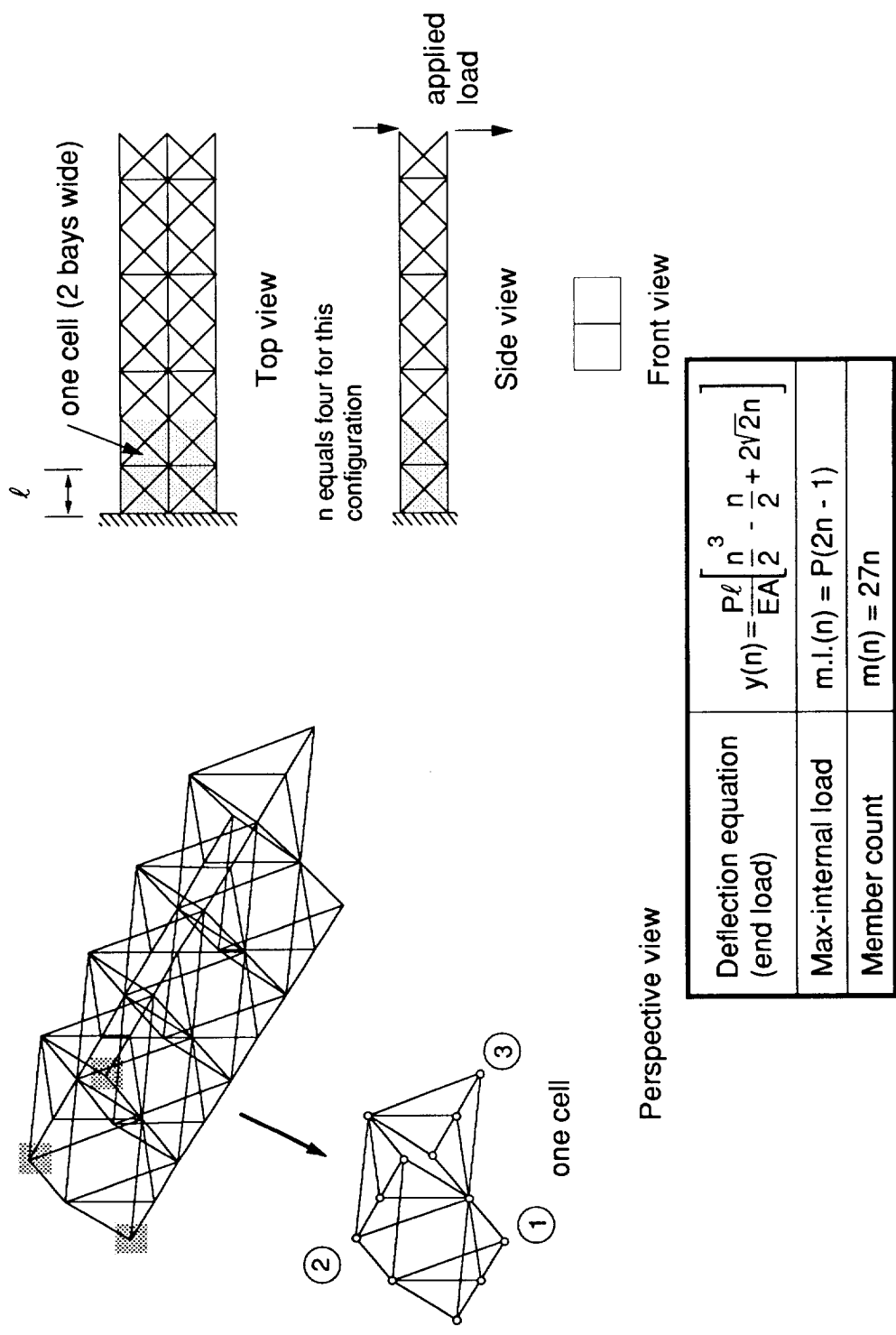


Figure 4.9. Deflection equation of a cantilevered Warren lattice, two bays wide.



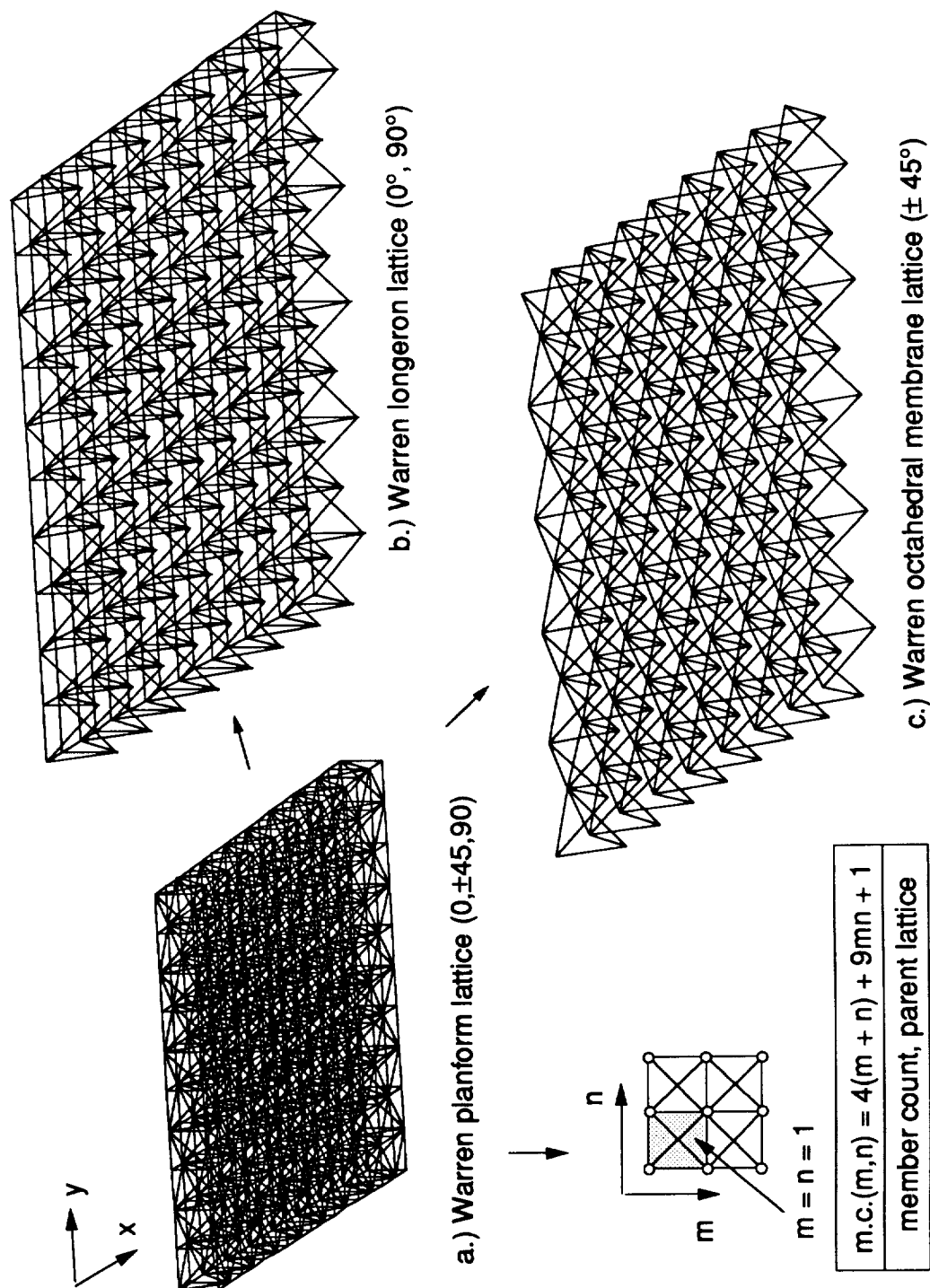


Figure 4.10. Warren planform lattice and component longeron and membrane lattices.

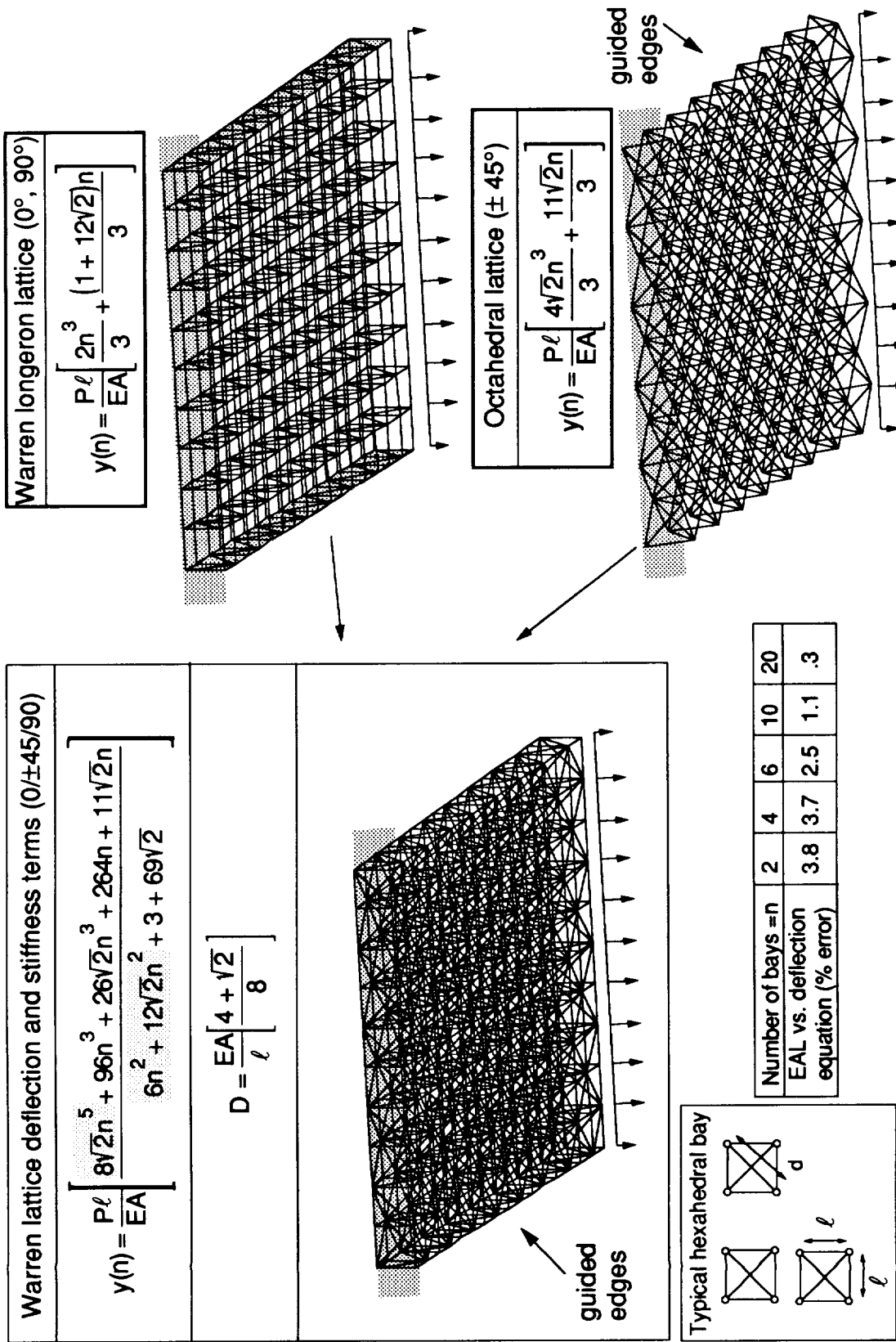


Figure 4.16. Deflection equation and stiffness coefficient for Warren lattice plate.

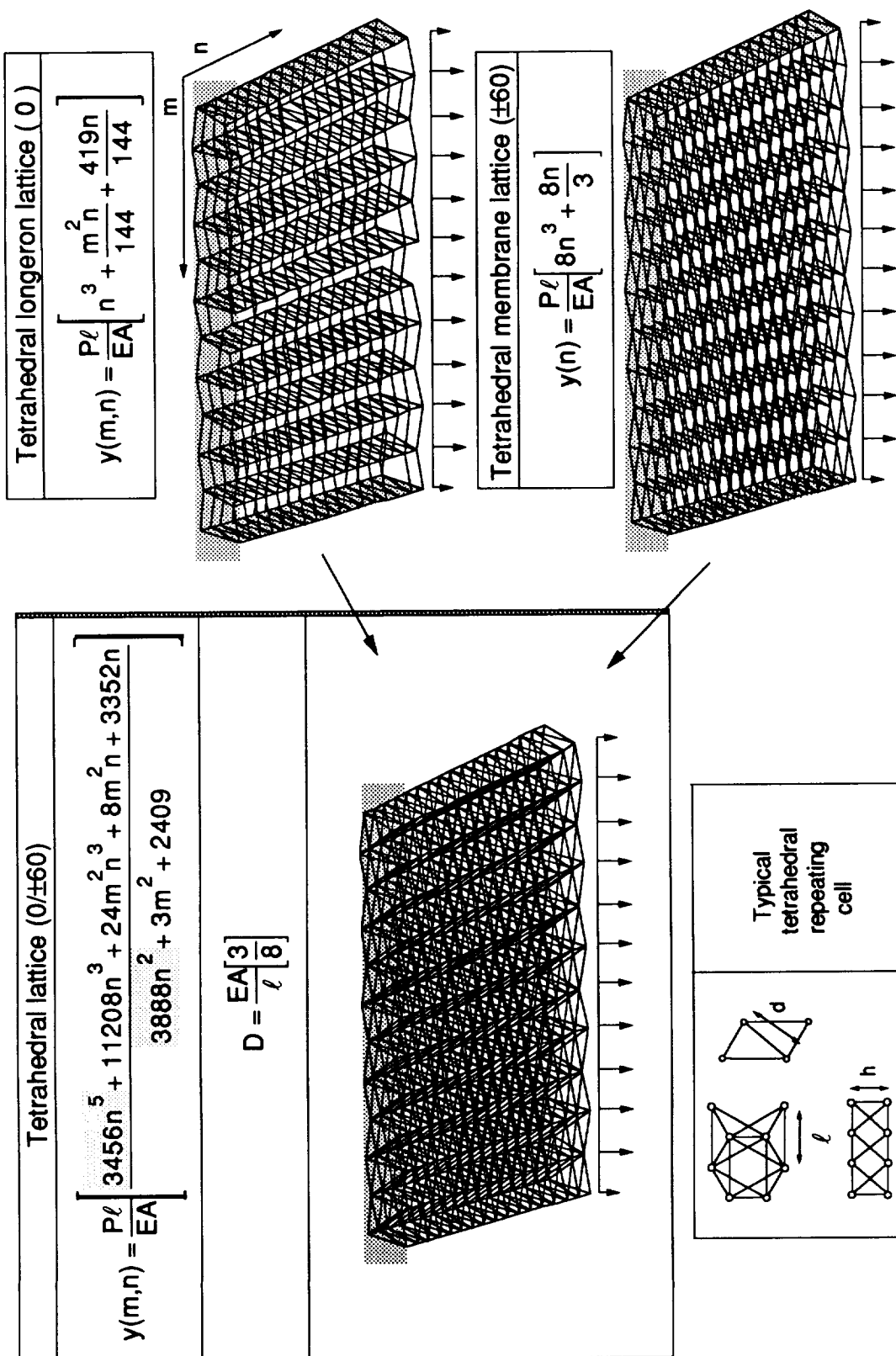


Figure 4.17. Deflection equations and stiffness coefficient of tetrahedral lattice plate.

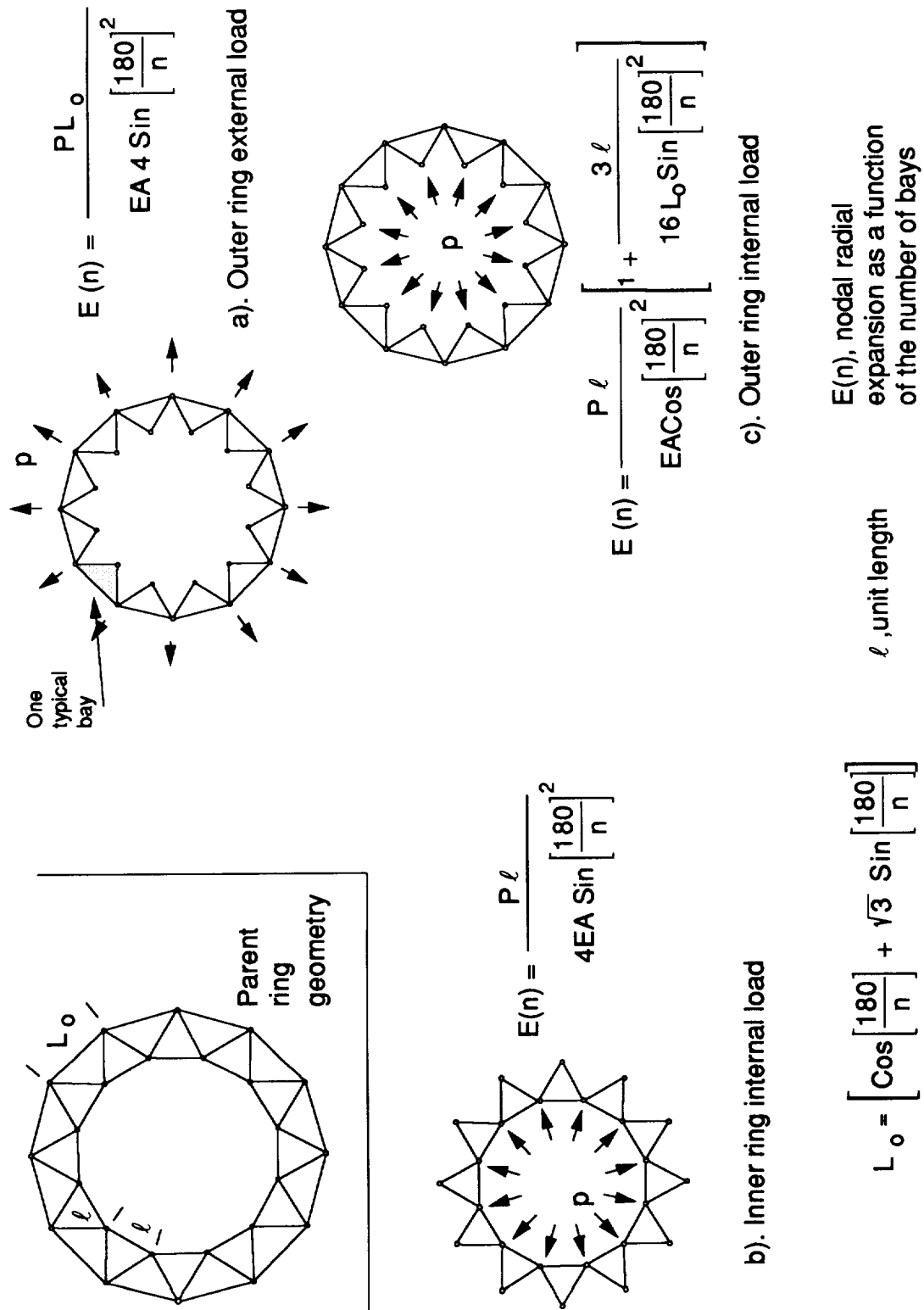


Figure 4.18. Expansion equation of triangular bay lattice ring.

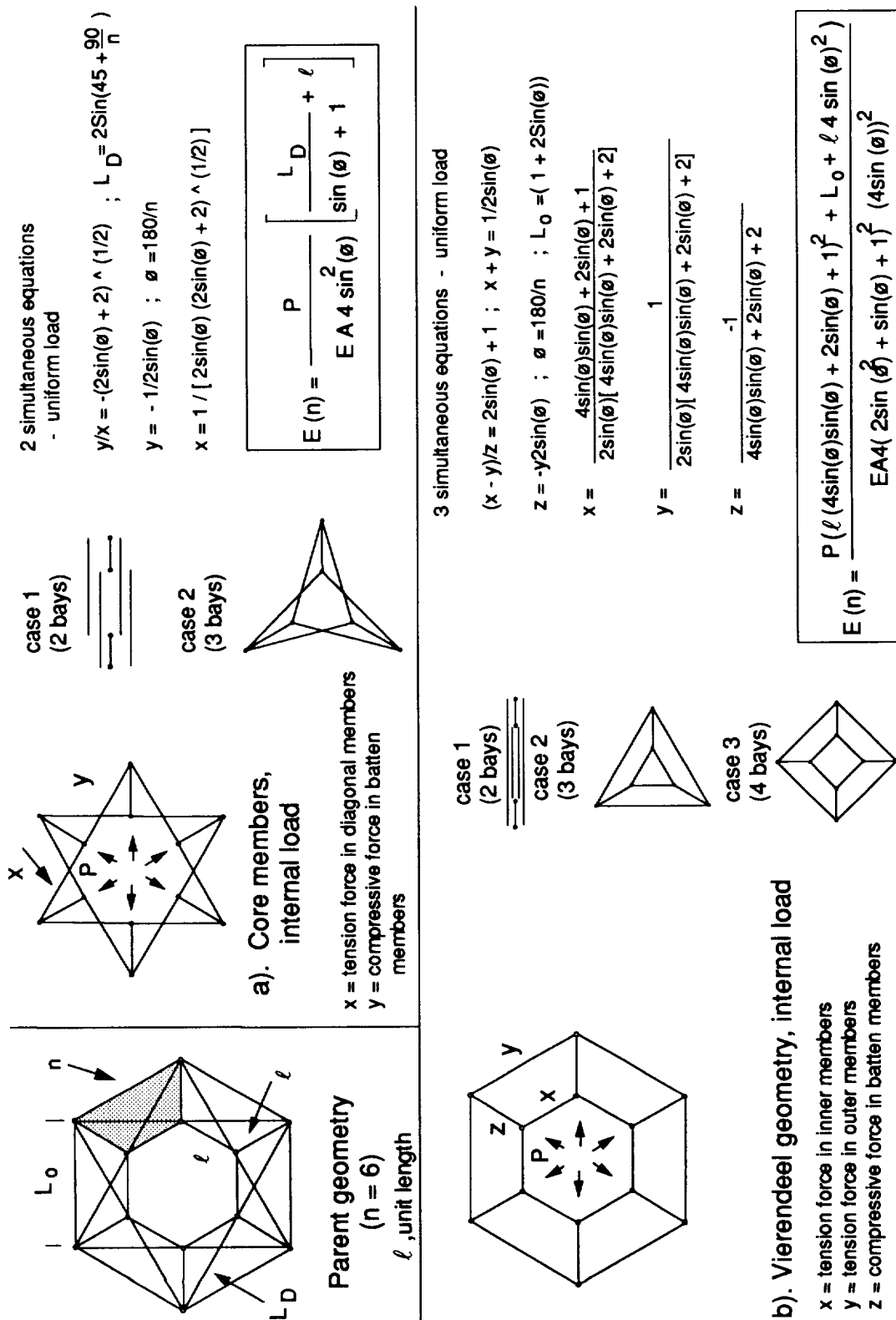


Figure 4.19. Expansion equations for square bay lattice ring.

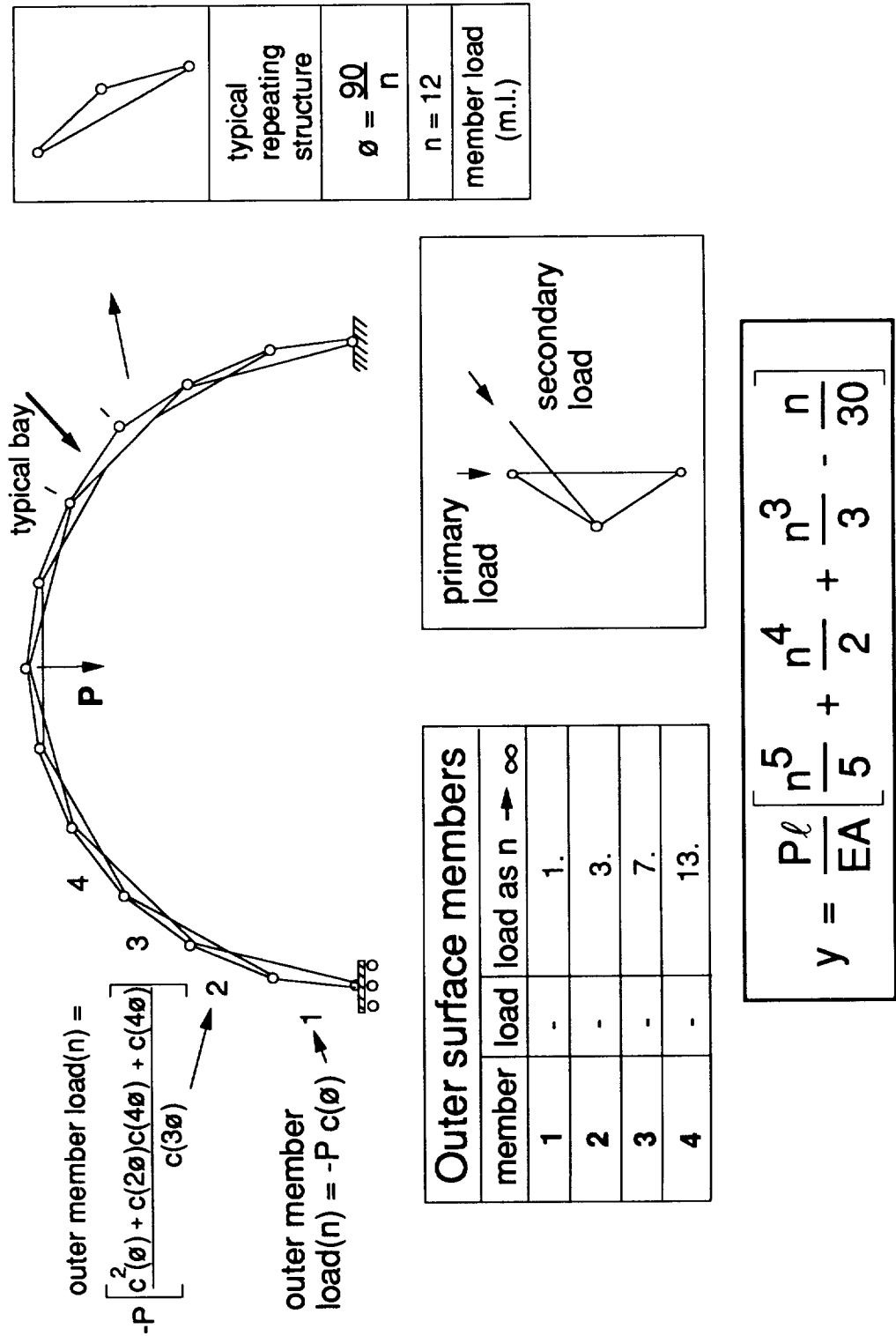


Figure 4.20. Statically determinate symmetric circular arch lattice.

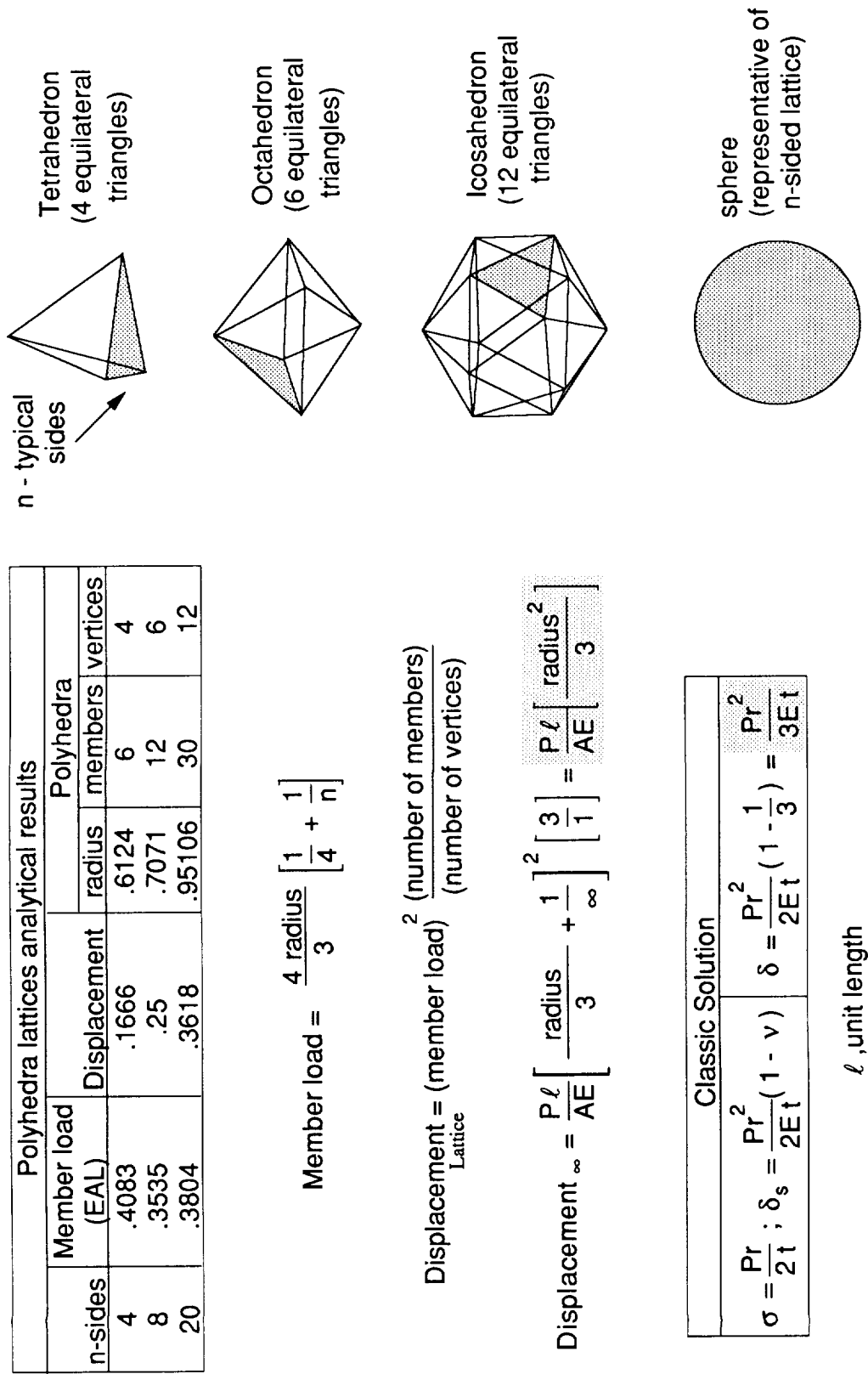


Figure 4.21. Spherical lattice member loads and displacements.

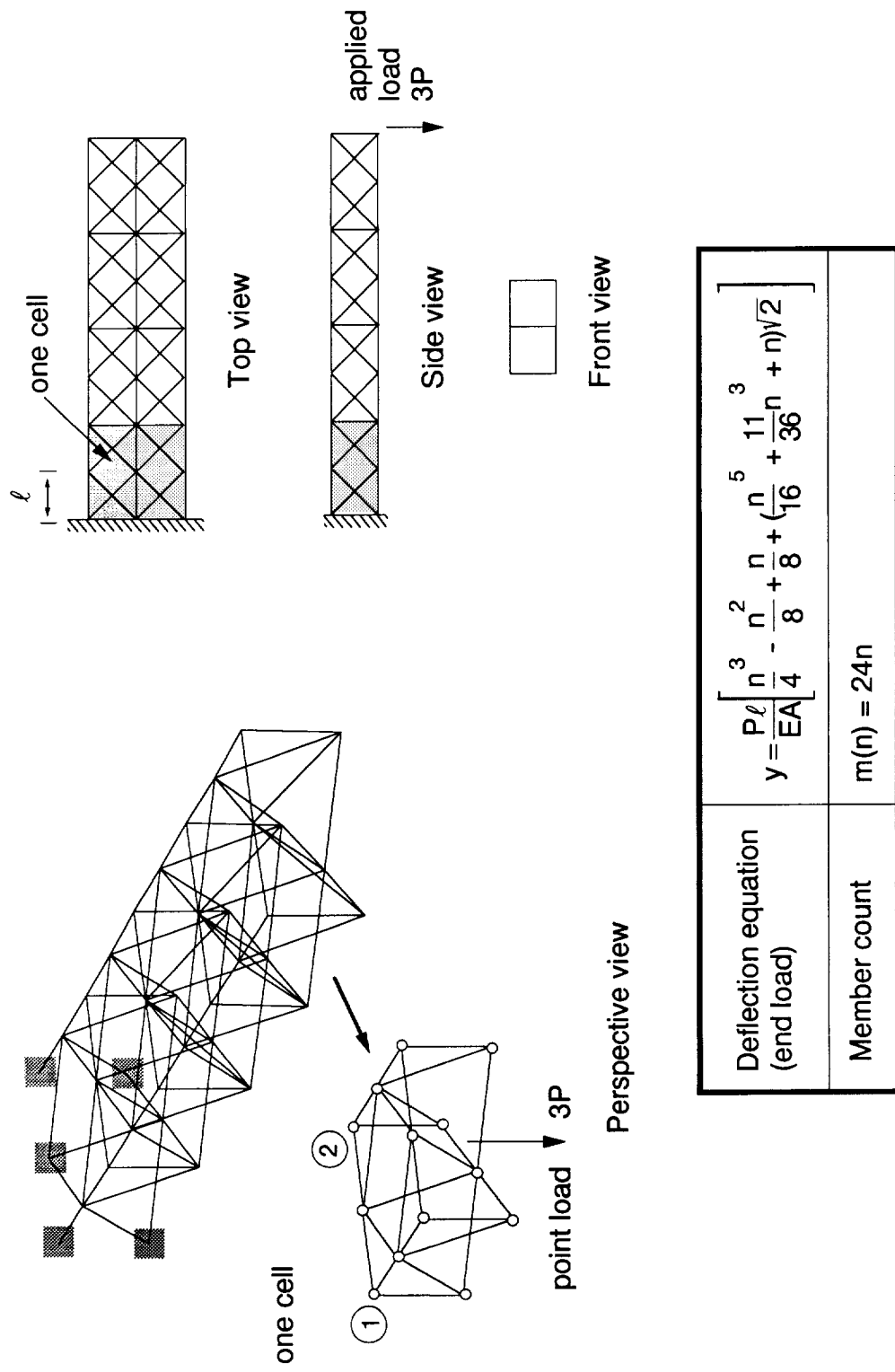


Figure 4.22. Deflection equation of soft sixth-order Warren lattice with end load, two rows of longerons.



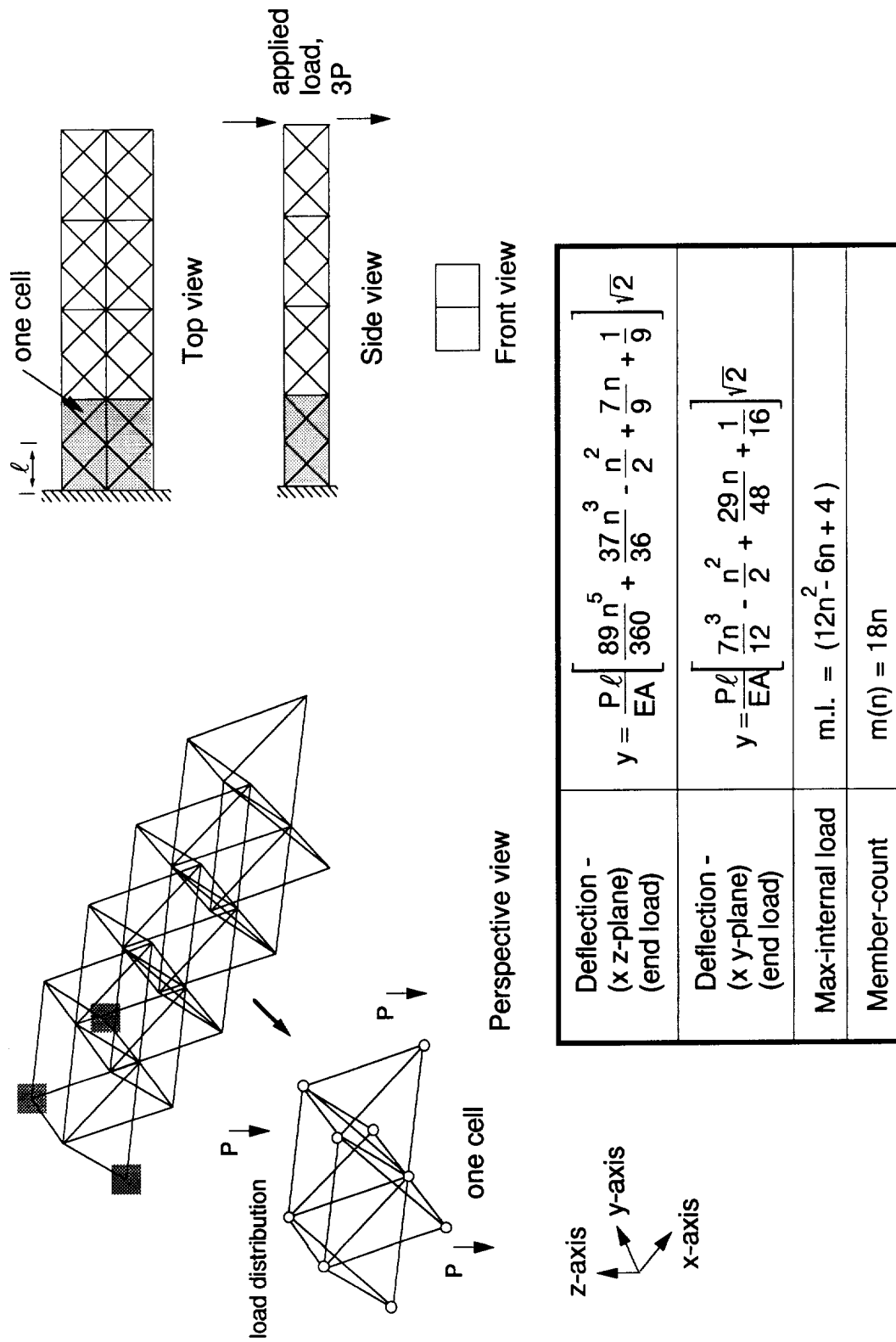
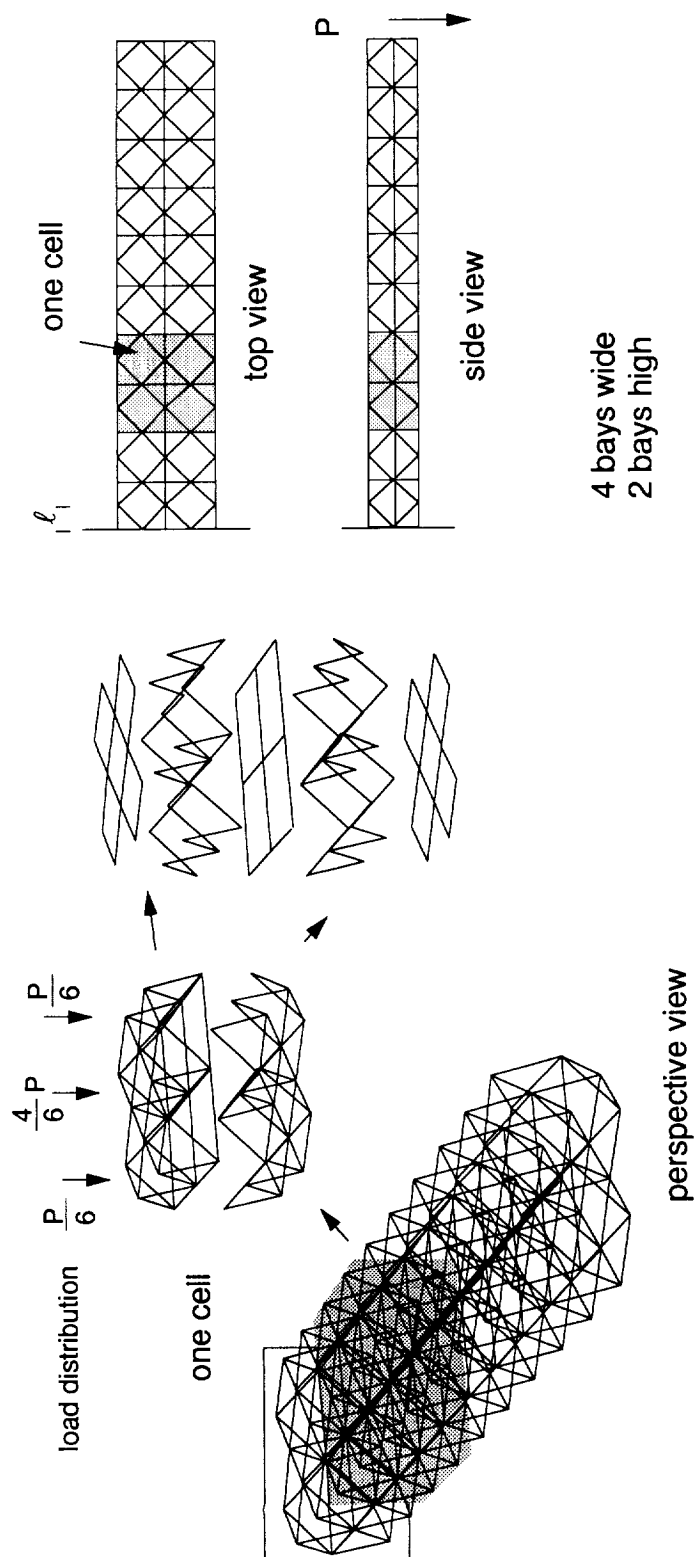
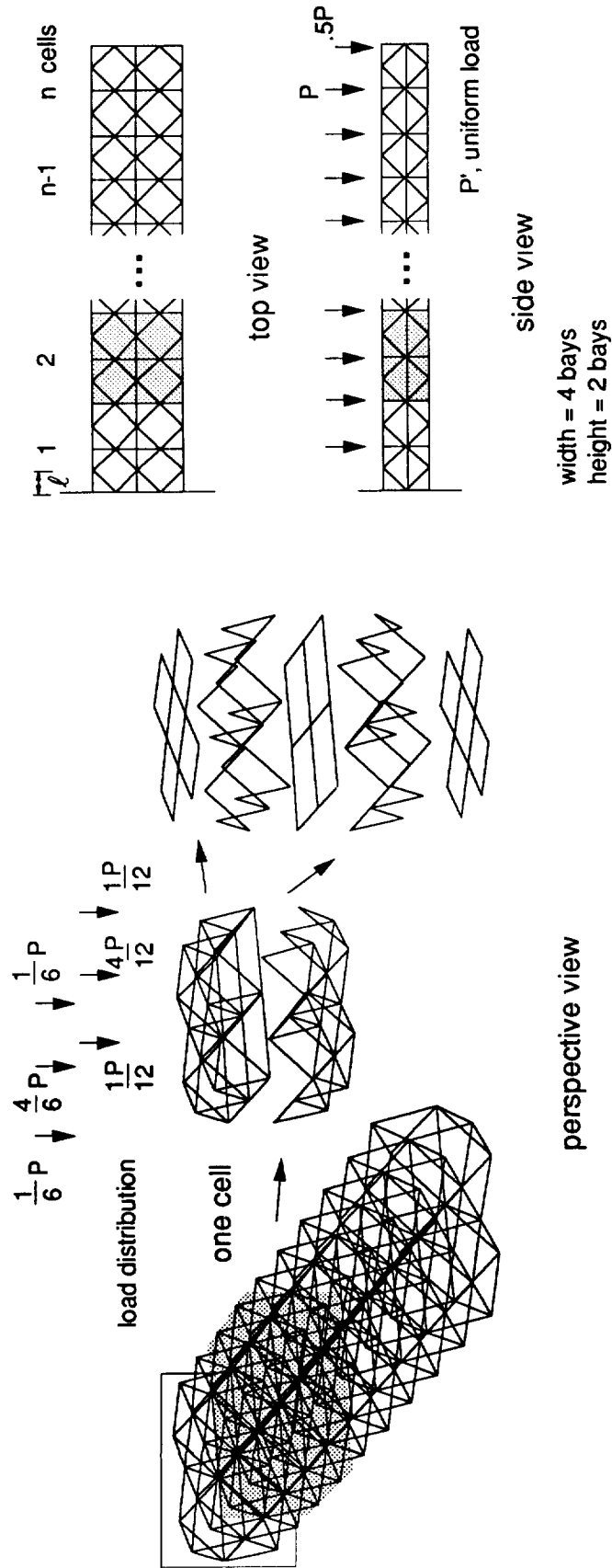


Figure 4.23. Deflection equations of a soft sixth-order Warren lattice with end load, longeronless.



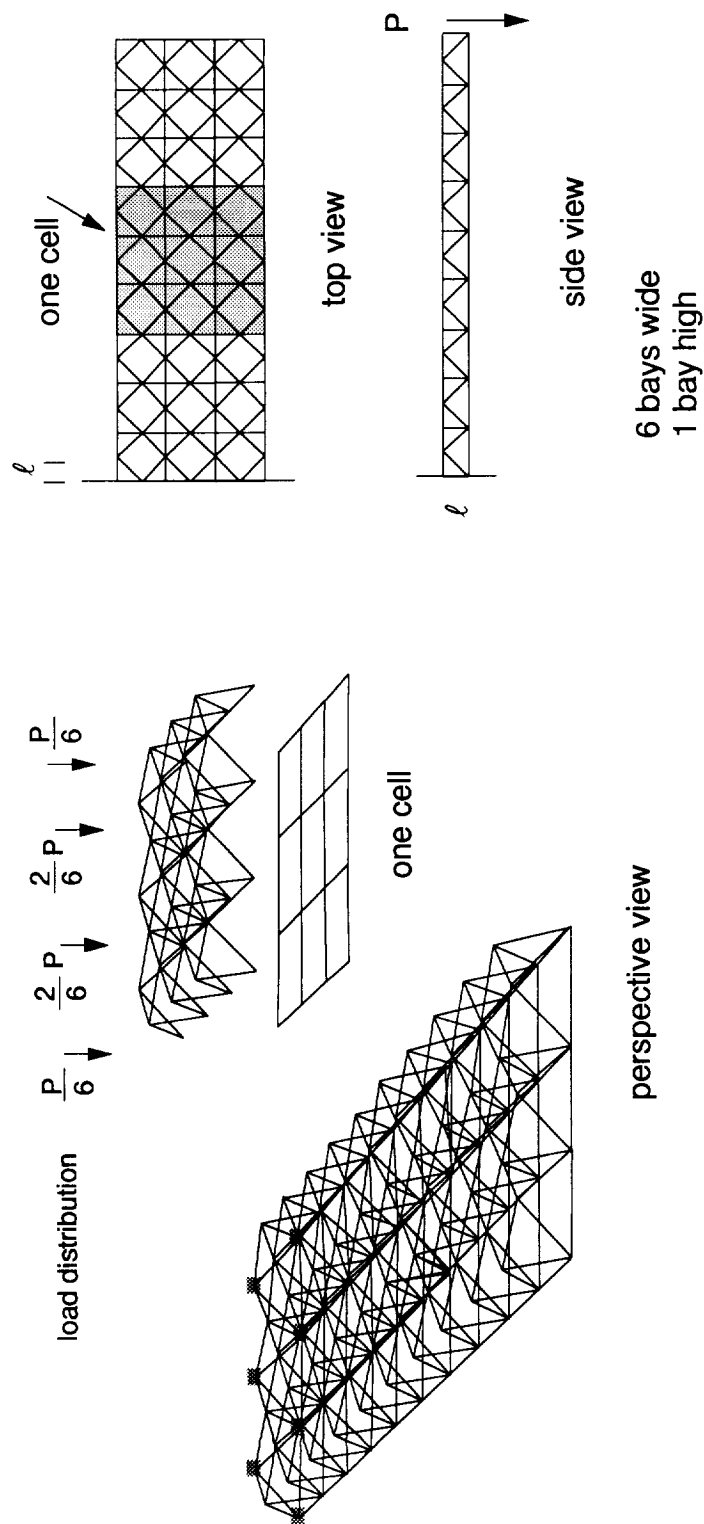
Deflection equation (end load)	$y(n) = \frac{P\ell}{AE} \left[ 15360n^5 + 24320n^3 - 960n^2 + 2248n + 30 \right] \left( \frac{\sqrt{2}}{1920} \right)$
Member count	$m(n) = 82n$

Figure 4.24. Deflection equation of a symmetric soft sixth-order Warren lattice with end load.



Deflection equation : m, number of bays in truss; n, designated bay deflection	
$y(m,n) = \frac{P'\ell}{AE} \left[ -128m^6 + 768nm^5 + (48 - 1920n^2)m^4 + (-192n + 2560n^3)m^3 + (-192 + 3744n^2)m^2 + (-96 + 1952n - 576n^2 + 1024n^3)m + 96n^2 + 16 \left( \frac{\sqrt{2}}{576} \right) \right]$	
Beam end, deflection	$y(n) = \frac{P'\ell}{AE} \left[ 1280n^6 + 1664n^4 - 576n^3 + 1856n^2 - 96n + 16 \left( \frac{\sqrt{2}}{576} \right) \right]$
Member count	$m(n) = 82n$

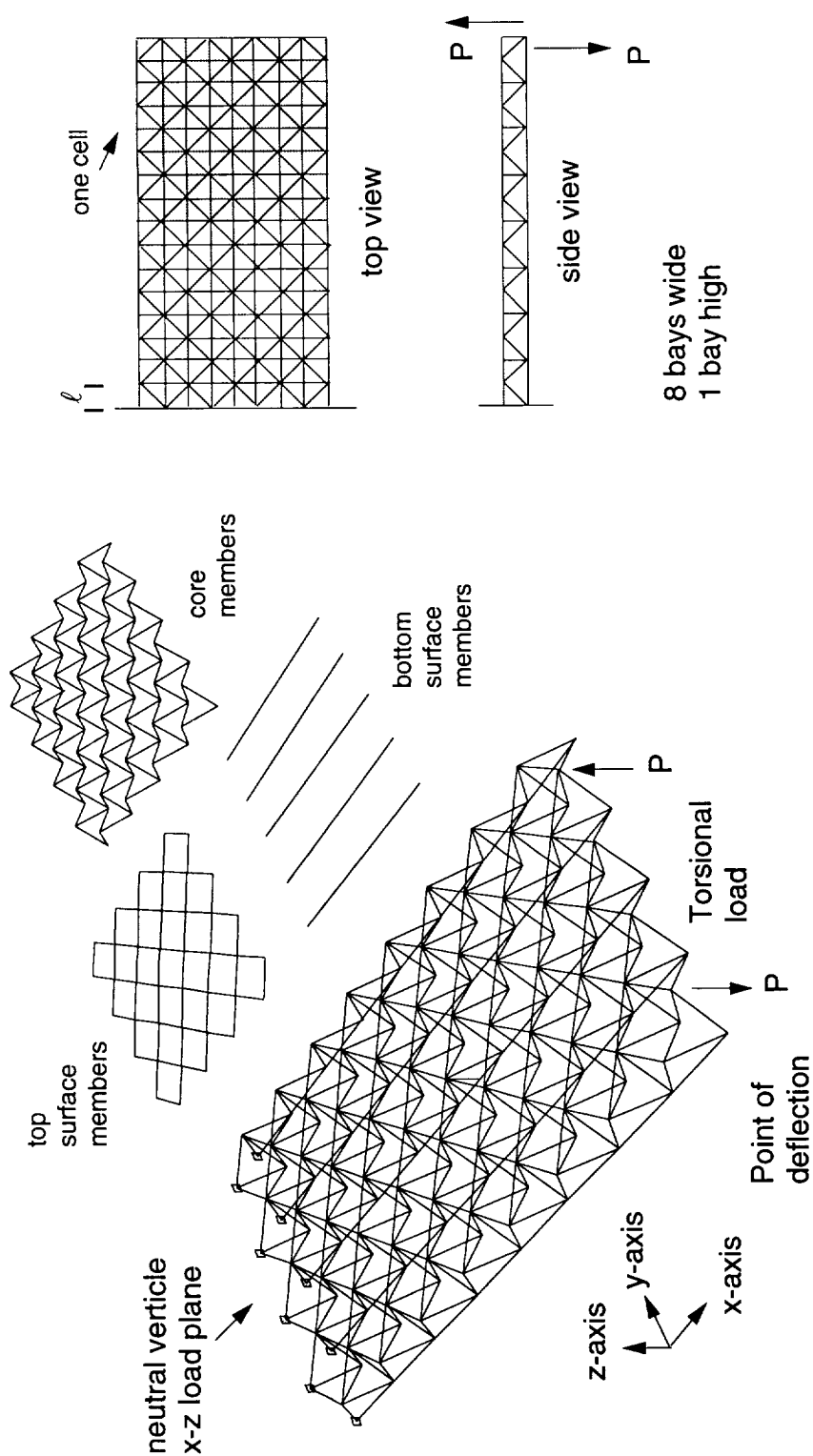
Figure 4.25. Deflection equations of a symmetric soft sixth-order Warren lattice with distributed load.



$$y = \frac{P\ell}{AE} \left[ 4374n^5 + 34560n^3 + 424n \right] \frac{1}{5} + \left[ 43740n^7 + 42525n^5 + 75880n^3 - 8505n^2 + 2373n + 210 \right] \frac{\sqrt{2}}{5040}$$

Deflection equation  
(end load)

Figure 4.26. Deflection equation for a soft eighth-order Warren lattice with end load.



$$y(n) = \frac{P\ell}{AE} \left[ \left[ \frac{2560}{7} n^7 + \frac{1800}{5} n^5 + \frac{554}{3} n^3 - \frac{40}{105} n \right] + \sqrt{2} \left[ 784 n^5 + 820 n^3 - 50 n^2 + \frac{97}{4} n + \frac{9}{4} \right] \right]$$

Figure 4.27. Deflection equation of soft eighth-order Warren lattice with point loads.

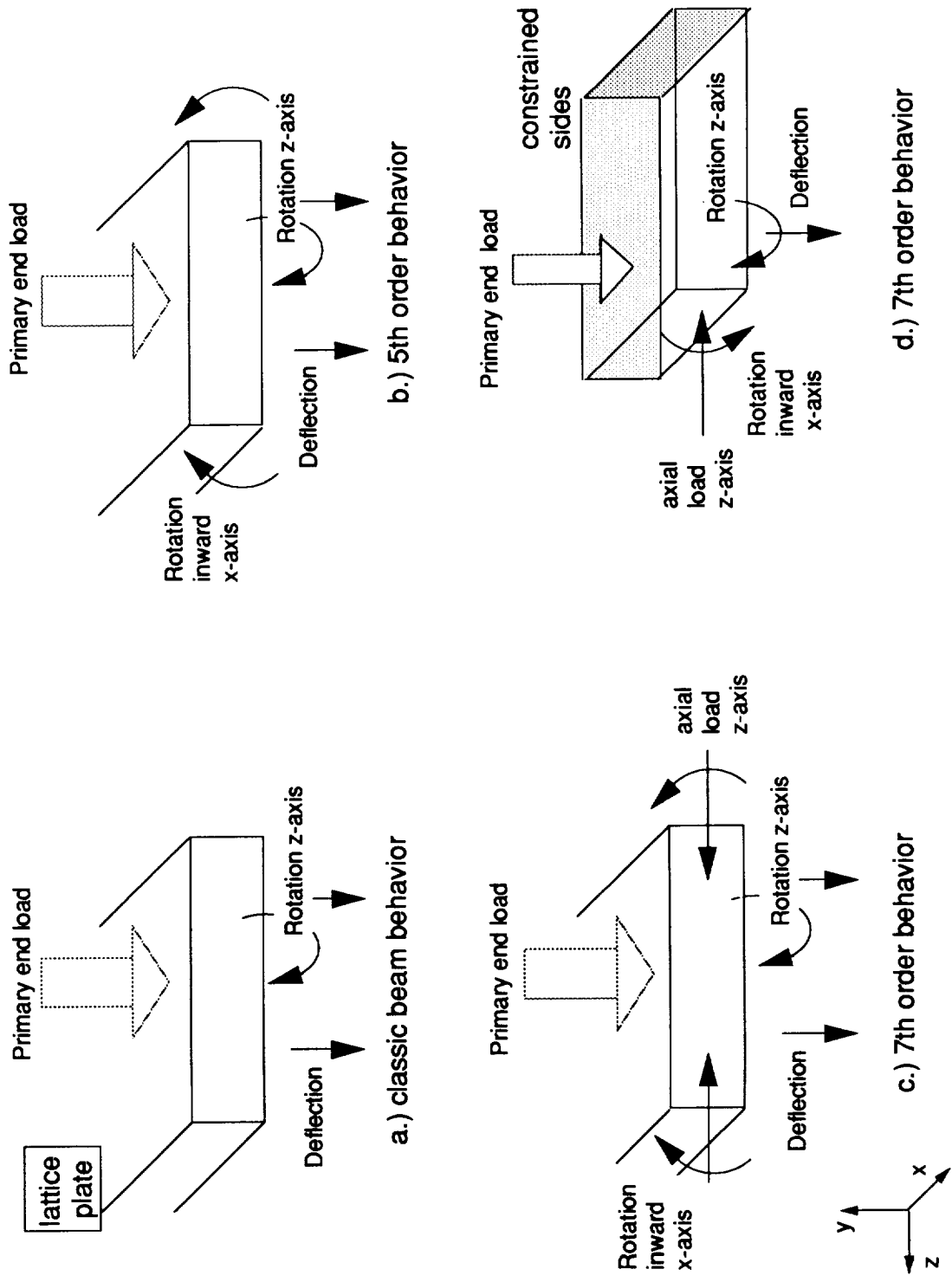
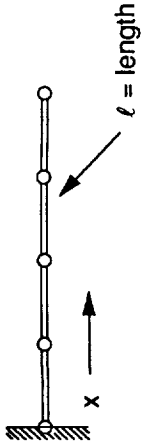


Figure 4.28. Overview of soft lattices endured loads and subsequent behavior.



a.) rod lattice, fixed left end

Eigenvalues

$$w_2 = a \pm \frac{a}{2} \sqrt{2}$$

$$f_1 = \frac{a}{2} \sqrt{2}$$

$$w_4 = a \pm \frac{a}{2} \sqrt{2 \pm \sqrt{2}}$$

$$f_2 = \frac{a}{2} \sqrt{2 \pm \sqrt{2}}$$

$$w_8 = a \pm \frac{a}{2} \sqrt{2 \pm \sqrt{2 \pm \sqrt{2}}}$$

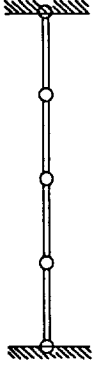
$$f_4 = \frac{a}{2} \sqrt{2 \pm \sqrt{2 \pm \sqrt{2}}}$$

$$\text{Eigenvalue } 2n = a - f_n$$

Fundamental eigenvalue

$$\text{Eigenvalues } 2n = a \pm f_n$$

General eigenvalue equation  
(recursion relationship)



b.) rod lattice, fixed ends

$$w_3 = a \pm \frac{a}{2} \sqrt{2} ; a \quad f_1 = \frac{a}{2} \sqrt{2}$$

$$w_7 = a \pm \frac{a}{2} \sqrt{2 \pm \sqrt{2}} ; a \pm \frac{a}{2} \sqrt{2} ; a$$

$$f_3 = \frac{a}{2} \sqrt{2 \pm \sqrt{2}} \quad f_1 = \frac{a}{2} \sqrt{2}$$

$$\text{Eigenvalue } 2n+1 = a - f_n$$

Fundamental eigenvalue

$$\text{Eigenvalues } 2n+1 = \sum_1^{n-1} \text{Eigenvalues } 2n-1$$

General eigenvalue equation  
(recursion relationship)

$$a = \frac{2EA}{\ell} \quad \text{density} = 1 \text{ unit mass/volume}$$

Figure 4.29. Axial eigenvalue relationships for two rod-like lattices.

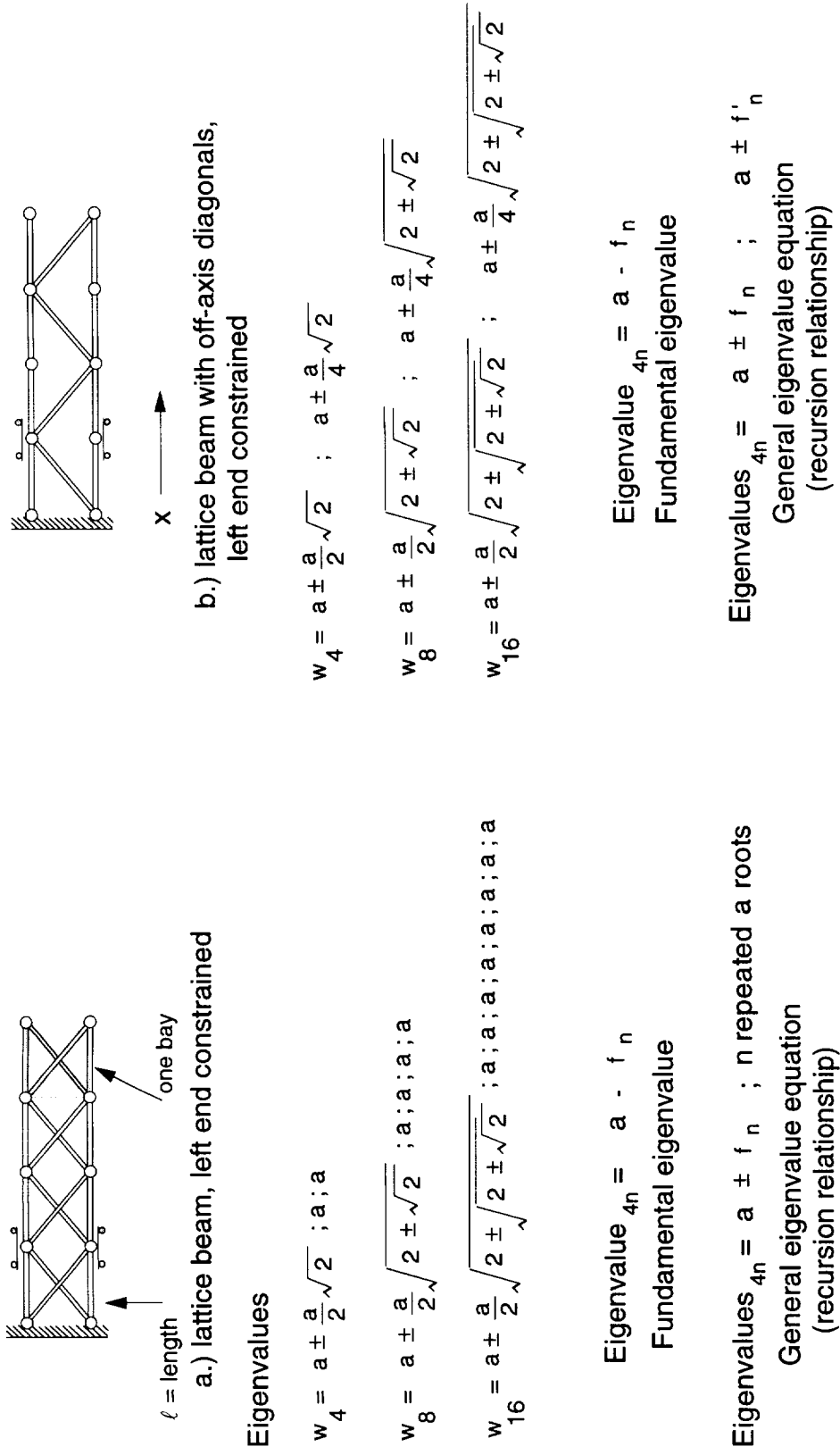


Figure 4.30. Axial eigenvalue relationships for two beam-like lattices.



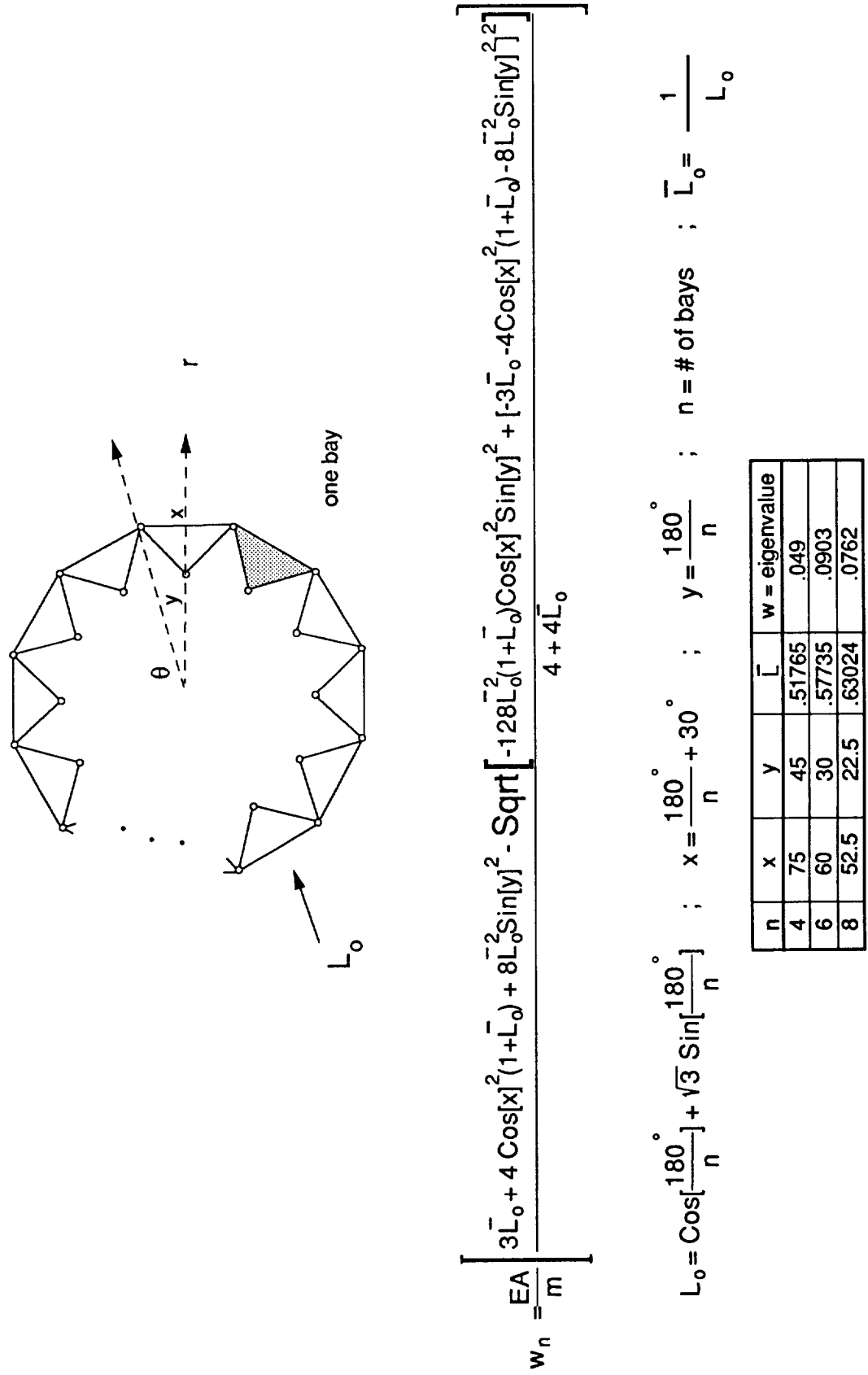


Figure 4.31. Fundamental eigenvalues for a lattice ring.

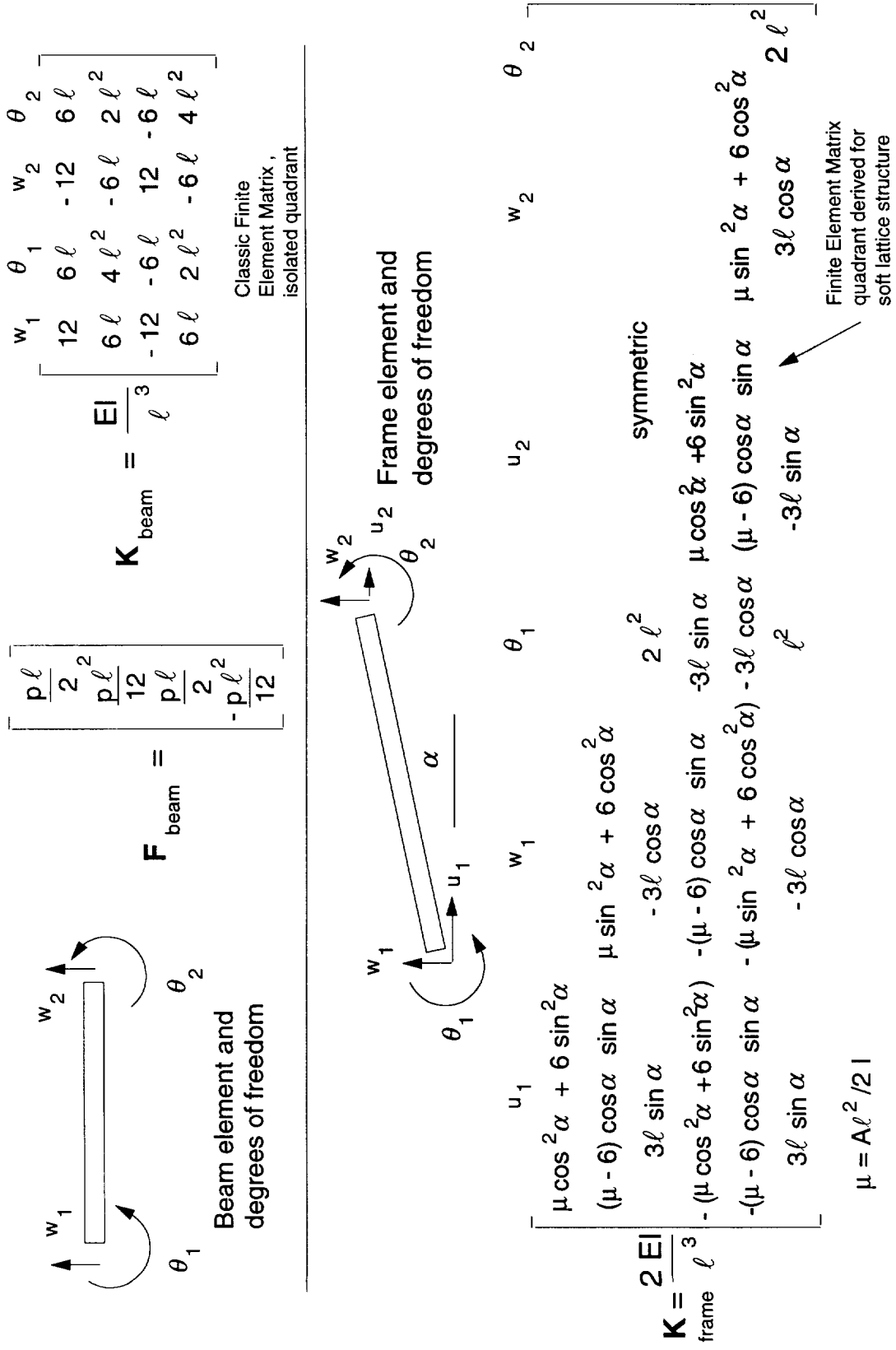


Figure 5.1. Finite Element stiffness matrices for elastic beam and frame elements.

$$[D] = [K]^{-1} [F]$$

$$\begin{bmatrix} w \\ \theta \\ \tau \end{bmatrix} = \begin{bmatrix} P(192n^5 + 304n^3 - 12n^2) + M(120n^4 + 142n^2 - 12n) + S(40n^3 + 16n) \\ P(120n^4 + 142n^2 - 12n) + M(80n^3 + 55n) + S30n^2 \\ P(40n^3 + 16n) + M30n^2 + S15n \end{bmatrix} \frac{\sqrt{2}}{AE24}$$

a.) Exact displacement matrix

$$\begin{bmatrix} w \\ \theta \\ \tau \end{bmatrix} = \begin{bmatrix} P(192n^5 + 304n^3) + M(120n^4 + 142n^2) + S40n^3 \\ P(120n^4 + 142n^2) + M80n^3 + S30n^2 \\ P40n^3 + M30n^2 + S15n \end{bmatrix} \frac{\sqrt{2}}{AE24} = [K]^{-1} \begin{Bmatrix} P \\ M \\ S \end{Bmatrix}$$

b.) Truncated displacement matrix

$$[K][D] = [F]$$

$$[K] = \begin{bmatrix} 300n^4 & -2130n^3 - 600n^5 & 4260n^4 + 400n^6 \\ -2130n^3 - 600n^5 & 4560n^4 + 1280n^6 & -3440n^5 - 960n^7 \\ 4260n^4 + 400n^6 & -3440n^5 - 960n^7 & -2016n^4 - 9760n^6 + 960n^8 \end{bmatrix} \frac{12\sqrt{2}EA}{-302460n^5 - 79200n^7 + 1600n^9}$$

c.) K-stiffness matrix, (b-inverse)

Figure 5.2. Finite element stiffness matrix derivation for soft sixth-order cantilevered lattice with end load.



$$\begin{aligned}
 & \mathbf{K} = \mathbf{L}^T \mathbf{K}' \mathbf{L} \\
 & [\mathbf{L}] = \begin{bmatrix} \text{Cos}[p] & \text{Sin}[p] & 0 & 0 \\ -\text{Sin}[p] & \text{Cos}[p] & 0 & 0 \\ 0 & 0 & 1 & 0 \\ 0 & 0 & 0 & 1 \end{bmatrix} \\
 & [\mathbf{K}] = \begin{bmatrix} \frac{10 \text{ Cos}[p]^2}{11 n} + \frac{900 \text{ Sqrt}[2] n^4 \text{ Sin}[p]^2}{-75615 n^5 - 19800 n^7 + 400 n^9} - \frac{10 \text{ Cos}[p] \text{ Sin}[p]}{11 n} - \frac{900 \text{ Sqrt}[2] n^4 \text{ Cos}[p] \text{ Sin}[p]}{-75615 n^5 - 19800 n^7 + 400 n^9} - \frac{\text{Sqrt}[2] (-6390 n^3 - 1800 n^5) \text{ Sin}[p]}{-75615 n^5 - 19800 n^7 + 400 n^9} - \frac{\text{Sqrt}[2] (12780 n^4 + 1200 n^6) \text{ Sin}[p]}{-75615 n^5 - 19800 n^7 + 400 n^9}, \\ \frac{10 \text{ Cos}[p] \text{ Sin}[p]}{11 n} - \frac{900 \text{ Sqrt}[2] n^4 \text{ Cos}[p] \text{ Sin}[p]}{-75615 n^5 - 19800 n^7 + 400 n^9} + \frac{10 \text{ Sin}[p]^2}{11 n} - \frac{900 \text{ Sqrt}[2] n^4 \text{ Cos}[p]^2}{-75615 n^5 - 19800 n^7 + 400 n^9} + \frac{\text{Sqrt}[2] (-6390 n^3 - 1800 n^5) \text{ Sin}[p]}{-75615 n^5 - 19800 n^7 + 400 n^9} - \frac{\text{Sqrt}[2] (12780 n^4 + 1200 n^6) \text{ Cos}[p]}{-75615 n^5 - 19800 n^7 + 400 n^9}, \\ \frac{\text{Sqrt}[2] (-6390 n^3 - 1800 n^5) \text{ Sin}[p]}{-75615 n^5 - 19800 n^7 + 400 n^9} - \frac{\text{Sqrt}[2] (-6390 n^3 - 1800 n^5) \text{ Cos}[p]}{-75615 n^5 - 19800 n^7 + 400 n^9}, \\ \frac{\text{Sqrt}[2] (12780 n^4 + 1200 n^6) \text{ Sin}[p]}{-75615 n^5 - 19800 n^7 + 400 n^9} - \frac{\text{Sqrt}[2] (12780 n^4 + 1200 n^6) \text{ Cos}[p]}{-75615 n^5 - 19800 n^7 + 400 n^9} \end{bmatrix}
 \end{aligned}$$

Figure 5.3 (b). Beam and frame stiffness matrix for cantilevered soft sixth-order lattice with end load.